

THESIS

PALEO-FLUID MIGRATION AND DIAGENESIS IN THE PENNSYLVANIAN-PERMIAN
FOUNTAIN FORMATION

Submitted by

Ian Hogan

Department of Geosciences

In partial fulfillment of the requirements

For the Degree of Master of Science

Colorado State University

Fort Collins, Colorado

Summer 2013

Master's Committee:

Advisor: Sally Sutton

John Ridley
Thomas Sale

ABSTRACT

PALEO-FLUID MIGRATION AND DIAGENESIS IN THE PENNSYLVANIAN-PERMIAN FOUNTAIN FORMATION

The Pennsylvanian-Permian Fountain Formation is an arkosic conglomeratic sandstone that was deposited in fluvial environments along the eastern flanks of the ancestral Rocky Mountains. The formation owes its pinkish red color to hematite cement that was precipitated early in its diagenetic history. Within the formation are whitened strata that crosscut laminations and facies boundaries, indicating that they are the result of a post depositional process. Whitened features are seen in core, indicating that they are not caused by modern weathering processes. Whitened strata similar to those present in the Fountain Formation are usually the result of the migration of reducing fluids. These fluids reduce and remove hematite cement leaving the fluid migration pathways whitened. Fluids that can cause large-scale reduction and removal of iron oxides include basinal aqueous brines and hydrocarbons.

Whitening within the Fountain Formation appears in a predictable stratigraphically-controlled manner and is most common in coarse channel sandstone facies that are adjacent to laterally continuous paleosol mudstones. The predictable distribution of whitened strata in outcrop suggests that fluid followed preferential pathways. Outcrop analysis indicates that these pathways are closely associated with thin paleosol mudstones and overbank deposits that seem to have focused the paleo-fluids that then flowed laterally along them in the coarser channel sandstones. Laterally

continuous paleosol mudstones therefore may have played an important role in determining the spatial location of paleo-fluid migration pathways. Fluids moved through the formation as stringers that took up less than 15% of the total rock volume.

The Fountain Formation has a complex diagenetic history and has undergone multiple stages of cementation. A late stage dolomite cement contains organic matter, hydrocarbon inclusions, and is associated with bitumen. This cement is restricted to whitened strata and likely precipitated from a hydrocarbon-bearing fluid. The hydrocarbon-bearing fluid may have been the fluid that was responsible for whitening sections of the Fountain. Fluid inclusion data indicate that the precipitation of this cement took place after the formation was buried to a depth of at least 1.3km, which would have been during or after Laramide deformation. The presence of bitumen and hydrocarbon inclusions in strata that were not buried to hydrocarbon generating depths indicates that the hydrocarbon-bearing fluid likely migrated through the formation from deeper in the basin.

The amount of whitening in outcrop decreases in the northern study sites and may be related to a decrease in coarse channel sandstone facies. The lesser abundance of those facies at northern study sites may be because those sites were further from the sources for coarse material and were associated with lower energy environments. Although there is less whitened rock at the northern sites, the amount of fluid that passed through them may have been similar to the amount of fluid that passed through the southern sites. Evidence of this is a higher amount of feldspar alteration in whitened strata in the northern site, which may have been caused by more fluid flow per volume of rock because there were fewer coarse channel facies to act as conduits.

ACKNOWLEDGEMENTS

I would like to thank my thesis committee: Dr. Sally Sutton, Dr. John Ridley, and Dr. Thomas Sale for their support during this project. I particularly want to thank Dr. Sally Sutton for her guidance regarding research methods and interpretation and for the many hours spent editing several drafts of this thesis. Thanks go to Dr. John Ridley for his time spent helping with fluid inclusion analysis. Thanks also go to Dr. Frank Ethridge for his time spent helping with facies interpretations. Thanks go to Boulder County Parks and Open Space and Larimer County Parks and Open Space for allowing fieldwork to be conducted on public land. Finally thanks go to the Rocky Mountain Association of Geologists, the Geological Society of America, and the Colorado State University geosciences department for funding which made this project possible.

TABLE OF CONTENTS

ABSTRACT	ii
ACKNOWLEDGEMENTS.....	iv
LIST OF TABLES	vi
LIST OF FIGURES	vii
CHAPTER 1: INTRODUCTION.....	1
1.1 PROJECT BACKGROUND.....	1
1.2 OBJECTIVES.....	2
1.3 PREVIOUS WORK	2
1.4 GEOLOGICAL SETTING	6
CHAPTER 2: METHODS	12
2.1 LOCATION OF STUDY AREA.....	12
2.2 DESCRIPTION OF FIELD SITES	15
2.3 FIELD WORK.....	21
2.4 LAB WORK	28
CHAPTER 3: RESULTS.....	31
3.1 WHITENED STRATA IN THE FOUNTAIN FORMATION	31
3.2 FACIES CLASSIFICATION.....	36
3.3 RELATIONSHIP BETWEEN FACIES TYPE AND WHITENING	42
3.4 PETROGRAPHIC ANALYSIS.....	50
3.5 FLUORESCENT MICROSCOPY ANALYSIS	67
3.6 FLUID INCLUSION ANALYSIS.....	73
CHAPTER 4: DISCUSSION	78
4.1 STRATIGRAPHY	78
4.1.1 FINING UPWARD SEQUENCES	78
4.1.2 SANDSTONES AND CONGLOMERATES.....	79
4.1.3 SANDSTONE AND CONGLOMERATE FACIES.....	79
4.2 PETROGRAPHIC AND FLUID INCLUSION INTERPRETATIONS FROM SANDSTONE SAMPLES.....	82
4.3 MUDSTONES	86
4.4 LIMESTONES	87
4.5 DIAGENESIS IN THE FOUNTAIN FORMATION	90
4.6 FLUORESCENT MICROSCOPY.....	97
4.7 FLUID INCLUSIONS AND BURIAL TEMPERATURES.....	98
4.8 WHITENING OF THE FOUNTAIN FORMATION	102
4.8.1 PREFERENTIAL FLUID-FLOW PATHWAYS.....	105
4.8.2 GEOGRAPHIC TRENDS OF WHITENING	108
CHAPTER 5: CONCLUSION	113
LIST OF REFERENCES	118
APPENDIX	125

LIST OF TABLES

Table 1: Location of field sites	14
Table 2: Features recorded in point counts	29
Table 3: Abundance of each facies and amount of whitening in all measured strata.....	43
Table 4: Abundance of each facies and amount of whitening at Hall Ranch	43
Table 5: Abundance of each facies and amount of whitening at the Devil's Backbone .	44
Table 6: Abundance of each facies and amount of whitening at the Bobcat Ridge	44
Table 7: Abundance of each facies and amount of whitening at the Blue Sky Trail.....	45
Table 8: Abundance of each facies and amount of whitening at the Hwy 38.....	45
Table 9: Abundance of each facies and amount of whitening at the Dixon Cove	46
Table 10: Abundance of each facies and amount of whitening at the Owl Canyon	46
Table 11: Percent of whitened strata at each outcrop	49
Table 12: Percent of strata whitened if outcrops are divided into vertical sections	50
Table 13: Mineralogy of grains in each facies	54
Table 14: Percentage of each facies composed of cement.....	63
Table 15: Mineralogical differences in whitened and non-whitened samples.....	66
Table 16: Mineralogical differences between outcrops	66
Table 17: Data from inclusions in calcite cement in sample C3	76
Table 18: Data from inclusions in quartz grains in sample C3	77
Table 19: Data from inclusions in quartz grains in sample D1	77
Table 20: Data from inclusions in quartz grains in sample E10.....	77

LIST OF FIGURES

Figure 1: Reconstruction of North America before the uplift of the Ancestral Rocky Mountains	10
Figure 2: Reconstruction of North America after the uplift of the Ancestral Rocky Mountains	10
Figure 3: Stratigraphic column of the Denver basin	11
Figure 4: Regional map of the study area	13
Figure 5: Map of field sites and Fountain Formation exposures.....	14
Figure 6: Map with the location of the Owl Canyon study site.....	15
Figure 7: Map with the location of the Dixon Cove study site.....	16
Figure 8: Photograph of the Dixon Cove study site	16
Figure 9: Map with the location of the Highway 38 study site.....	17
Figure 10: Map with the location of the Blue Sky Trail study site	18
Figure 11: Map with the location of the Bobcat Ridge study site.....	18
Figure 12: Map with the location of the Devil's Backbone study site.....	19
Figure 13: Map with the location of the Hall Ranch study site.....	20
Figure 14: Regional map of all seven study sites	20
Figure 15: Stratigraphic position of samples taken at Hall Ranch	23
Figure 16: Stratigraphic position of samples taken at Devil's Backbone	24
Figure 17: Stratigraphic position of samples taken at Blue Sky Trail	25
Figure 18: Stratigraphic position of samples taken at Dixon Cove	26
Figure 19: Stratigraphic position of samples taken at Owl Canyon	27
Figure 20: Photograph of whitened strata cross cutting bedding	31
Figure 21: Photograph of whitened strata composed of two different facies.....	32
Figure 22: Photograph of wedge shaped whitened strata	33
Figure 23: Photograph of laterally continuous whitened strata.....	33
Figure 24: Photograph of whitened laminations	34
Figure 25: Photograph of coarse sand in whitened laminations.....	35
Figure 26: Photograph of whitening around a paleo-root	35
Figure 27: Photograph of facies SC	36
Figure 28: Photograph of facies TS.....	37
Figure 29: Photograph of facies CSM	38
Figure 30: Photograph of facies VFS	39
Figure 31: Photograph of facies MS	40
Figure 32: Photograph of facies MUD	41
Figure 33: Photograph of facies LS	42
Figure 34: Representation of idealized fining upward sequences	48
Figure 35: Chart of the mineralogy of all point counted samples	51
Figure 36: Photomicrograph of a quartzite clast in facies CSM.....	52
Figure 37: Photomicrograph of large dolomite crystals in facies MUD.....	53
Figure 38: Chart of the mineralogy of grains in all point counted samples.....	54
Figure 39: Chart of the degree of feldspar alteration in various facies	55
Figure 40: Photomicrograph of an altered feldspar in facies TS	55
Figure 41: Chart of the composition of lithic grains in all point counted samples	56

Figure 42: Chart of the distribution of opaque minerals in various facies	56
Figure 43: Photomicrograph of grains without hematite coatings in poikilotopic carbonate cement (cross polarized light).....	58
Figure 44: Photomicrograph of grains without hematite coatings in poikilotopic carbonate cement (plane polarized light)	59
Figure 45: Photomicrograph of replacement dolomite and calcite cement.....	59
Figure 46: Photomicrograph of blocky dolomite cement filling a fracture in a clastic grain.....	60
Figure 47: Photomicrograph of blocky dolomite cement and hematite cement.....	60
Figure 48: Photomicrograph of pore filling hematite cement.....	61
Figure 49: Photomicrograph of hematite and clay cement.....	61
Figure 50: Photomicrograph of clay cement.....	62
Figure 51: Photomicrograph of dolomite cement.....	62
Figure 52: Chart of cement types from all point counted samples	63
Figure 53: Chart of cement type distribution in various facies.....	64
Figure 54: Chart of porosity in various facies	65
Figure 55: Photomicrograph of fluorescent carbonate cement (fluorescent light)	68
Figure 56: Photomicrograph of fluorescent carbonate cement (cross polarized light) ...	68
Figure 57: Photomicrograph of fluorescent carbonate cement (fluorescent light)	69
Figure 58: Photomicrograph of fluorescent carbonate cement (plane polarized light) ...	69
Figure 59: Photomicrograph of fluorescent carbonate cement and bitumen.....	70
Figure 60: Photomicrograph of a hydrocarbon inclusion (fluorescent light)	71
Figure 61: Photomicrograph of a hydrocarbon inclusion (cross polarized light).....	71
Figure 62: Photomicrograph of a hydrocarbon inclusion (fluorescent light)	72
Figure 63: Photomicrograph of a hydrocarbon inclusion (plane polarized light).....	72
Figure 64: Photomicrograph of a fluid inclusion in blocky calcite cement	73
Figure 65: Chart of calcite cement fluid inclusion data from sample C3.....	74
Figure 66: Chart of quartz grain fluid inclusion data from sample C3.....	74
Figure 67: Chart of quartz grain fluid inclusion data from sample D1.....	75
Figure 68: Chart of quartz grain fluid inclusion data from sample E10.....	75
Figure 69: Chart of quartz grain fluid inclusion data from all samples.....	76
Figure 70: Photograph of facies SC	79
Figure 71: Photograph of paleo-channel	80
Figure 72: Photograph of facies VFS	82
Figure 73: Photograph of carbonate nodules in facies MUD.....	87
Figure 74: Photomicrograph of fossils in facies LS	88
Figure 75: Photomicrograph of intraclasts and a ripple in facies LS	89
Figure 76: Photomicrograph of carbonate clasts in facies VFS.....	89
Figure 77: Photomicrograph of abundant carbonate cement in facies SC	94
Figure 78: Photomicrograph of dolomite and hematite cement.....	94
Figure 79: Photomicrograph of a ghost of a grain due to dolomite replacement.....	95
Figure 80: Photomicrograph of replacement calcite cement	95
Figure 81: Photomicrograph of pore filling clay cement	96
Figure 82: Sequence of diagenetic events	97
Figure 83: Stratigraphic column of the study area pre-exhumation.....	101
Figure 84: Photograph of whitening above and below a paleosol mudstone bed	107

Figure 85: Photograph of transition of whitening in facies SC and TS	107
Figure 86: Photograph of whitening ending abruptly at the contact between facies TS and CSM.....	108
Figure 87: Chart of the amount of whitened strata vs. the amount of channel sandstone facies at various study sites.....	111
Figure 88: Map of paleo-alluvial fans overlain by study site locations.....	112
Figure 89: Complete list of sequence of diagenetic events	117

CHAPTER 1 INTRODUCTION

1.1 PROJECT BACKGROUND

The Pennsylvanian-Permian Fountain Formation outcrops along the Front Range in Colorado and southern Wyoming and is composed primarily of arkosic conglomerates and sandstones. Although the Fountain Formation has been studied for several decades, whitened strata within the otherwise red to pink sandstones have not. Whitened strata are widespread throughout the Fountain Formation and are found in both marine and non-marine facies (Garner, 1963). Whitened features can be observed in core from several thousand feet below the surface so they are not the result of modern surface weathering. Depositional features such as laminations, bedding, and even facies boundaries are crosscut by whitening, which indicates that they formed after deposition. Whitened strata, such as the ones found in the Fountain Formation, may be caused by diagenetic alteration resulting from the migration of reducing paleo-fluids (Parry et al., 2004; Beitler, 2005). Reducing paleo-fluids are typically associated with hydrocarbons, organic acids, or hydrogen sulfide (Beitler, 2005). Although they are of great importance to the petroleum industry, formational-scale fluid migration pathways are poorly understood because little data can be gathered from them in the subsurface (Larter et al., 1996; Dembicki, 1989). The laterally extensive whitened strata in the Fountain Formation provide an unusual opportunity to directly observe paleo-fluid pathways in a complex and heterogeneous formation and to tie them to the diagenetic history of the Fountain Formation.

1.2 OBJECTIVES

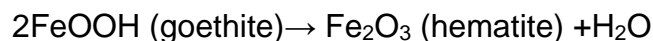
The objectives of this project are: (1) to characterize the lithology and facies of the Fountain Formation in the study area, (2) to determine whether lithological variation controlled the pathways of paleo-fluid migration, (3) to determine what diagenetic effects the paleo-fluid had on the Fountain Formation, (4) to determine the composition of the paleo-fluid, and (5) to constrain the timing of paleo-fluid migration.

1.3 PREVIOUS WORK

Numerous studies have focused on the lithology, environment of deposition, paleo-climate, tectonic history, and paleogeography of the Fountain Formation. The first description of the Fountain Formation was by Cross (1894) and since then many detailed studies have been carried out on the formation. Most authors agree upon the depositional environments of the formation. Knight (1929), Hubert (1960), Howard, (1966), Napp and Ethridge (1985), Maples & Suttner (1990), El-Banna (1993), Meyer (2007), and Sweet and Soreghan (2009) have all concluded that along the Front Range the formation was deposited as a series of alluvial fans and fluvial systems being shed eastward off the Ancestral Rocky Mountains. A shallow sea was located east of the Ancestral Rockies so the formation grades into marine shales and carbonates as it dips into the Denver Basin. Some marine facies are also exposed in outcrop near Manitou Springs and are thought to represent a shallow embayment (Garner, 1963). Howard (1966) used paleo-current data to locate and describe eleven alluvial fans that acted as source areas for the Fountain Formation. Napp and Ethridge (1985) conducted a detailed study of the lithology and facies of the Fountain Formation on the northwest

margin of the Denver Basin and concluded that the Fountain formed in fluvial environments along the Ancestral Rockies before grading into marine facies deeper in the basin. They defined several facies including conglomerates, coarse trough cross-bedded sandstones, horizontally bedded and ripple laminated sandstones, planar cross-bedded sandstones, massive sandstones, and shales and limestones. These facies were interpreted as conglomerate lag, migrating dunes, longitudinal and transverse bars, flood plain deposits, and soil horizons (Napp and Ethridge, 1985).

The Fountain Formation owes its red, pink, and purple colors to hematite cement. Various processes of precipitation for large quantities of hematite cement have been proposed by Friend, (1966), Walker (1967), Berner, (1969), and Turner (1980). Berner explained how, with rising temperatures, unstable amorphous ferric hydroxides such as goethite dehydrate to hematite shortly after burial by the following reaction:



Friend, Walker, and Turner indicated that large quantities of hematite cement can precipitate shortly after burial by the alteration of ferromagnesian silicates by oxygenated groundwaters. Iron bearing silicates, such as hornblende, are common in plutonic and metamorphic-sourced sediments and break down fairly quickly during weathering and diagenesis. The breakdown of hornblende commonly produces minerals such as goethite and kaolinite and the reaction above shows how goethite could dehydrate into hematite.

Although there are numerous reports describing the Fountain, there have only been a few studies that record the whitened strata in the otherwise red and pink formation. Hubert (1960) noted that whitened strata are not depositional features because laminations crosscut red and white boundaries. He suggested that the whitened strata probably formed very shortly after deposition and were caused by hydrogen sulfide produced by decaying plants on buried floodplains seeping down into the underlying channel sandstones. He suggested that the hydrogen sulfide reduced the hematite grain coatings and during compaction was pushed out of the channel sandstones and back into the floodplain sediments along with the ferrous iron (Hubert, 1960). While Hubert's assumption that whitening occurred after deposition based on his observation of cross cutting relationships was sound, his mechanism for early whitening is not supported by later observations. Garner (1963) briefly discussed whitening in the Fountain Formation and addressed Hubert's hypothesis. Whitened strata occur in both marine and non-marine sediments in the Fountain Formation, so it is not possible that hydrogen sulfide from localized floodplain plant decay caused whitening throughout the entire Fountain Formation. Both McLaughlin (1947) and Garner (1963) observed whitening in marine and non-marine facies in outcrops southwest of Colorado Springs. Garner also pointed out that during compaction fluids would likely have been pushed out of the mudstone floodplain facies and into the channel sandstones, not the other way around (Garner, 1963).

In depth studies of whitened strata have been carried out in other formations (Levandowski et al., 1973; Lee & Bethke, 1994; Garden, 2001; Parry, Chan, & Beitler

2004; Beitler, 2005; Parry & Blamey, 2010). Fluids that can cause large-scale reduction and removal of iron oxides include basinal aqueous brines, hydrocarbons, or a combination of both. Levandowski et al. (1973) and Lee and Bethke (1994) studied the close association of whitened strata and hydrocarbons in the Permian Lyons Formation in the Denver Basin. Both studies concluded that basinal brine migrated upwards into the formation and caused dolomite and anhydrite precipitation in some parts of the formation, creating an impermeable layer. Hydrocarbons migrated along the same pathways and were trapped by the impermeable layer sometime after the Late Cretaceous (Lee and Bethke, 1994). Hydrocarbons removed hematite from the otherwise orange and red Lyons Formation leaving those sections a white to grey color (Levandowski et al., 1973; Lee and Bethke, 1994). A study by Garden (2001) showed that widespread whitening of the Jurassic Entrada Formation in southeast Utah was due to a hydrocarbon migration event. Bitumen and hydrocarbon inclusions were found within the whitened strata.

Garden (2001) used the spatial distribution of whitened strata to infer how the hydrocarbon-bearing fluid moved through the Entrada Formation. He concluded that fluids migrated through carrier beds as stringers that took up less than 10% of the total volume of the formation and were in the coarser sandstones. This was explained by the fact that capillary pressure is one of the most important resistant forces to hydrocarbon movement and is ultimately controlled by the radius of the pore throats between grains, which would often be larger in coarser grain sand (Garden, 2001). Other studies also show that hydrocarbon-bearing fluids move in the subsurface as stringers that take up a

small portion, usually less than 10%, of the total volume of rock, and may migrate laterally tens to even hundreds of kilometers in carrier beds (Dembicki, 1989; Larter et al., 1996).

1.4 GEOLOGIC SETTING

The Fountain Formation along the Front Range extends for about 215 miles north to south from Canon City, Colorado to Iron Mountain, Wyoming (Howard, 1966). The southern third of the formation overlies Ordovician, Devonian, and Mississippian sedimentary rocks and the northern two-thirds of the formation lie unconformably on Precambrian basement (Howard, 1966). The Fountain is exposed along the western margin of the Denver Basin and dips eastward into the basin. Dips along the western margin of the basin are highly variable ranging from less than twenty degrees to close to vertical at the Flatirons near Boulder, Colorado. As the Fountain Formation dips eastward into the Denver Basin it grades from conglomerates and sandstones into marine shales and limestones (Howard, 1966). The thickness of the formation ranges from over 1300m near Colorado Springs to 200m in southern Wyoming (El-Banna, 1993). On the eastern flank of the basin the dip reverses and Fountain equivalents gradually shallow near Kansas and Nebraska to about 1,500-2,000 meters depth (Garbarini and Veal, 1968).

The Fountain Formation formed as a wedge of immature sediment along the Ancestral Rocky Mountains and was the earliest formation to form due to erosion of those mountains. In the study area the Fountain sediment was deposited in alluvial

fans and braided streams that sloped northeast off the highlands and graded into marine sediments further northeast in the Denver Embayment. The age of the Fountain Formation is based on paleontological and stratigraphic evidence. Suttner et al. (1984) described Atokan age marine invertebrate and plant fossils in the lower Fountain and Maughan and Ahlbrandt (1985) described Virgilian age fusulinids in the upper Fountain. The Fountain is overlain by the Permian Ingleside and Lyons Formations and it is possible that the uppermost Fountain is lower Permian in age (Sweet and Soreghan, 2009).

The Ancestral Rocky Mountains were Precambrian fault-bounded basement blocks that were uplifted during the Pennsylvanian due to severe cratonic deformation (Fig. 1 and Fig. 2). The orientation of these mountains was roughly northwest-southeast (Kluth and McCreary, 2006). Structural relief was likely close to 6km (Soreghan and Gilbert, 2006). Uplift of the mountains resulted in erosion of earlier overlying Paleozoic sediments and exposure and erosion of basement rock (Kluth and Coney, 1981). The cause of the intracratonic stresses that uplifted the Ancestral Rockies is still debated, in part because uplift occurred hundreds miles from any active plate boundary. Several hypotheses have been proposed. The most prominent hypothesis is that the Ouachita-Marathon orogeny directed compressional stresses to the northwest into the craton and reactivated zones of weakness (Kluth and Coney, 1981; Dickinson and Lawton, 2003; Soreghan et al., 2012). The Ouachita-Marathon orogeny was a collision front that trended roughly northeast-southwest, but the Ancestral Rockies trended roughly northwest-southeast. This may be explained by

wrench faulting of the uplifted basement blocks and that suturing of Gondwana and Laurasia along an irregular margin or convergence of an oblique front would produce a range of stress trajectories into the interior (Kluth and Coney, 1981; Thomas, 1983). Another hypothesis is that the Alleghenian orogeny far to the east caused reactivation of a megashear running through the center of the continent resulting in the uplift of the Ancestral Rockies (Budnik, 1986). This hypothesis would require stress to have propagated over 800 miles into the interior of the continent from the deformation front. A third hypothesis is that a subduction zone to the southwest caused northeast-directed stresses that resulted in uplift of the Ancestral Rockies. Pennsylvanian volcanics found in northeastern Mexico have been interpreted as evidence for a subduction zone (Ye et al., 1996). Aside from the volcanic rocks, there is no other evidence that this subduction zone existed (Kluth et al., 1998).

Uplift continued through the Permian and by the Mesozoic the Ancestral Rockies had been eroded (Kluth, 1981). The Ancestral Rocky Mountains were also the source of many of the sediments of the later Paleozoic formations in the Denver Basin that buried the Fountain (Kluth, 1981; Hoy and Ridgway, 2002). Current thicknesses of Paleozoic and early Mesozoic formations are less than 1km (Braddock, 1989) so it is unlikely that the Fountain was buried to depths greater than 1km before the latest Cretaceous. Beginning in the Late Cretaceous rapid subsidence of the basin allowed for thick deposits of the Pierre shale to accumulate in the Interior Seaway causing the Fountain to be buried much deeper. Higley and Cox (2007) report that during the latest Cretaceous subsidence near the center of the basin may have exceeded 2km over the

course of only ten million years. At the end of the Cretaceous the Paleozoic sediments near the center of the basin were buried by about 3km of sediment (Lee and Bethke, 1994). Deep burial brought organic rich shales and carbonates in the center of the basin into the oil window, where they became sources for Dakota Formation hydrocarbons that make up a majority of the oil and gas plays in the Denver Basin (Higley et al.,1995). Burial along the western margin of the basin ended with the onset of the Laramide Orogeny, which began in the latest Cretaceous and extended into the Eocene. The Laramide orogeny created numerous basement-cored uplifts and formed the current Rocky Mountains. The Front Range basement block was uplifted along the western side of the Denver Basin and exposed the Fountain, as well as other Paleozoic and Mesozoic formations (Meyer, 2007). Signs of uplift are seen in rocks that are about 66 million years old (Cole et al., 2010). Evidence for this timing includes deposition of synorogenic formations such as the Arapahoe Formation and Denver Formation in the latest Cretaceous (Cole et al., 2010) and the presence of numerous volcanic clasts at the base of the Arapahoe Formation that were likely derived from uplifted volcanic centers along the Front Range (Cole and Braddock, 2009). A progressive increase in arkosic material from the uplift and deroofting of Precambrian basement in these formations (Wilson, 2002), large fans that extended out from the Front Range block beginning at the end of the Cretaceous (Obradovich, 2002), and long periods of erosion or non-deposition beginning around 63 million years ago (Cole et al., 2010) also provide evidence of uplift during this time. The Laramide Orogeny also resulted in the rotation of Paleozoic strata derived from the northwestern trending Ancestral Rockies to the current north-south orientation of the Denver Basin (Rall, 1996).

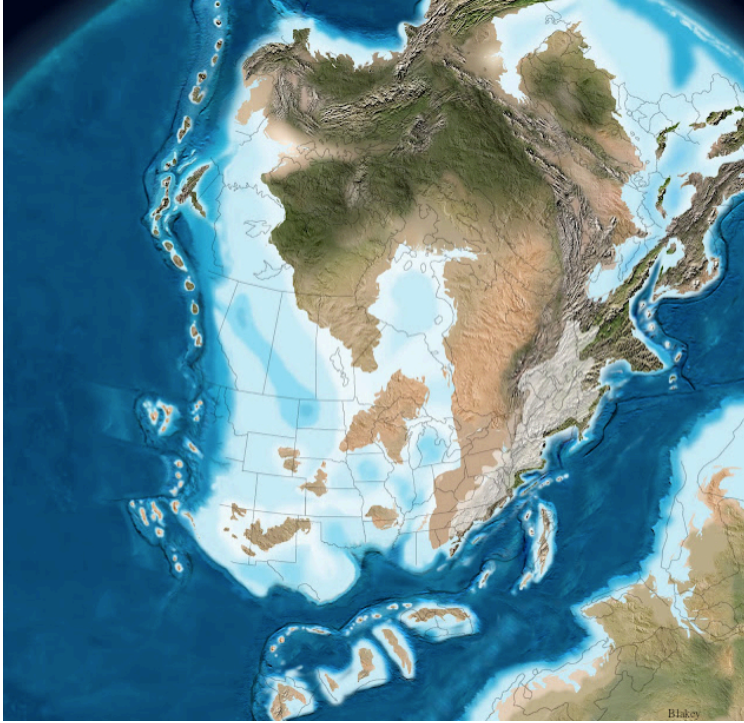


Figure 1. Reconstruction of Gondwana approaching Laurasia during the Late Devonian (Blakey, 2011)



Figure 2. Reconstruction of the Alleghenian and Ouachita-Marathon orogenies during the early Pennsylvanian. Ancestral Rocky Mountains circled in red. (modified from Blakey, 2011)

ERA	PER.	FORMATION	THICKNESS (m)
CEN.	QUAT.	Undiff.	0-120
	TERT.	Undiff.	0-420
MESOZOIC	CRETACEOUS	Laramie	0-30
		Fox Hills Ss.	0-45
		Pierre Sh.	300-2500
		Niobrara	6-112
		Codell SS.	0-6
		Carlile Sh.	12-30
		Greenhorn Ls.	60-85
		Graneros/ Mowry Sh.	50-65
		Dakota Gp.	60-150
	JUR.	Morrison	27-75
		Entrada	0-40
		Jelm	0-40
	TRI.	Lykins	150-200
		Lyons	6-40
	PERM.	Satanka/ Owl Canyon	30-75
Ingleside		30-100	
Fountain Fm.		30-365	
PENN.			
PRECAMBRIAN			

Figure 3. Stratigraphic column of the Denver basin (Sutton et al., 2004)

CHAPTER 2

METHODS

2.1 LOCATION OF STUDY AREA

The study area is along the western flank of the Denver Basin near Fort Collins, Colorado. Field observations and samples were taken at outcrops along the Front Range where the Fountain Formation has been exposed by uplift of the Rocky Mountains. The formation outcrops along a north-south transect. The length of the study area is approximately fifty miles (Fig. 4). Seven field sites were chosen based on most complete outcrop exposure and accessibility and are shown in map view in Figure 5. The northernmost site is at the Owl Canyon roadcut on Highway 287 seventeen miles north of Fort Collins, Colorado. The southernmost site is at Hall Ranch near Lyons, Colorado. Other sites are in Bobcat Ridge Natural Area, Devils Backbone Open Space, and near Horsetooth Reservoir. Exact locations of field sites are listed below in Table 1. The Fountain Formation in the study area is about 800 feet thick (Wolfe, 1953), but in the northern Denver Basin the lower portion of the Fountain is rarely exposed because it consists of mostly paleosol deposits that result in it forming strike valleys (Maughan and Wilson, 1963). Therefore, this study focuses on the upper third of the Fountain Formation.

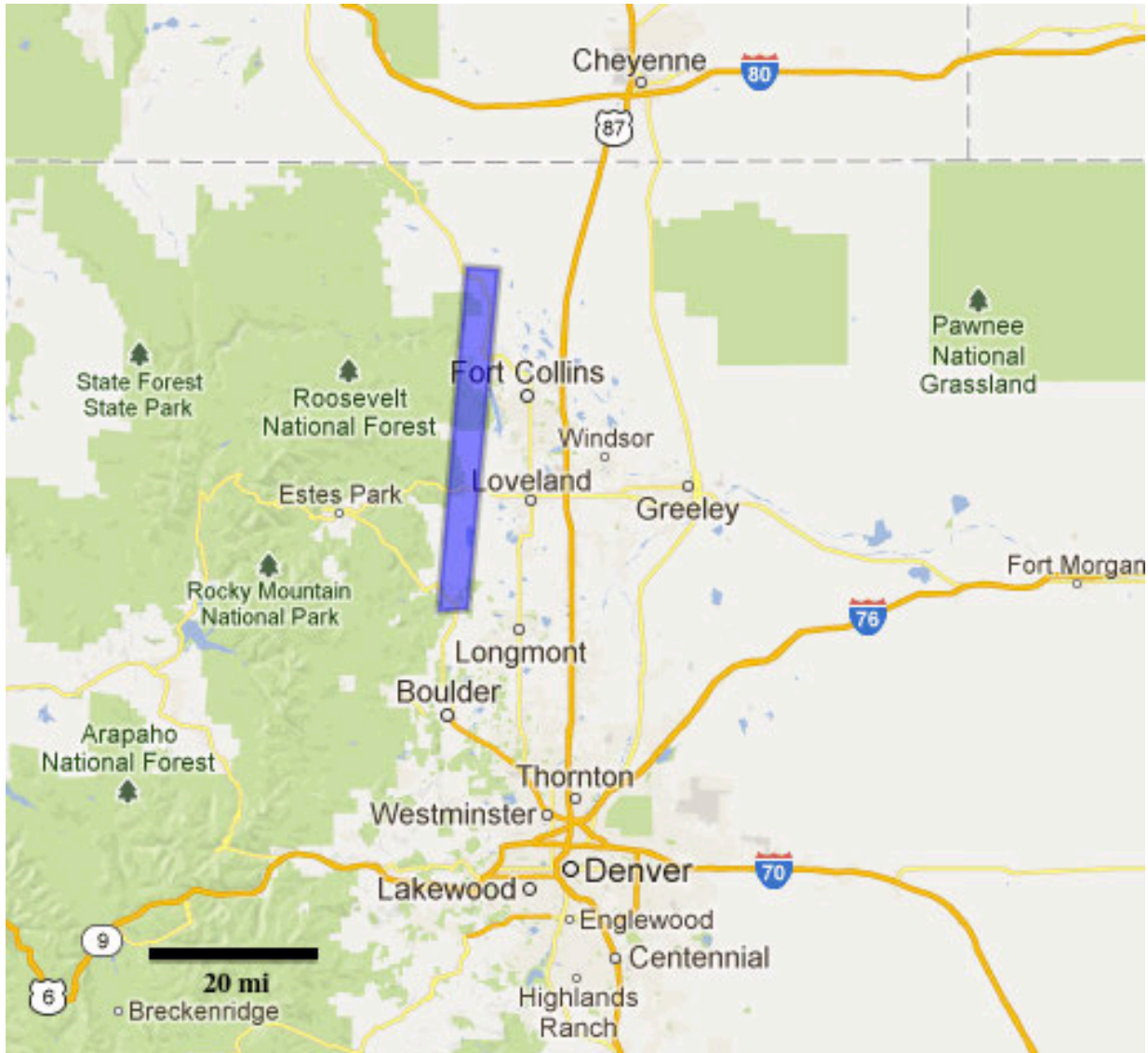


Figure 4. Regional study area shown in purple

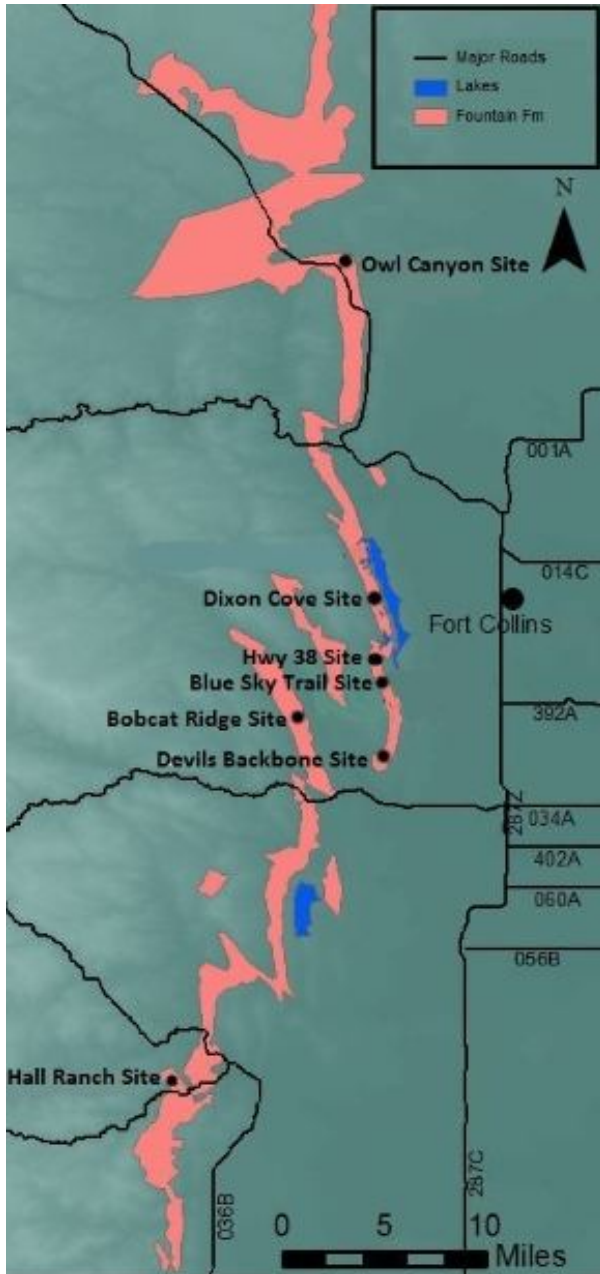


Figure 5. Location of field sites and Fountain Formation exposures

Table 1. Location of field sites in order from north to south

Owl Canyon Roadcut on Hwy 287	SE1/4 of the NW1/4, Sec. 12, T9N, R70W
Dixon Cove at Horsetooth Reservoir	SW1/4 of the NE1/4, Sec. 30, T7N, R69W
Hwy 38 Roadcut at Horsetooth Reservoir	SE1/4 of the NW1/4, Sec. 6, T6N, R69W
Blue Sky Trail at Horsetooth Reservoir	NW1/4 of the SW1/4, Sec. 17, T6N, R69W
Bobcat Ridge Natural Area	SW1/4 of the SE1/4, Sec. 15, T6N, R70W
Devil's Backbone Open Space	NE1/4 of the NE1/4, Sec. 6, T5N, R69W
Hall Ranch	SW1/4 of the NE1/4, Sec. 24, T3N, R71W

2.2 DESCRIPTION OF FIELD SITES

Owl Canyon: This is the northernmost field site and is a roadcut along highway 287 about three miles southeast of Livermore, Colorado (Fig. 6). It is a continuous exposure of 143 feet of section and is very easily accessible.

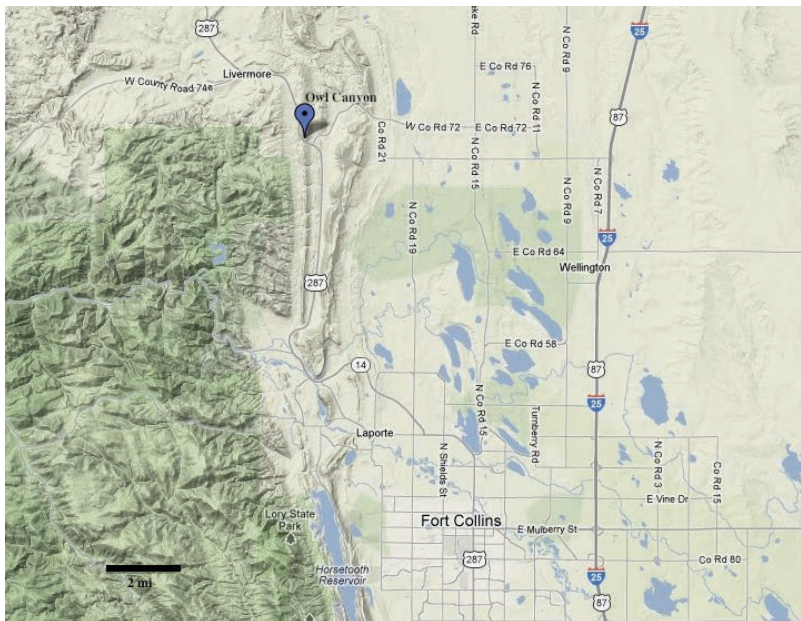


Figure 6. Location of the Owl Canyon roadcut field site

Dixon Cove: This field site is located along the western bank of Horsetooth Reservoir and is about two miles west of Fort Collins (Fig. 7). It consists of a large outcrop along one of the hogbacks in the area. About 170 feet of section are exposed at this site. The outcrop is accessible via the Shoreline Trail, which begins in the Soderberg Open Space parking area.



Figure 7. Location of Dixon Cove field site.



Figure 8. Dixon Cove outcrop

Hwy 38 Roadcut: This field site is located at the southern end of Horsetooth Reservoir along Highway 38 (Fig. 9). A 208ft continuous section is exposed here and is easily accessible.

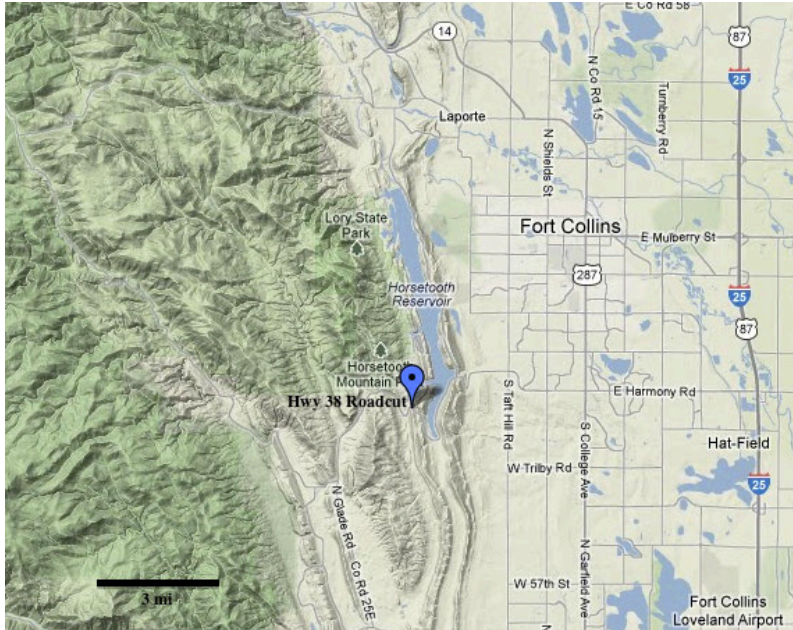


Figure 9. Location of Highway 38 Roadcut field site

Blue Sky Trail: This field site is located along the Blue Sky Trail in Rimrock Open Space about two miles south of Horsetooth Reservoir (Fig. 10). The outcrop is along a large hogback and 102 feet of section are exposed. The field site is accessible via the Blue Sky Trail, which has a trailhead along Highway 38.

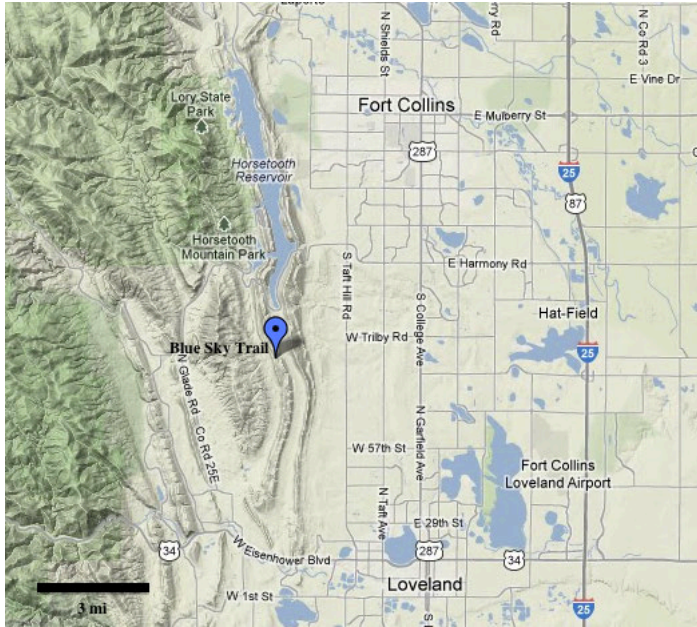


Figure 10. Location of the Blue Sky Trail field site

Bobcat Ridge: This field site is located in the Bobcat Ridge Natural Area about eight miles southwest of Fort Collins (Fig. 11). It is an outcrop with about 68 feet of exposed section. The outcrop is easily accessible along CO Road 32C near Masonville.

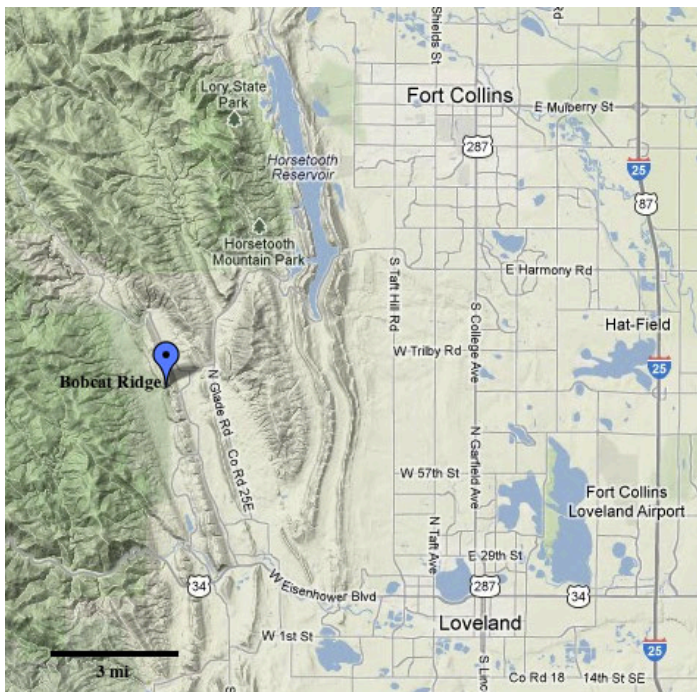


Figure 11. Location of the Bobcat Ridge study site

Devil's Backbone: This field site is at an outcrop along a hogback in Devil's Backbone Open Space near Loveland, Colorado (Fig. 12). About 75 feet of section are exposed and the lateral extent of the outcrop is excellent. The site is accessible via the Hunter Loop Trail that starts at the Devil's Backbone Trailhead.

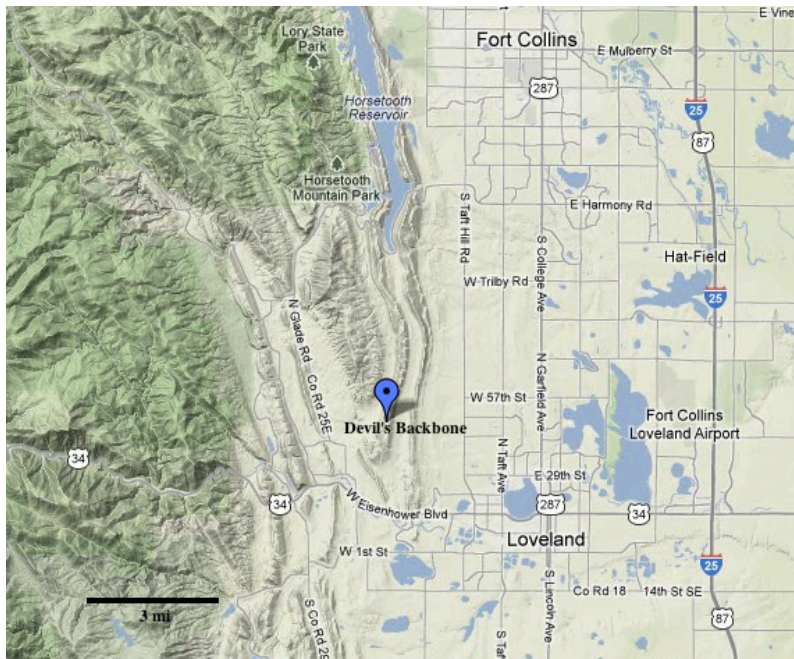


Figure 12. Location of the Devil's Backbone field site

Hall Ranch: This is the southernmost field site and is located near Lyons, Colorado (Fig. 13). This outcrop has 126 feet of exposed section and is accessible from the southern parking area in Hall Ranch.

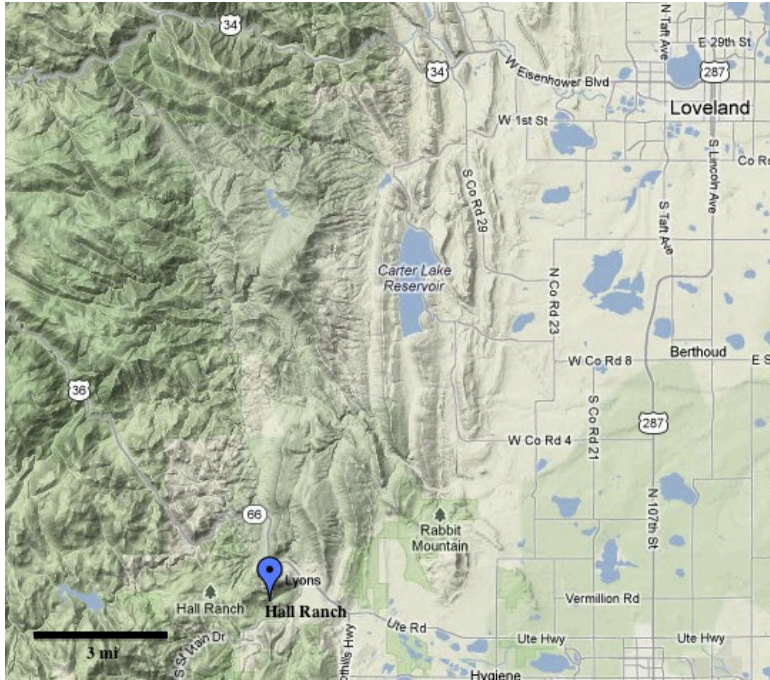


Figure 13. Location of the Hall Ranch field site

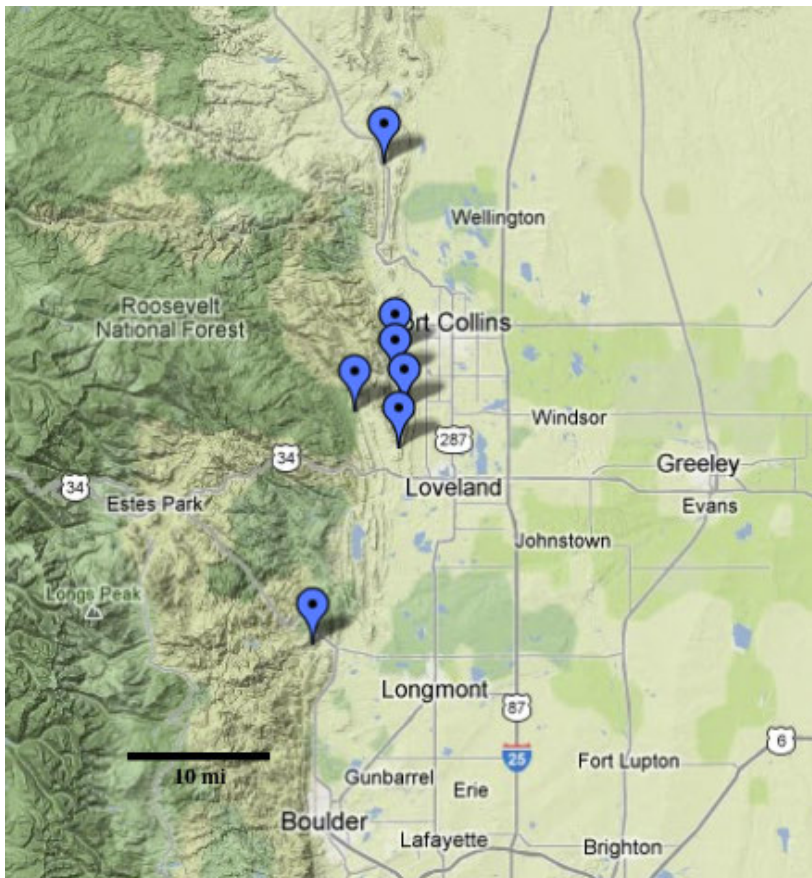


Figure 14. Regional map of all seven field sites

2.3 FIELD WORK

Fieldwork was an important component of this project and was conducted during the summer of 2012. Field data were used to define the spatial distribution of whitened strata and their relationship to sedimentary facies. These relationships were studied in order to determine if the reducing paleo-fluid that caused whitening in the formation had followed preferential pathways and to determine what features controlled those pathways. Sections were measured in detail at each of the seven field sites. Strata were measured from the bottom of exposures up to the Fountain-Ingleside contact. This contact is marked by a sharp transition from the arkosic sandstones and conglomerates in the Fountain Formation to the planar cross-bedded, fine grained, orange sandstones in the Ingleside Formation. The contact shows evidence of a hiatus and clastic dykes extending up to 15 feet into the Fountain are common along the contact. Strata in measured sections were broken down into distinct units based on observable features and were then documented. Features recorded included grain size and sorting, sedimentary structures, cement type, bedding type and thickness, bioturbation, paleosol structures, and color. Careful attention was paid to the distribution of whitened strata and whether beds were completely whitened, whitened only in laminations, or had some other distribution of whitening. Each unit within the measured section was described and usually photographed or sketched. Each unit was classified as one of the following seven facies: structureless conglomerate, trough cross-bedded sandstone, coarse sand and mud, very fine sandstone, massive sandstone, mudstone, or limestone. Lateral continuity was also noted and in some cases beds were measured laterally along the outcrop. Measurements of units were

taken using a 50-foot tape and strike and dip was taken using a Brunton compass. Owl Canyon, Dixon Cove, Blue Sky Trail, Devil's Backbone, and Hall Ranch were selected as sample sites and fifteen hand samples were taken from each site. The 75 hand samples were selected based on color and facies type and would later be used for thin sections. Although samples were taken from fresh-appearing rock faces, there may be some degree of modern weathering. Most samples were taken from whitened strata and red strata directly adjacent to whitened strata and a few samples were taken in red strata several feet from whitened strata to be used as controls. Figures 15 through 19 show the exact stratigraphic position where each sample was taken in the measured sections.

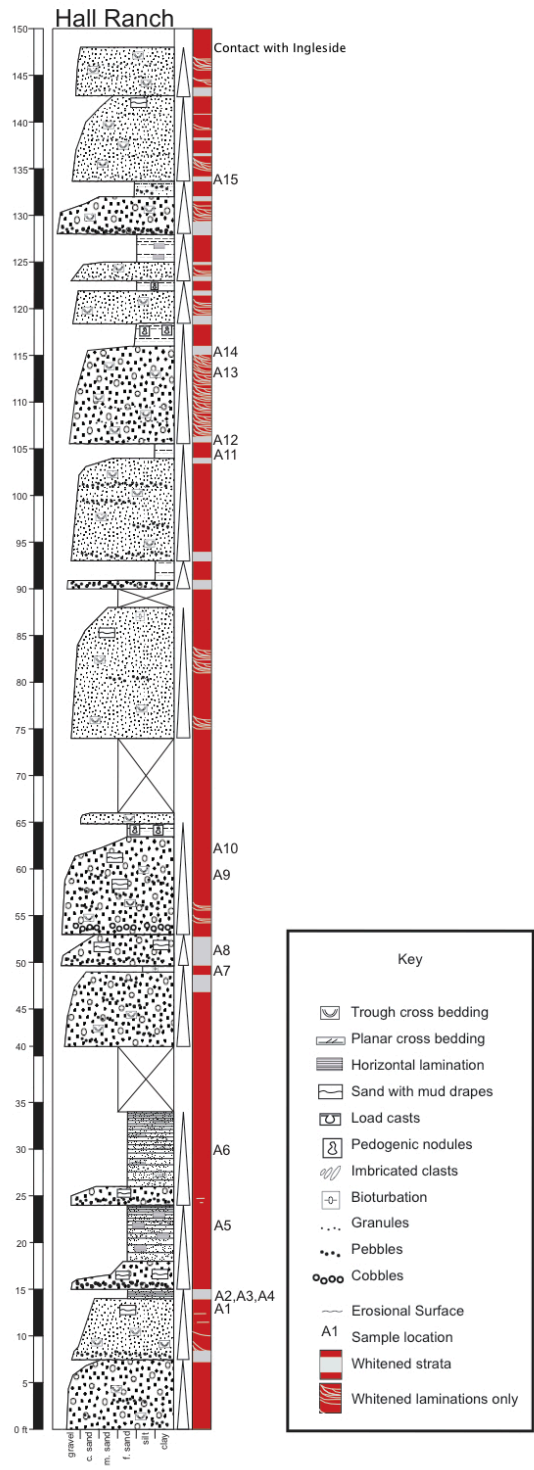


Figure 15. Stratigraphic position of samples taken at the Hall Ranch field site

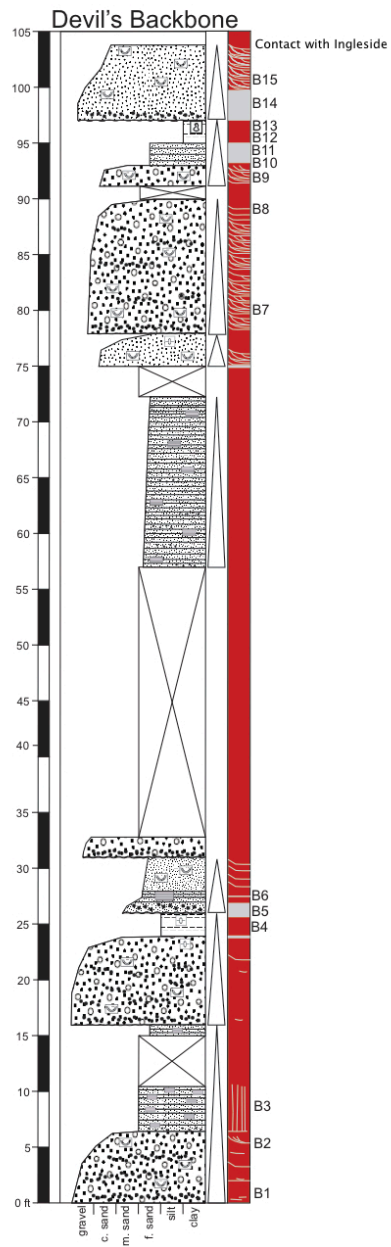


Figure 16. Stratigraphic position of samples taken at the Devil's Backbone field site

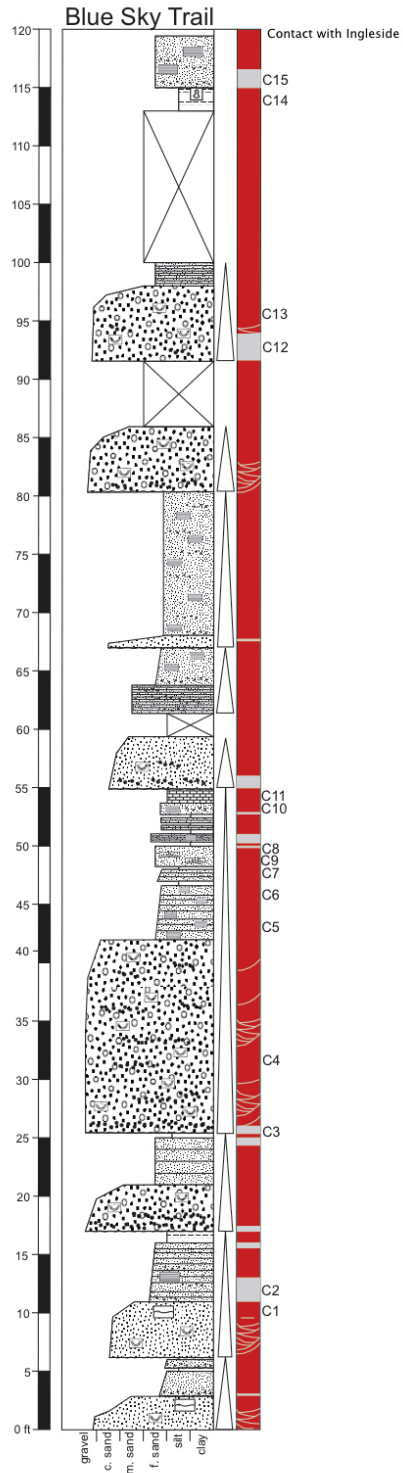


Figure 17. Stratigraphic position of samples taken at the Blue Sky Trail field site

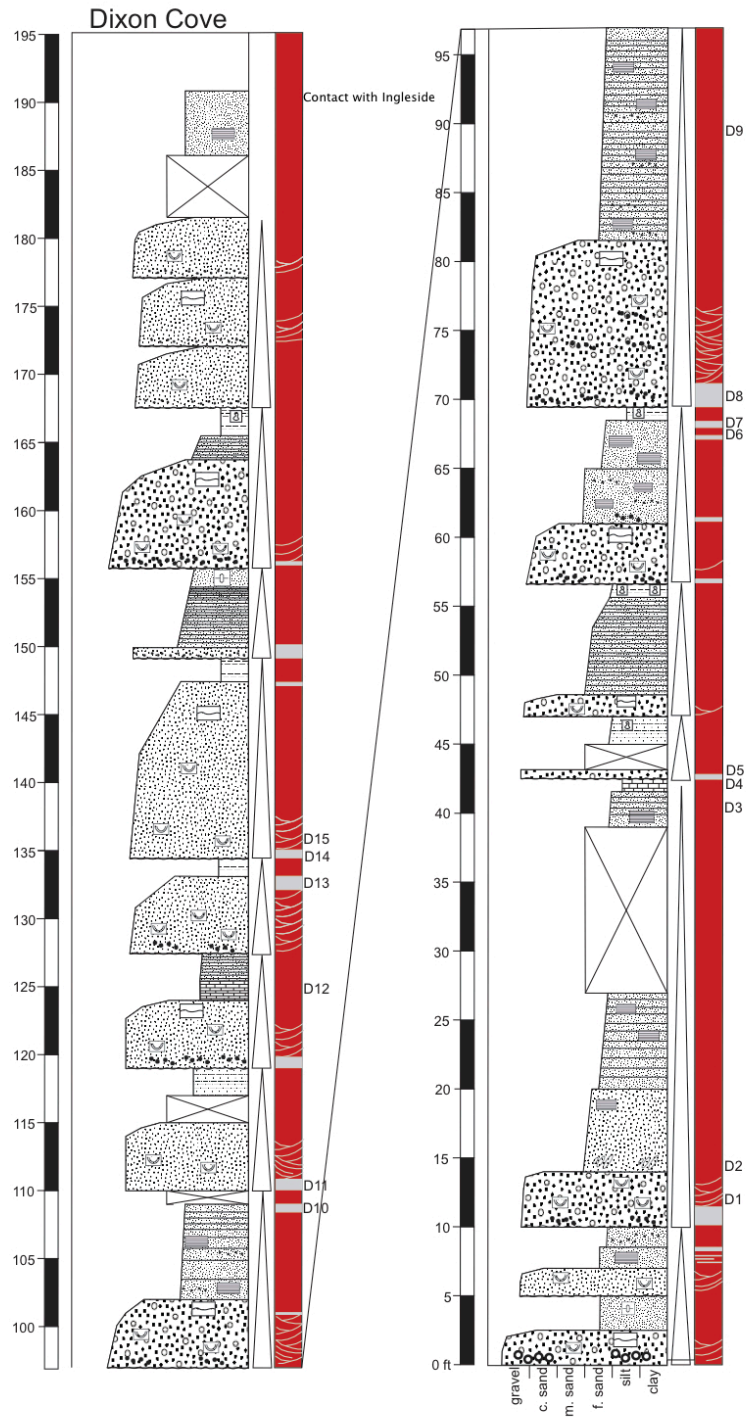


Figure 18. Stratigraphic position of samples taken at the Dixon Cove field site

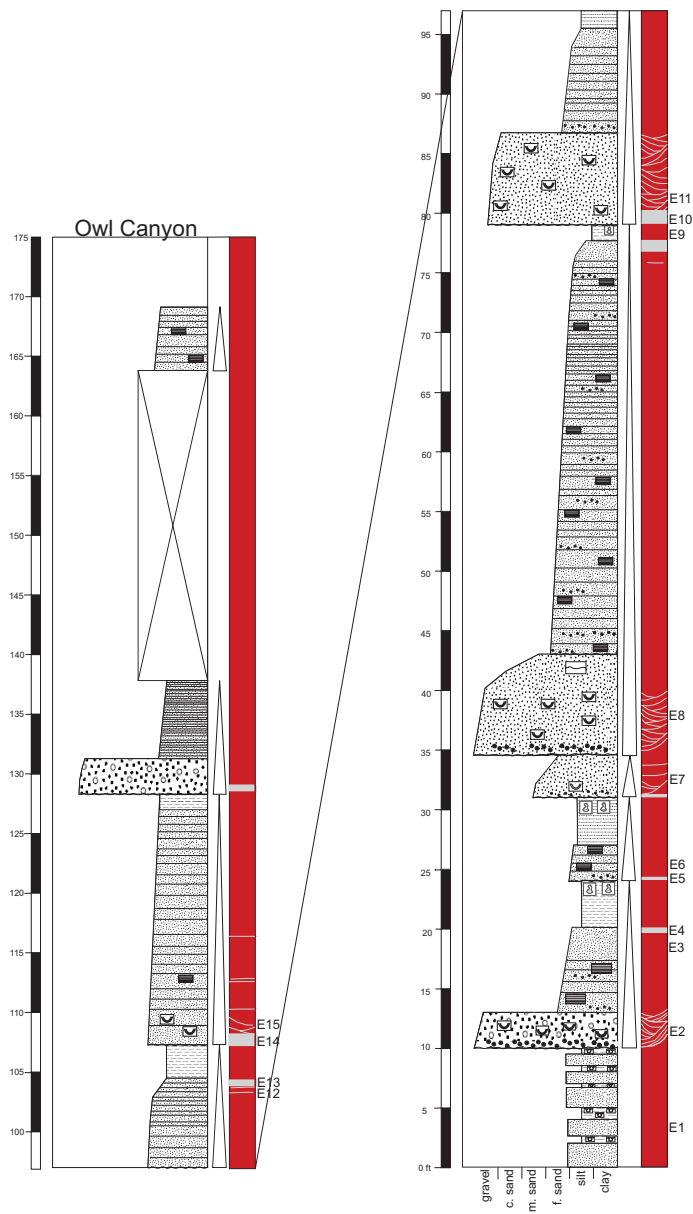


Figure 19. Stratigraphic position of samples taken at the Owl Canyon field site

2.4 LAB WORK

Petrographic analysis, fluorescent microscopy, and fluid inclusion analysis were used in order to study the diagenetic history of the formation, determine how fluid flow affected diagenesis, determine what the composition of the paleo-fluid was, and petrographically characterize facies. Hand samples collected in the field were used to make 75 thin sections and 25 polished fluid inclusion sections. Hand samples were cut to billet size and then sent to Spectrum Petrographics where they were impregnated with epoxy and processed. Thin sections were polished to the standard 30 micron thickness whereas fluid inclusion sections were polished to 60 microns. Alizarin red dye was used to help distinguish carbonates and blue dyed mounting epoxy was used to help identify porosity. All thin sections were described in detail based on qualitative observations and 55 thin sections were selected for point counting in order to obtain quantitative data. Thin sections were selected to represent all facies, study sites, and both red and white strata. For point counting 250 points were analyzed on each thin section using a Leica DM 2500P petrographic microscope and photos were taken using a Clemex C mount camera. Point counting was done on a mechanical stage using a grid method with one-millimeter increments. Features that were point counted included mineralogy of grains, cement type, composition of matrix, and porosity. A complete list of counted features is shown below (Table 2).

Table 2. Features recorded in point counts

Grains Counted	Cements Counted	Matrix Counted	Porosity
Quartz, k-feldspars (altered and non-altered), plagioclase feldspars (altered and non-altered), plutonic lithics, metamorphic lithics, sedimentary lithics (clastic), sedimentary lithics (carbonate), biotite, muscovite, chlorite, anhydrite, gypsum, opaque minerals, zircon	Clay (kaolinite), clay (other), calcite, dolomite, hematite, quartz	Clay (kaolinite), clay (other)	Porosity

Diagenetic features such as cement, replaced minerals, and compacted, dissolved, and deformed grains were recorded. The relationships among these features were used to determine a diagenetic sequence of events. Fluorescent light was used to identify bitumen, hydrocarbon inclusions, and carbonate cements that contained organic matter. Fluid inclusion analysis was used to determine paleo-fluid composition and the maximum burial temperature of the formation at three of the sample sites. The three samples were chosen based on the quantity and quality of the fluid inclusions they contained. Two-phase fluid inclusions were found in carbonate cement and in secondary inclusion trails in healed fractures within clastic quartz grains. Sample C3 from the Blue Sky Trail field site contained 13 workable inclusions in calcite cement and 12 inclusions in quartz grains, sample D1 from the Dixon Cove field site contained 27 inclusions in quartz, and sample E10 from the Owl Canyon field site contained 18 inclusions in quartz. Inclusions in quartz were only used if they were along secondary inclusion trails. No inclusions in grain overgrowths were observed. An Olympus BX51 petrographic microscope and Linkam THMSG 600 heating and freezing stage were

used for the fluid inclusion analysis. Inclusions were frozen to a temperature of -70°C and then slowly heated. The number of solid phases that formed and the final melting temperature were recorded for larger inclusions. Inclusions were then heated and the homogenization temperature was recorded. Ice was impossible to see in many of the smaller inclusions, so only homogenization temperatures were recorded for these inclusions.

CHAPTER 3

RESULTS

3.1 WHITENED STRATA IN THE FOUNTAIN FORMATION

Colors of rock in the Fountain Formation range from purple, pink, red, and orange to white and dull grey. Large amounts of hematite cement occur within the red, purple, pink, and orange colored strata. Samples of rock from colored strata are composed of an average of 11 percent hematite cement and samples of rock that had been whitened are composed of an average of less than 0.5 percent hematite cement according to petrographic analysis. Whitened strata cut across laminae and facies boundaries (Fig. 20). They are widespread in outcrop and can be easily observed in core from depths of over 9,000 feet (Denver Core Research Center, 2013). Of 892 feet of section measured, 14.6% of strata had been whitened.



Figure 20. Whitening cross cutting bedding at the Devil's Backbone study site. Outcrop is approximately 5 feet thick from bottom to top of photograph

Whitened strata in the Fountain Formation can be classified into three categories. One is complete whitening of strata in which whitening may cross cut laminations, bedding, and facies (Fig. 20, 21). Completely whitened strata range from less than an inch to over 2.5 feet thick. The lateral extent of individual whitened strata is extremely variable. Some take on wedge shapes in outcrop and extend laterally for only several feet before pinching out (Fig. 22) whereas others extend laterally with fairly uniform thickness for several hundred feet (Fig. 23). Of all documented whitened strata, 58% were in the completely whitened category.



Figure 21. This zone of completely whitened strata at the Dixon Cove study site includes two different facies



Figure 22. This section of completely whitened strata at the Owl Canyon study site has little lateral extent and is wedge shaped



Figure 23. Completely whitened strata at the base of the outcrop maintains uniform thickness and was walked out laterally for over 1,500 feet at the Devil's Backbone field site

Another category is whitening of individual laminations within units that contain cross bedding (Fig. 24). The degree of whitening within these units is variable as some units contain only one or two whitened laminae, whereas laminations in other units are almost all whitened. Whitened laminae often contain coarser material than the colored laminae around them (Fig. 25). Because of the nature of cross bedding, white laminations are truncated in outcrop view by successive beds and are therefore not very continuous. Although individual laminae have poor continuity, the units themselves that contain white laminae are usually continuous. Whitened laminae made up 42% of all documented whitened strata.



Figure 24. Whitened laminations in a coarse sandstone unit at the Dixon Cove study site

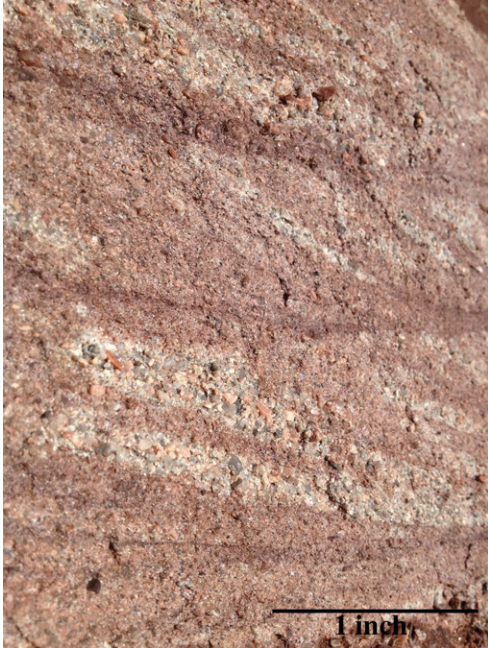


Figure 25. Whitened laminations often contain coarser sand than surrounding laminations. Scale is approximate

The final category consists of concentrations of white reduction spots or whitened rock along root traces (Fig. 26). The volume and extent of this type of whitening is less than 1% of the total amount of whitening observed.



Figure 26. Whitened rock around a paleo-root structure at the Highway 38 Roadcut study site

3.2 FACIES CLASSIFICATION

The Fountain Formation is made up of vertically stacked fining upward sequences. Seven different facies are defined within these sequences. It is rare for all seven facies to be present in a single sequence. In some cases only the first few facies in a sequence are present before a new sequence begins. Laterally these facies are discontinuous and unpredictable, but vertically they follow a pattern that is shown in figure 34. The following facies are listed from bottom to top of a fining upward sequence.

Structureless Conglomerate (Facies SC): This facies consists of structureless conglomeratic lag (Fig. 27) and its base is always on an erosional surface. It forms the bottom of almost all sequences. Clasts are poorly sorted subangular to subrounded quartz, feldspar, and lithics, with less common rip up clasts. Most clasts are 1-2 cm but some anomalous clasts are >10 cm. The matrix is coarse to very coarse sand. This facies is usually white, pink, or red in color. The overlying facies is usually trough cross-bedded sandstone and the contact with it is fairly abrupt. This facies makes up 6.9% of all measured section.



Figure 27. Structureless conglomerate facies at the Dixon Cove study site

Trough Cross-Bedded Sandstone (Facies TS): This facies consists of trough cross-bedded conglomeratic and coarse-grained sandstones (Fig. 28). Sorting is very poor and grains range from angular to subrounded. The angle of trough laminations at the bottom and middle of these units is highly variable, but is usually between 10 to 30 degrees. Bed thickness decreases in the upper portion of these units and commonly grades into very low angle trough laminations. Angles are as low as 4-5 degrees, so without wide outcrops these low angle trough laminations can easily be mistaken for horizontal laminae. This facies commonly has a mix of white and red laminations or is pink to red in color. The top consists either of a gradational contact with the coarse sandstone with mud drape facies or an abrupt contact with the very fine sandstone facies. This facies makes up 33.4% of all measured section.



Figure 28. Trough cross-bedded sandstone facies at the Dixon Cove study site

Coarse Sandstone with Mud Drapes (Facies CSM): This facies consists of thin sandstone beds (several mm to 5cm) separated by thin (1-2mm) mud drapes (Fig. 29). Sorting is extremely poor and grain size ranges from coarse sand to clay. This facies does not always appear in the fining upward sequences but when it does it always overlies facies TS. It differs from facies TS by a dramatic increase in mud content and mud drapes, a decrease in bedding thickness, and sharp color changes from mostly pink and white to dark purple and red. In some areas mud laminations are continuous whereas in others areas they are discontinuous but aligned and are made up of compacted mud rip-up clasts. This facies makes up 7.7% of all measured section.

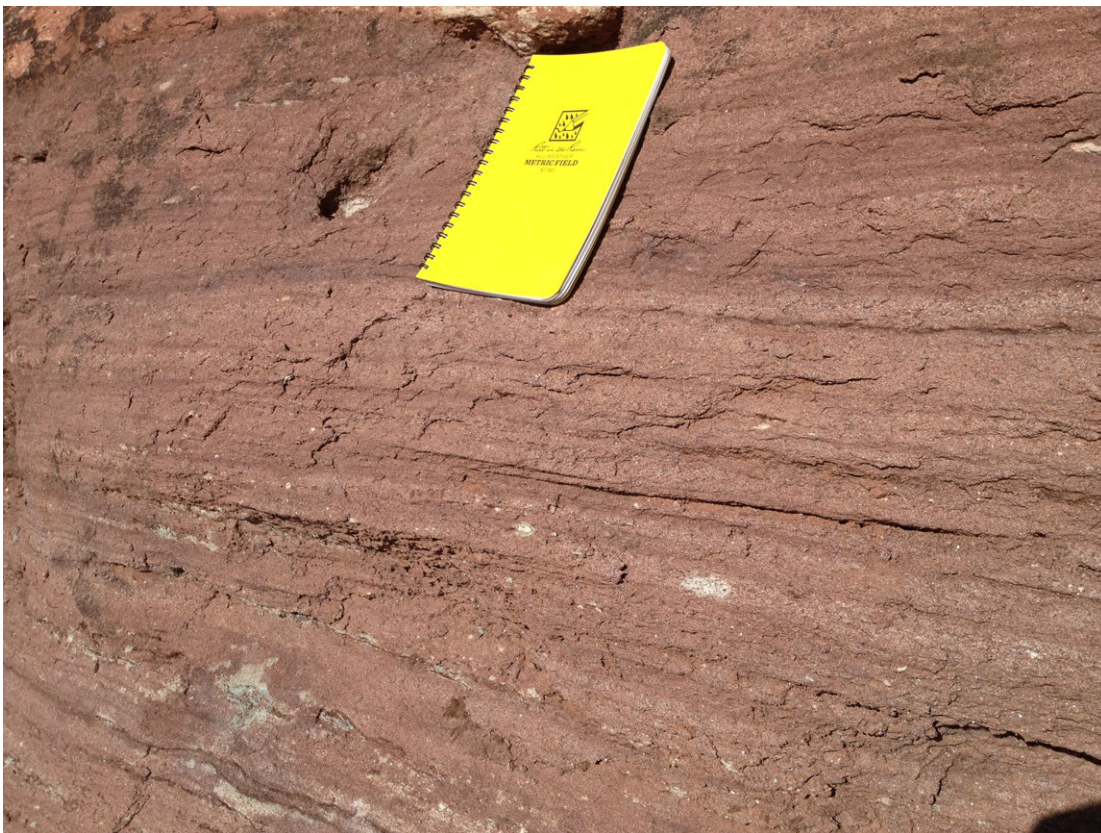


Figure 29. Coarse sand and mud facies at the Blue Sky Trail study site

Very Fine Sandstone (Facies VFS): This facies consists of well sorted, angular to subrounded, fine to very fine sandstone (Fig. 30). It is much better indurated than other facies and usually forms vertical rock faces. Beds are tabular to lenticular and range from several inches to one to two feet thick. Grain size in this facies is commonly bimodal with mostly very fine sand and a lesser amount of coarse to granular sized sand. In some beds coarse grains are concentrated in laminations, whereas other beds consist entirely of well-sorted fine to very fine sand. Many beds have horizontal laminations and a few display planar cross stratification with angles between 25 and 30 degrees. The color of this facies is usually orange although some beds are white. This facies commonly has a sharp contact with overlying mudstone facies or trough cross-bedded sandstone facies. This facies makes up 37.7% of all measured section.



Figure 30. Very fine sandstone facies at the Highway 38 Roadcut study site

Massive Sandstone (Facies MS): This facies consists of massive sandstone, although there is bioturbation in areas. The bioturbation is usually root traces that have been replaced by calcite and are white or purple in color (Fig. 26, 31). Grain size ranges from coarse to very fine sand and colors range from red, brown, orange, or purple with some mottling and white reduction spots. Unlike other facies, this one does not occur in any particular position in the fining upward sequences. This facies makes up 5.1% of all measured section.



Figure 31. Massive sandstone facies at the Highway 38 Roadcut study site

Siltstone/Mudstone (Facies MUD): This facies consists of brown to purple mottled siltstone or mudstone (Fig. 32) and is usually less than 2 feet thick. Some occurrences are well sorted while others contain significant amounts of coarse to granular sand. Platy, blocky, or nodular textures are present, layers of carbonate

nodules are common, and some units contain root structures and reduction spots. The lateral extent of this facies is highly variable. Some units form wedge shapes and are only a few feet across. Other units extend laterally for hundreds of feet and are fairly uniform in thickness except where overlying facies have eroded into them. This facies is fairly soft and is commonly covered. The tops of these units usually represent the top of fining upward sequences and are marked by an erosive contact with facies SC. This facies makes up 9.0% of all measured section.



Figure 32. Siltstone/Mudstone facies at the Owl Canyon study site

Limestone (Facies LS): This facies is uncommon and consists of limestone beds that are 1-2 feet thick (Fig. 33). It is found at the top of fining upward sequences in place of the mudstone facies and it was only observed at two study sites. The beds are blocky and contain intraclasts and microfossils including shell fragments and gastropods. This facies makes up 0.3% of all measured section.



Figure 33. Limestone facies (blocky) at the Blue Sky Trail study site

3.3 RELATIONSHIP BETWEEN FACIES TYPE AND WHITENING

Whitening within the Fountain Formation appears in a predictable manner within fining upward sequences and is much more common in some facies than others. Tables 4 through 10 show the percentage each facies makes up of the total 892 feet of measured section, as well as at each outcrop, and how much of each facies was whitened.

Table 3. Abundance of each facies and amount of whitening in all measured strata

Facies	Percent of Total Measured Sections	Percent of Total Whitened Strata	Percent of Facies Whitened
Structureless Conglomerate (SC)	8.9	24.1	49.3
Trough Cross-Bedded Sandstone (TS)	33.4	54.4	23.8
Coarse Sandstone with Mud Drapes (CSM)	5.6	0.4	0.8
Very Fine Sandstone (VFS)	37.7	14.7	5.7
Massive Sandstone (MS)	5.1	6.4	15.4
Siltstone/Mudstone (MUD)	9	0	0
Limestone (LS)	0.3	0	0

Table 4. Abundance of each facies and amount of whitening at the Hall Ranch study site

Facies	Percent of Total Measured Sections	Percent of Total Whitened Strata	Percent of Facies Whitened
Structureless Conglomerate (SC)	17.5	50.2	58.2
Trough Cross-Bedded Sandstone (TS)	48.6	44.1	18.4
Coarse Sandstone with Mud Drapes (CSM)	5.6	0	0
Very Fine Sandstone (VFS)	17.6	3.7	4.5
Massive Sandstone (MS)	2.5	2	26.3
Siltstone/Mudstone (MUD)	8.2	0	0
Limestone (LS)	0	0	0

Table 5. Abundance of each facies and amount of whitening at the Devil's Backbone study site

Facies	Percent of Total Measured Sections	Percent of Total Whitened Strata	Percent of Facies Whitened
Structureless Conglomerate (SC)	17.1	28	30.2
Trough Cross-Bedded Sandstone (TS)	44.3	59.1	26.7
Coarse Sandstone with Mud Drapes (CSM)	1.5	0	0
Very Fine Sandstone (VFS)	27.6	11.7	8.7
Massive Sandstone (MS)	3	1.2	29.7
Siltstone/Mudstone (MUD)	6.5	0	0
Limestone (LS)	0	0	0

Table 6. Abundance of each facies and amount of whitening at the Bobcat Ridge study site

Facies	Percent of Total Measured Sections	Percent of Total Whitened Strata	Percent of Facies Whitened
Structureless Conglomerate (SC)	8.1	29.6	57.7
Trough Cross-Bedded Sandstone (TS)	32.4	56.3	29.5
Coarse Sandstone with Mud Drapes (CSM)	1.9	0	0
Very Fine Sandstone (VFS)	43.4	0	0
Massive Sandstone (MS)	7.4	14.1	30
Siltstone/Mudstone (MUD)	6.8	0	0
Limestone (LS)	0	0	0

Table 7. Abundance of each facies and amount of whitening at the Blue Sky Trail study site

Facies	Percent of Total Measured Sections	Percent of Total Whitened Strata	Percent of Facies Whitened
Structureless Conglomerate (SC)	7.3	27.9	52.7
Trough Cross-Bedded Sandstone (TS)	33.1	36.1	15.2
Coarse Sandstone with Mud Drapes (CSM)	4.9	1.6	4.8
Very Fine Sandstone (VFS)	46.2	29.9	9.3
Massive Sandstone (MS)	4.3	4.5	15.4
Siltstone/Mudstone (MUD)	3.4	0	0
Limestone (LS)	0.8	0	0

Table 8. Abundance of each facies and amount of whitening at the Hwy 38 study site

Facies	Percent of Total Measured Sections	Percent of Total Whitened Strata	Percent of Facies Whitened
Structureless Conglomerate (SC)	5.8	16.9	63.1
Trough Cross-Bedded Sandstone (TS)	37.9	49.3	29.9
Coarse Sandstone with Mud Drapes (CSM)	6.3	1	2.3
Very Fine Sandstone (VFS)	33.3	19.6	13.6
Massive Sandstone (MS)	4.5	13.2	34.3
Siltstone/Mudstone (MUD)	12.2	0	0
Limestone (LS)	0	0	0

Table 9. Abundance of each facies and amount of whitening at the Dixon Cove study site

Facies	Percent of Total Measured Sections	Percent of Total Whitened Strata	Percent of Facies Whitened
Structureless Conglomerate (SC)	7.1	24	51.4
Trough Cross-Bedded Sandstone (TS)	39.9	55.1	17.5
Coarse Sandstone with Mud Drapes (CSM)	10.1	0	0.8
Very Fine Sandstone (VFS)	23.9	15.1	9.8
Massive Sandstone (MS)	6.1	5.8	14.6
Siltstone/Mudstone (MUD)	11.5	0	0
Limestone (LS)	1.4	0	0

Table 10. Abundance of each facies and amount of whitening at the Owl Canyon study site

Facies	Percent of Total Measured Sections	Percent of Total Whitened Strata	Percent of Facies Whitened
Structureless Conglomerate (SC)	1.2	3.8	41.7
Trough Cross-Bedded Sandstone (TS)	13.5	68.1	59.2
Coarse Sandstone with Mud Drapes (CSM)	0.7	0	0
Very Fine Sandstone (VFS)	69.5	24.4	3.2
Massive Sandstone (MS)	3	3.7	12.5
Siltstone/Mudstone (MUD)	12.1	0	0
Limestone (LS)	0	0	0

Facies SC and TS are the facies most likely to be whitened, but whitened rock still does not make up the bulk of these facies. In fact, only 23.8% of facies TS and 49.3% of facies SC is whitened and the remainder is red or pink. Whitening mostly occurs at the base and close to the top of the fining upward sequences, especially if mudstones are present at the top. At the bases of sequences whitening usually occurs in facies SC and TS and near the top of the sequence it usually occurs in facies VFS or MS directly under facies MUD. The mudstone facies make up only 9% of the measured sections yet 64% of the whitened strata are concentrated directly above and below these layers. Figure 34 shows two idealized fining upward sequence with the generalized location of whitened strata.

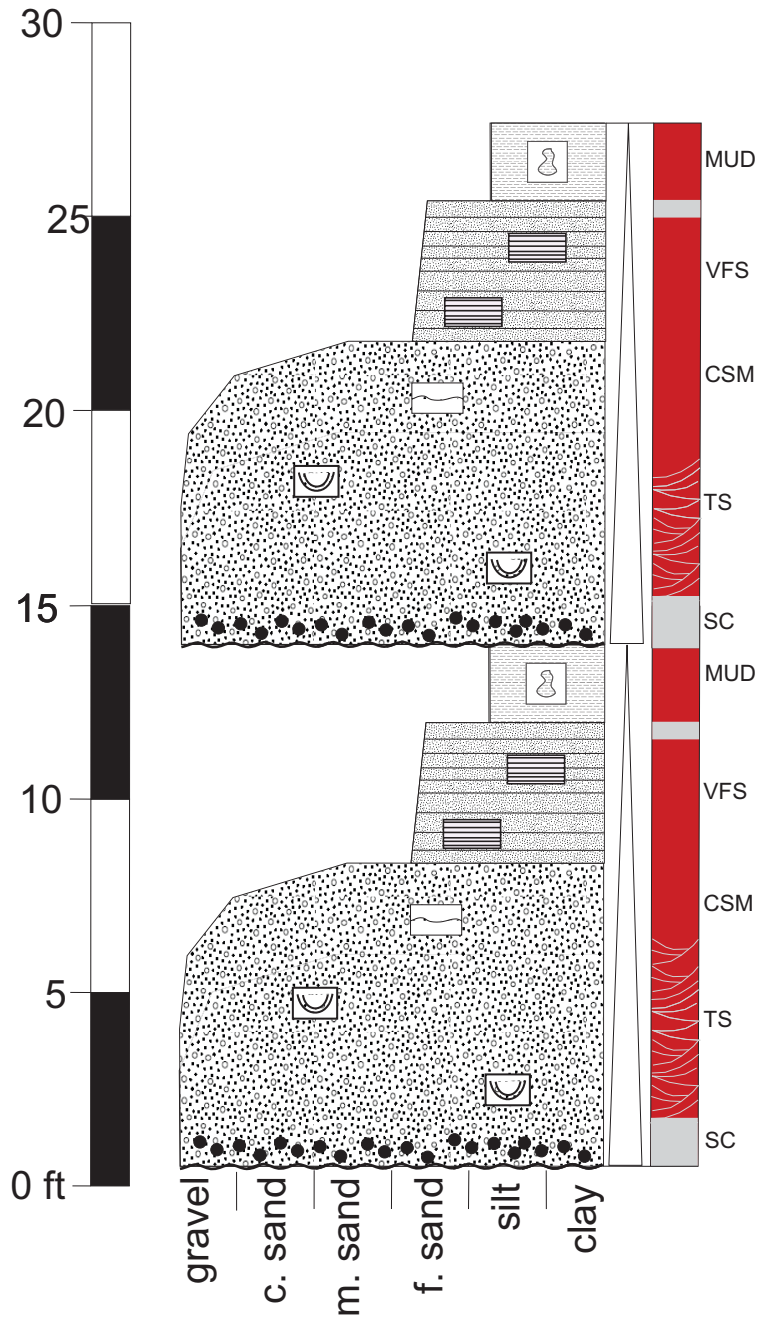


Figure 34. Idealized fining upward sequences showing the distribution of whitening commonly observed in outcrop. Refer to Figure 15 for symbols

Whitened strata and the abundance of channel sandstone facies follow a pattern geographically. The percent of whitened rock in the seven measured sections decreases to the north. The outcrops at southern sites consist of about 20 percent whitened rock, decreasing to about 9 percent at the northernmost field site. Most whitened strata are in channel sandstone facies SC and TS and these facies also decrease in abundance to the north.

Table 11. Percent of whitened strata at each outcrop

Location	% White	% of Outcrop that is composed of Facies SC or TS
Hall Ranch	20.3	65.8
Devil's Backbone	20.7	61.4
Bobcat Ridge	14.4	40
Blue Sky	14.3	41.2
Roadcut Hwy 34	11.7	43.6
Dixon Cove	15.2	55
Owl Canyon	9.2	15.6

When outcrops are broken down into a top, middle, and bottom section there are no patterns in the amount of whitening between sections. The top section is considered to be from the top of the formation at the Ingleside contact to 50 feet below the Ingleside contact. The middle section starts 50 feet below the Ingleside contact and ends 100 feet below the Ingleside contact. The bottom section starts 100 feet below the Ingleside contact. Results are shown below in Table 12.

Table 12. Percent of strata whitened when outcrops are divided into vertical sections

Outcrop Location	% Whitened in Bottom Section	% Whitened in Middle Section	% Whitened in Top Section
Hall Ranch	9.9	9.1	34.7
Devil's Backbone		6.7	27.6
Bobcat Ridge		10.0	15.7
Blue Sky		13.8	14.3
Roadcut 34	8.9	20.4	7.9
Dixon Cove	15.1	20.9	8.3
Owl Canyon	13	9.2	4.8

3.4 PETROGRAPHIC ANALYSIS

Petrographic analysis of samples representative of the lithology of the Fountain Formation was used to quantify the composition of the formation. Of all points counted 58.7% were framework grains, 35.7% were cement, 4.7% were porosity, and 0.9% were matrix. Several important observations were made during petrographic analysis. The first was that the degree of feldspar alteration is much higher in whitened strata than non-whitened strata. The second was that carbonates and clay are the dominant cements and clay cement is more common in whitened strata than non-whitened strata. The third was that the ratio of kaolinite cement to other clay cements is higher in whitened strata than non-whitened strata.

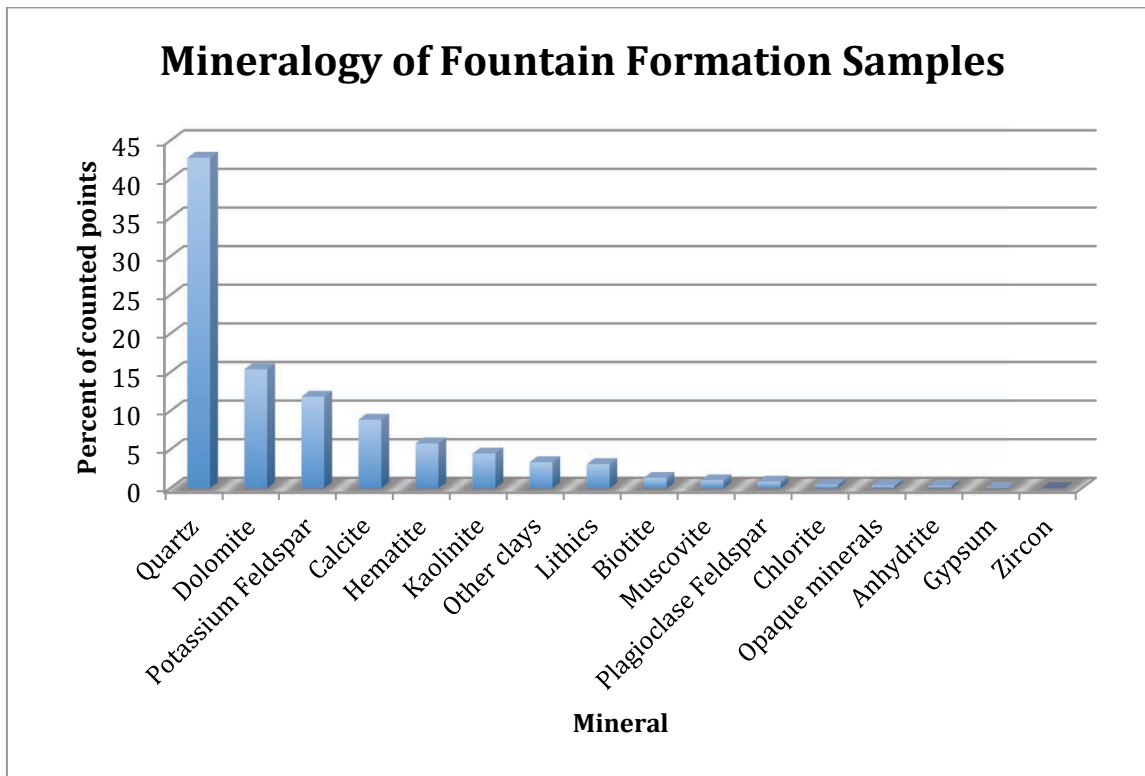


Figure 35. Composition of all minerals counted including grains, cement, and matrix n=13,098

Most of framework grains counted were quartz (69.0%), potassium feldspar (19.4%), lithic fragments (5.0%), biotite (2.2%), muscovite (1.7%), or plagioclase feldspar (1.4%). Other detrital grains included opaque minerals, chlorite, and zircon. A breakdown of grain mineralogy in each facies is shown below in Table 6.

Sandstones in the Fountain are angular to rounded subarkosic and arkosic arenites and grain size ranges from very coarse to very fine. Sandstone facies contain between 23.4 to 39.5 percent cement, including carbonates, hematite, and clays. The most common grains in the sandstone facies are quartz. Most quartz is monocrystalline although some polycrystalline quartz is present. The polycrystalline quartz exhibits undulose extinction and is most common in the coarser grained sandstones (Fig. 36).

Most feldspar is in the alkali group and almost all exhibits polysynthetic twinning. A small percent of plagioclase feldspar is present and is much more altered than the alkali feldspar and in many cases can barely be recognized. Of those that can be identified 76% of plagioclase feldspars and 61% of alkali feldspar have been partially altered to clay and in some instances calcite. Feldspar alteration is much more common in whitened rock than non-whitened rock. The ratio of altered to unaltered feldspar is 2.9 in whitened strata, 2.5 in strata with white laminations, and 0.7 in non-whitened strata. Alteration is also higher in certain facies with the highest being in facies SC and TS and the lowest being in facies MUD. Lithic clasts are common and consist mostly of plutonic and clastic sedimentary clasts. Biotite and muscovite are present in small amounts in most samples. Opaque minerals are present in some samples and usually consist of magnetite. Opaque minerals are much more common in non-whitened rock.

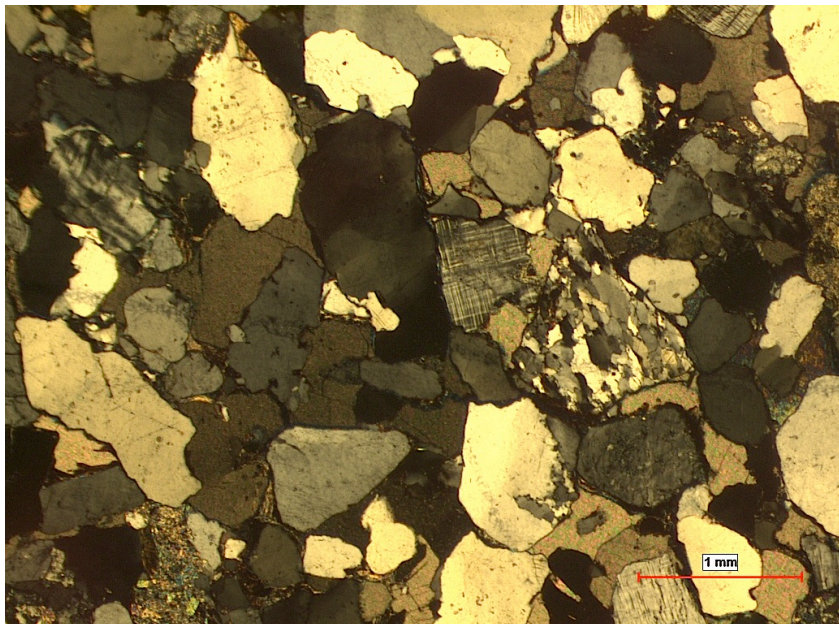


Figure 36. Quartzite clast in sample A1 (facies CSM) from the Hall Ranch study site

Mudstone samples are composed of dark silt and clay size material, quartz and feldspar sand grains, biotite, and very high amounts of cement. The percentage of cement in mudstones is 57.5%; 60% of it is carbonate cement and 40% is hematite cement. Over 98% of carbonate cement is large rhombic dolomite crystals and hematite cement fills the remaining pore space (Fig.37).

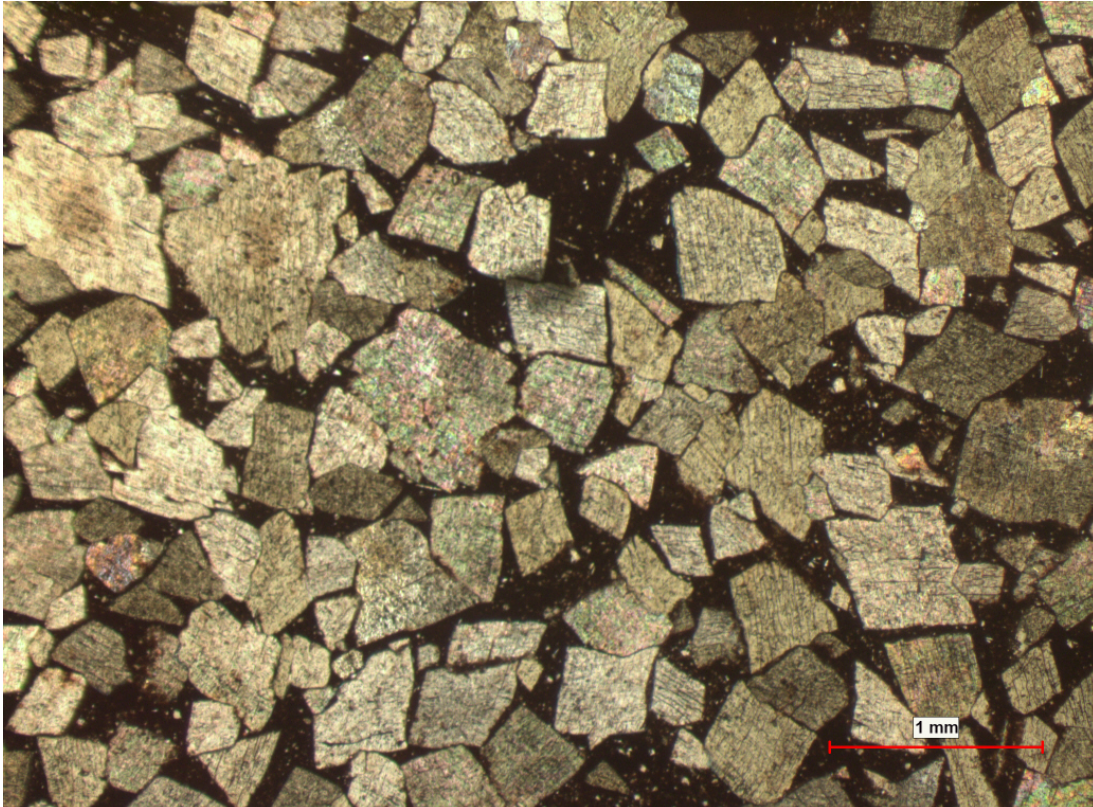


Figure 37. Large dolomite crystals surrounded by hematite cement in a carbonate nodule, sample B13 (facies MUD) from the Devil's Backbone study site

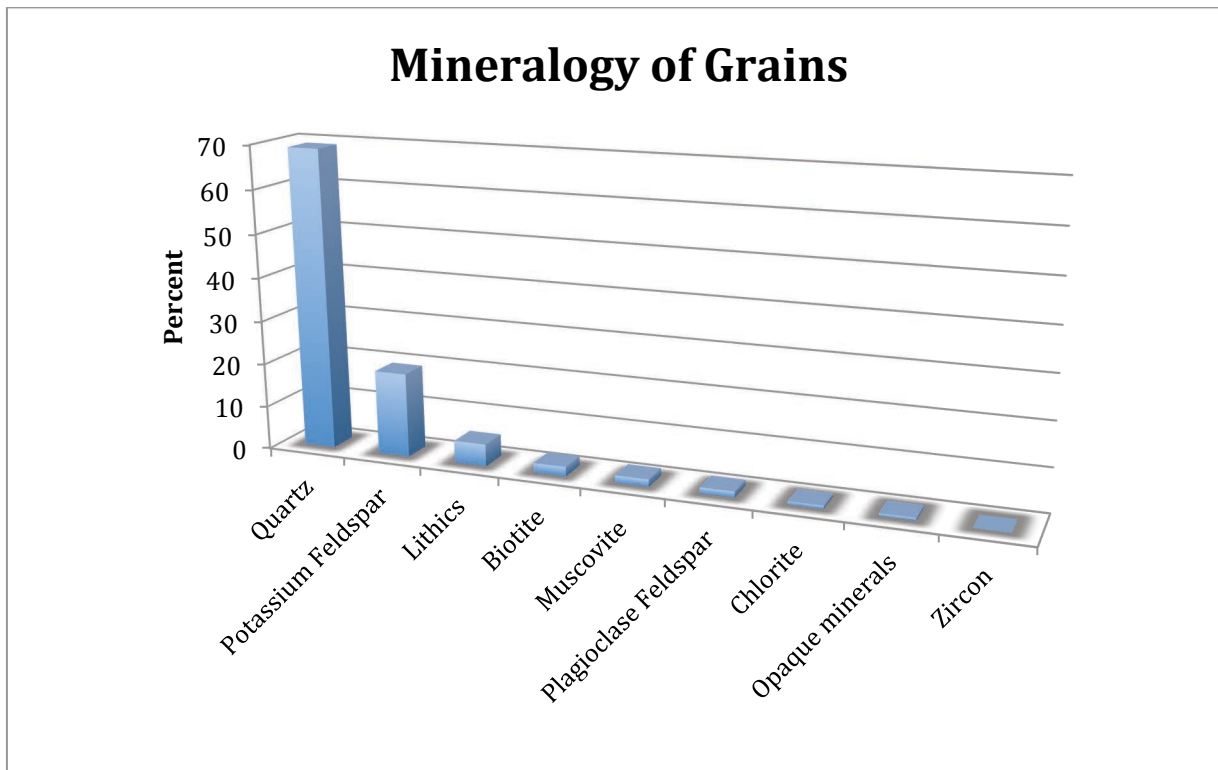


Figure 38. Composition of all grains counted n=8,087

Table 13. Mineralogy of grains in each facies

Mineral	Facies SC	Facies TS	Facies VFS	Facies MS	Facies CSM	Facies MUD
Quartz	63.0	67.1	75.1	75.1	59.3	55.8
Potassium Feldspars	24.5	22.0	16.8	12.2	22.9	13.5
Plagioclase Feldspars	1.4	1.8	1.1	1.8	2.1	1.0
Lithics	7.9	5.5	3.3	1.0	7.8	7.1
Biotite	1.2	0.9	1.2	4.0	3.8	14.1
Muscovite	1.5	1.9	0.7	2.0	2.3	6.2
Chlorite	0.3	0.3	1.1	3.2	0.2	0.4
Opaque Minerals	0.3	0.4	0.6	0.8	1.7	2.0
Zircon	0.0	0.0	0.1	0.0	0.0	0.0

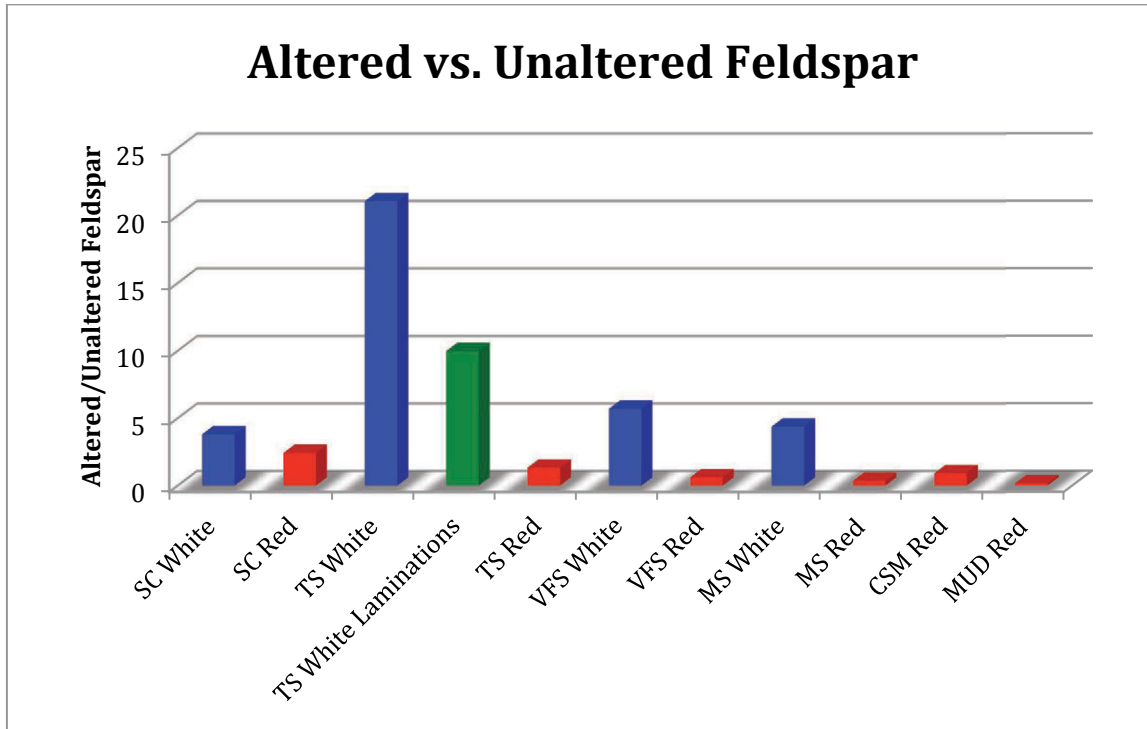


Figure 39. Feldspar alteration in various facies

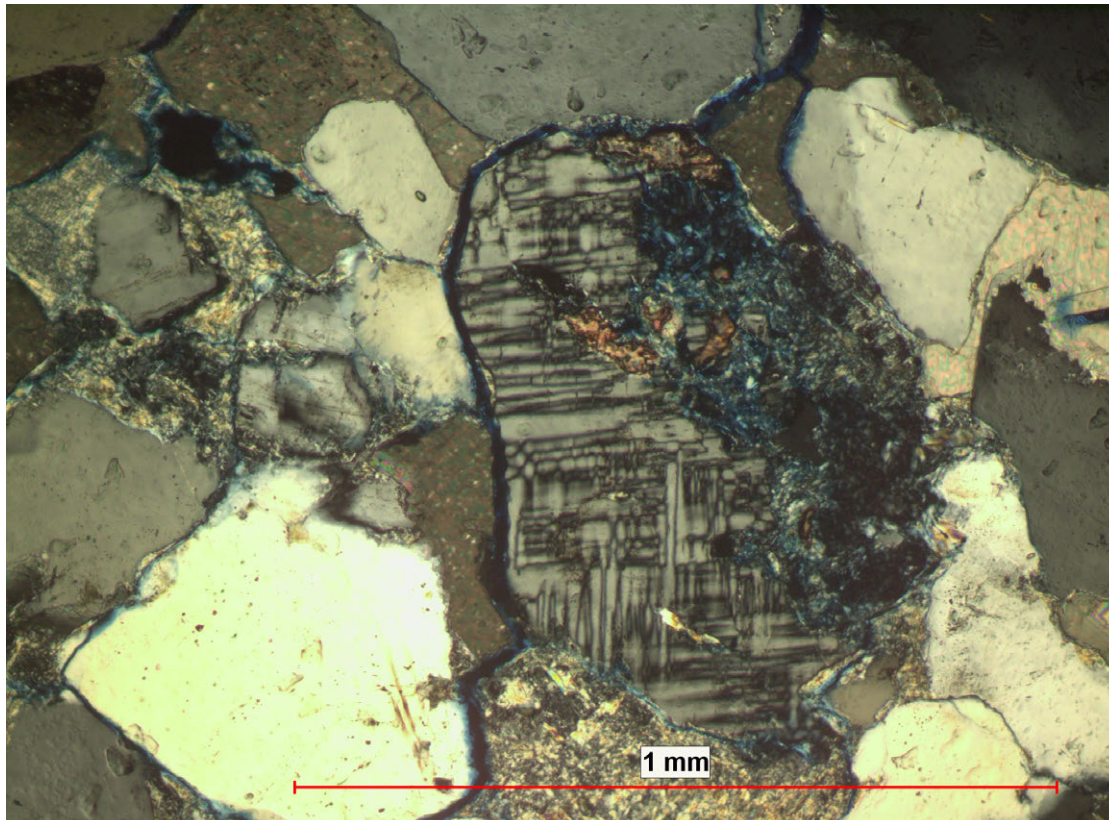


Figure 40. Diagenetic alteration of k-feldspar to calcite, kaolinite, illite, and intragranular porosity in whitened sample B14 (facies TS) from the Devil's Backbone study site

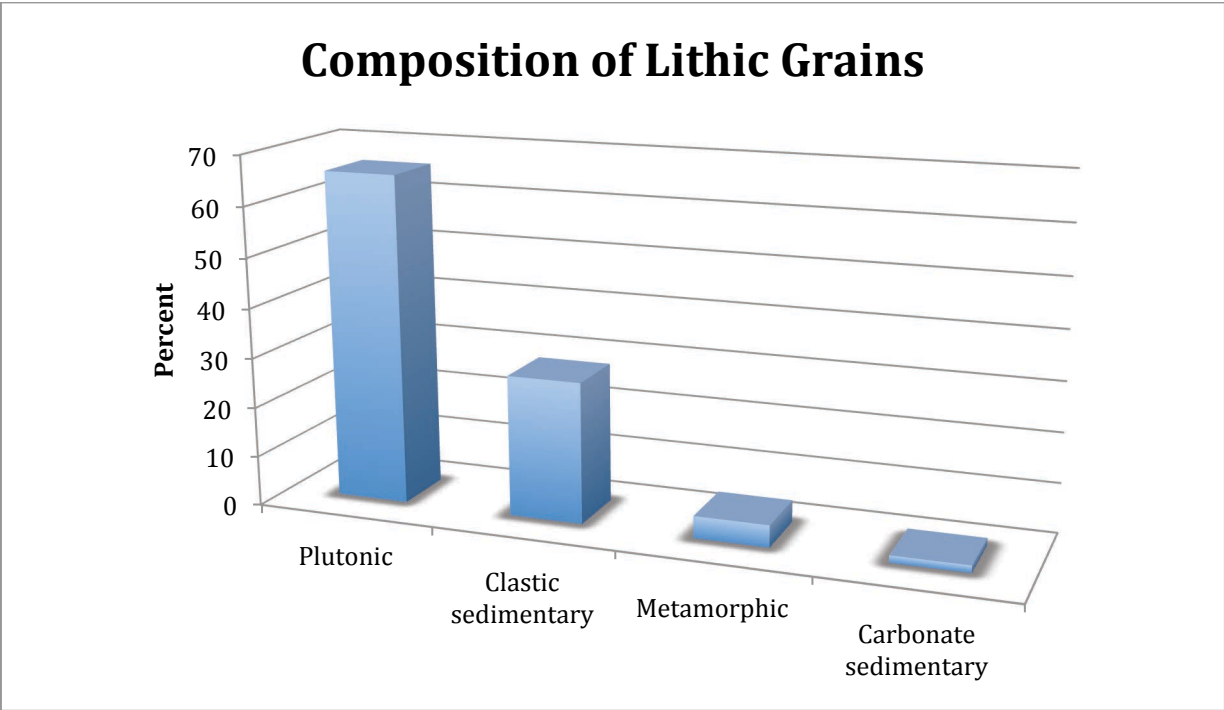


Figure 41. Lithic grain type of all lithic clasts counted n=407

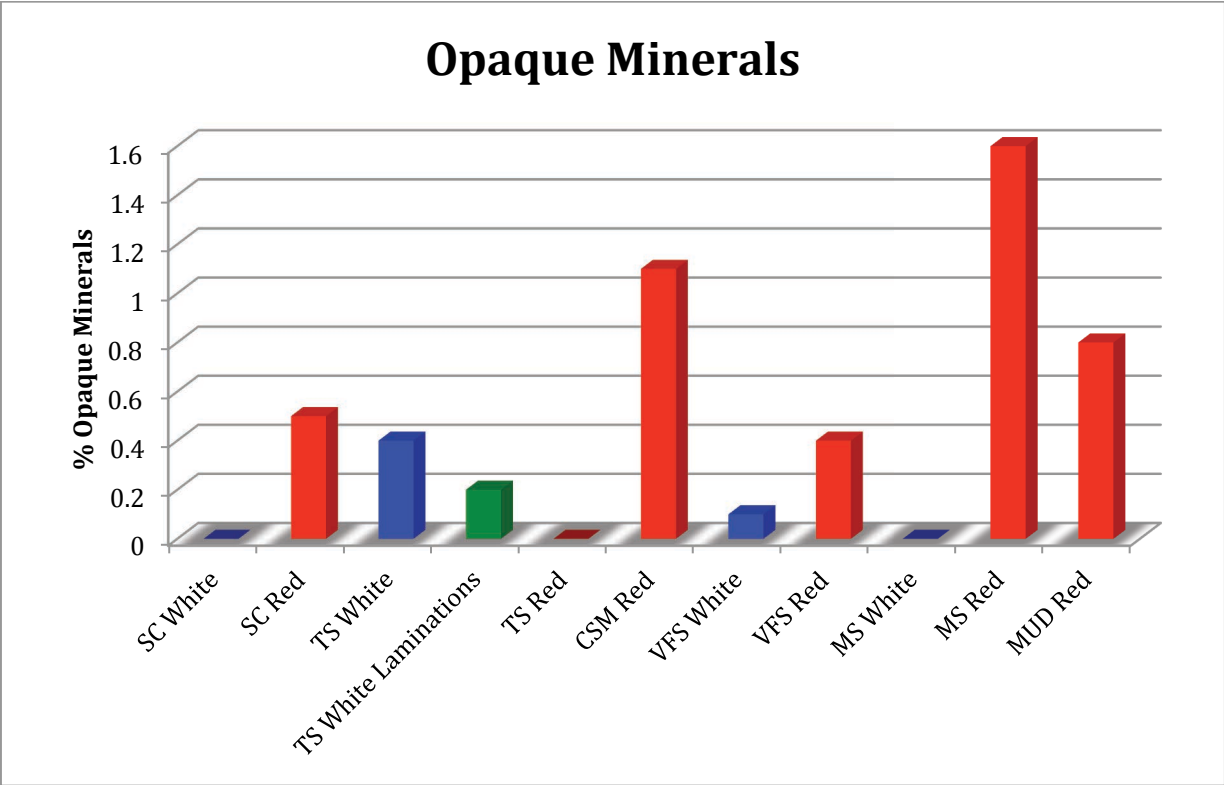


Figure 42. Distribution of opaque minerals in various facies

Cements include dolomite (41.0%), calcite (23.6%), hematite (15.4%), kaolinite (11.3%), other clays (7.2%), and quartz (1.4%). Four types of carbonate cement are present in the samples. The first is a patchy poikilotopic dolomite cement. Clastic grains within it do not show signs of significant compaction and even in colored samples there is no hematite coating on grains in the center of the poikilotopic cement (Fig. 43, 44). The second carbonate cement is a blocky cement and at some outcrops it is calcite and at others is dolomite. It may form rhombic crystals, very commonly replaces clastic grains, and fills fractures in clastic grains (Fig. 45, 46). Clastic grains in this cement show signs of compaction and are coated with hematite. In rare instances hematite cement is also present in the spaces between carbonate crystals and within the cement itself. The third carbonate cement is calcite cement that has partially replaced some of the blocky dolomite cement. In some cases it only replaced the outside rims of the blocky dolomite and is platy, in other cases the blocky dolomite was almost completely replaced. The fourth carbonate cement is a dark microcrystalline dolomite cement that is patchy, seems to have replaced the earlier cements, and is fluorescent. The first three types of carbonate cement are more common in non-whitened rock whereas the fourth type of carbonate cement is almost exclusive to whitened rock.

Hematite cement is abundant in many samples and varies from partial coating of clastic grains to completely filling large pore spaces. Hematite cement is present between grains that had been compacted and exhibit grain-to-grain contact (Fig. 47, 48). Kaolinite and other clay cements are also common in some samples. They are

usually associated with altered feldspars. They may coat grains, completely fill large pore spaces, and replace clastic grains (Fig. 49, 50). Most clay cement fills spaces between grains but some of the larger patches of clay cement are grain shaped and are rimmed with hematite cement. Some patches of clay cement have mild fluorescence. Clay cement, especially kaolinite, is much more common in whitened rock (Fig. 50, 51). Quartz cement is rare and consists of overgrowths on quartz grains.

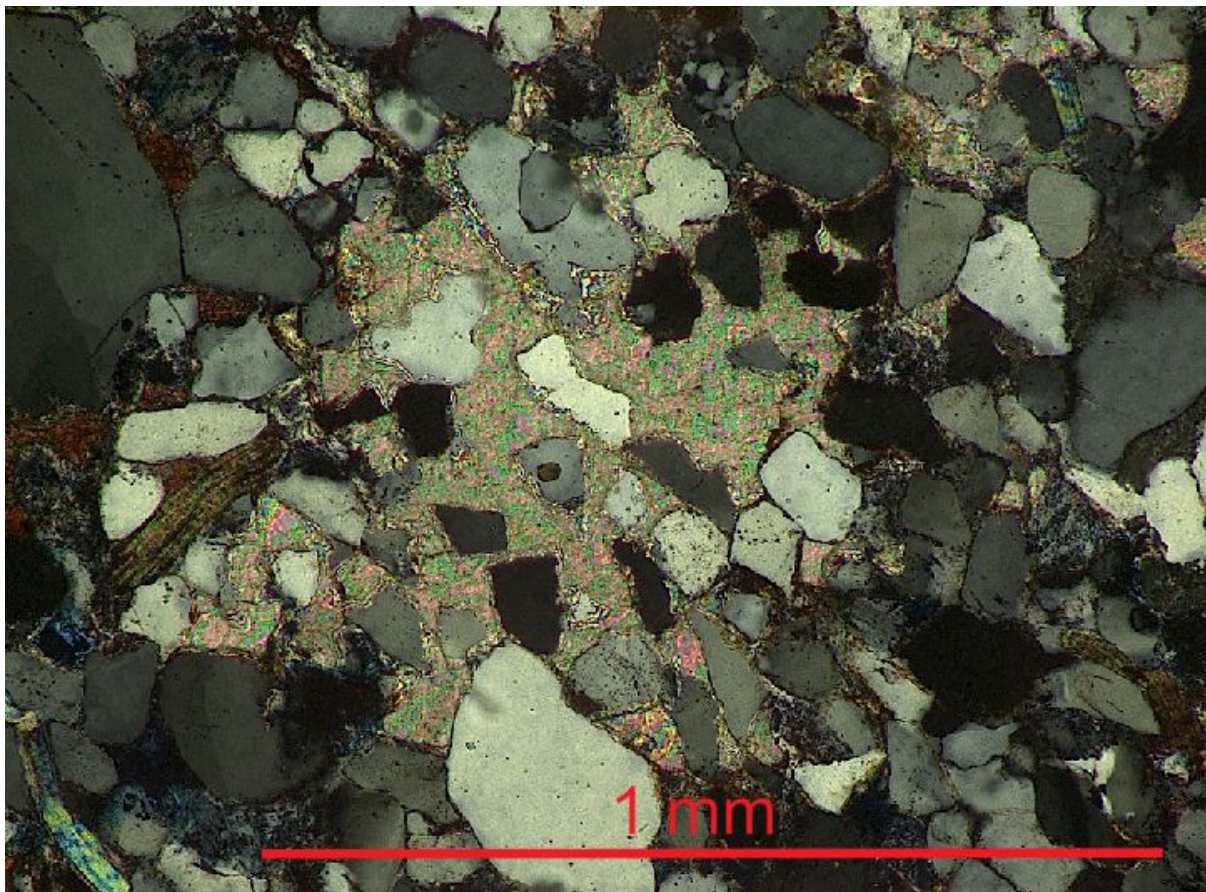


Figure 43. Poikilotopic carbonate cement in non-whitened sample A5 (facies VFS) from the Hall Ranch study site

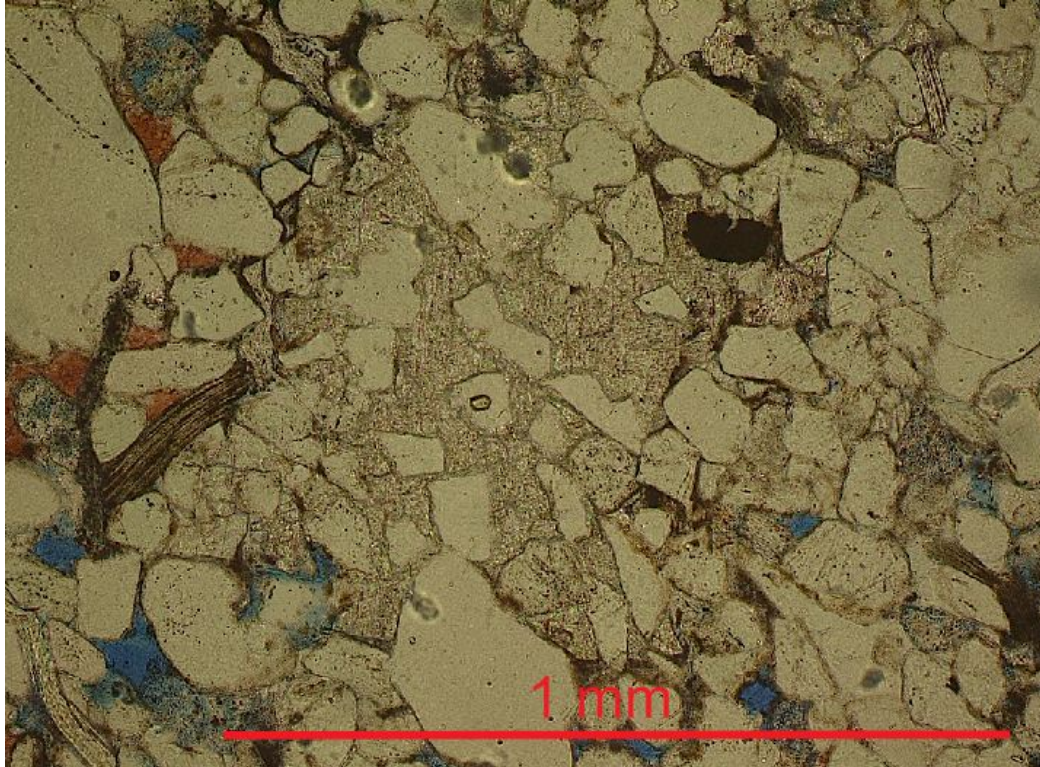


Figure 44. Poikilotopic carbonate cement from Figure 43 in plane polarized light. Note that grains within the patch of cement are not rimmed by hematite cement

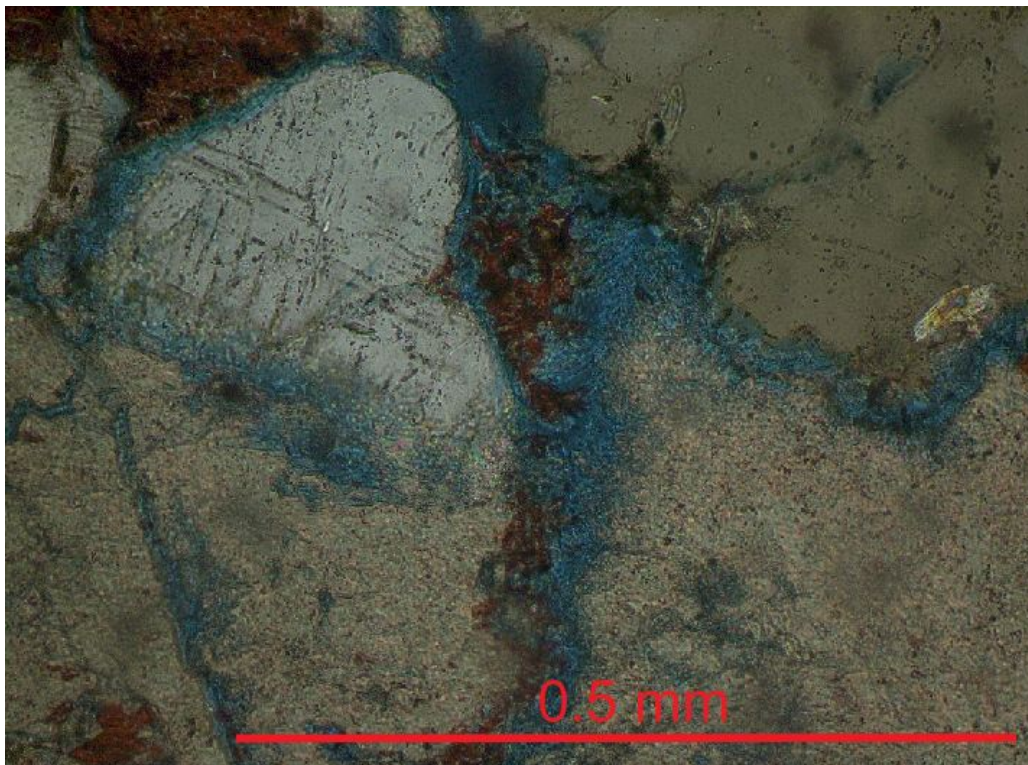


Figure 45. Dolomite cement replacing clastic grains and calcite replacing outer edge of dolomite cement in whitened sample D14 (facies SC) from the Dixon Cove field site

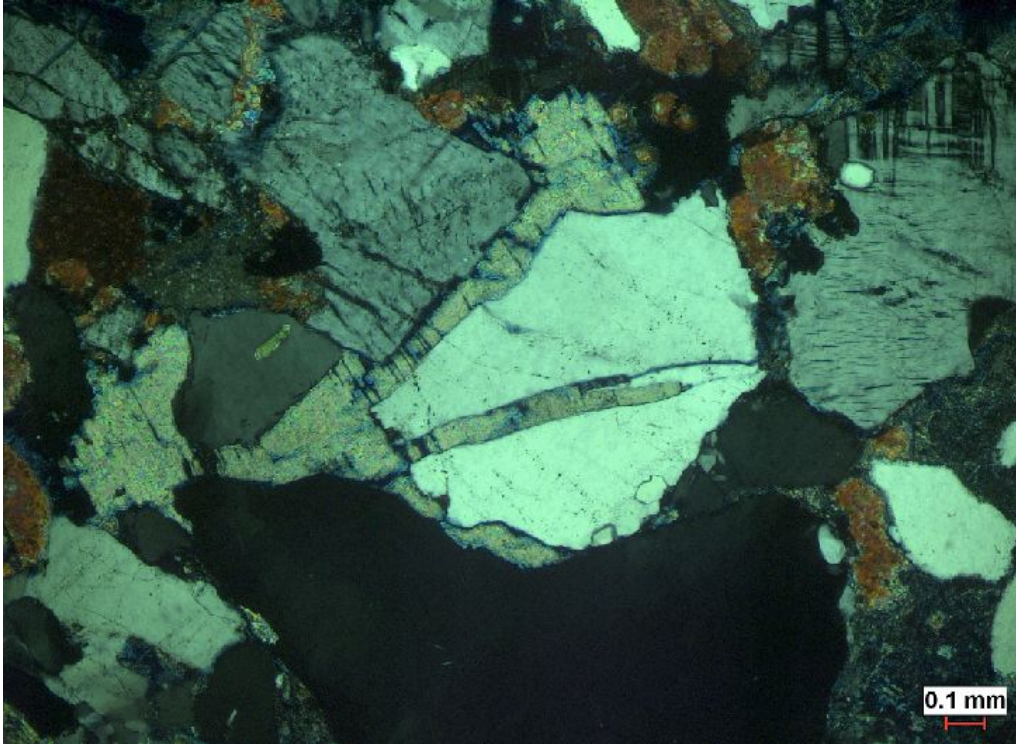


Figure 46. Blocky dolomite cement filling a fracture in a clastic grain in non-whitened sample C13 (facies TS) from the Blue Sky Trail study site

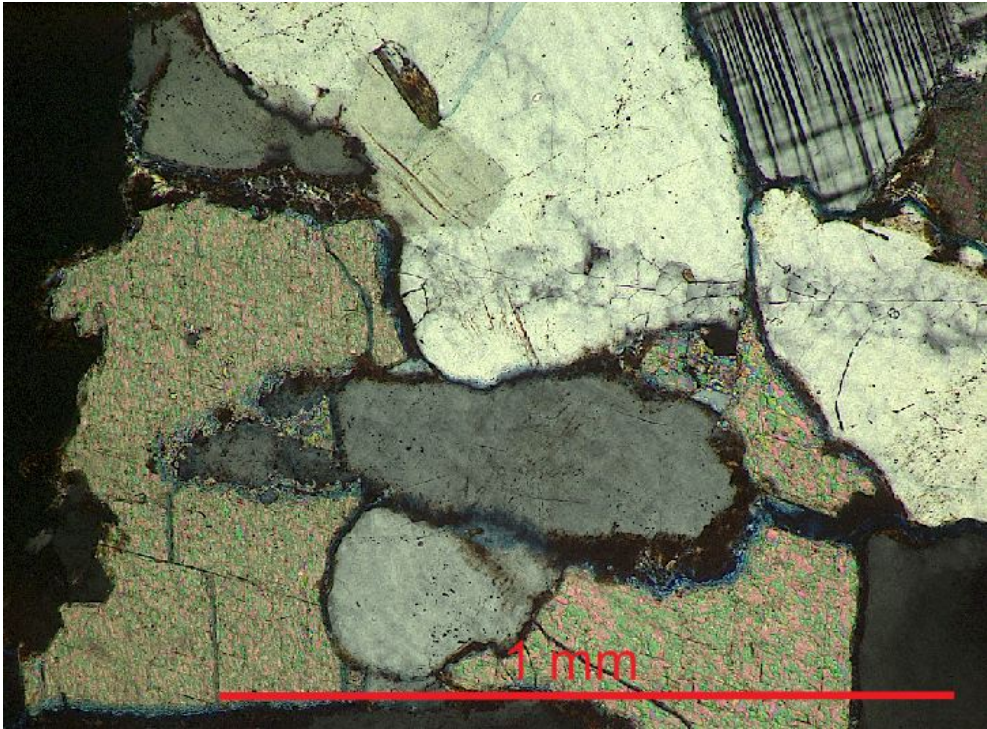


Figure 47. Blocky dolomite cement replacing a clastic grain in non-whitened sample A1 (facies CSM) from the Hall Ranch study site. Note that hematite cement coats the clastic grains and is between compacted grains

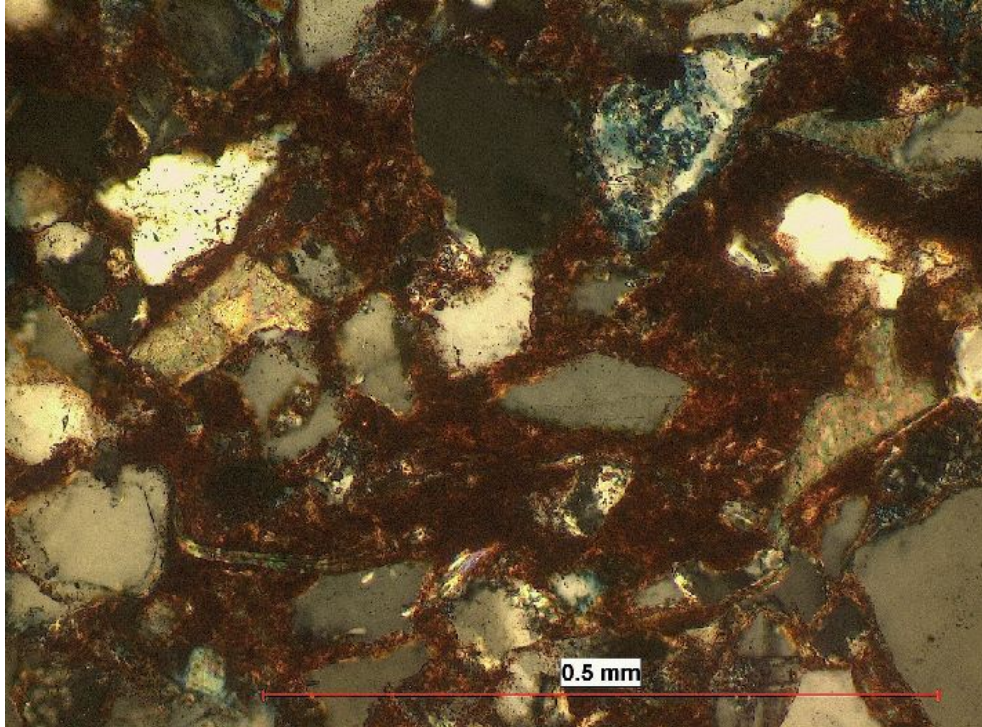


Figure 48. Hematite cement filling pores in non-whitened sample B8 (facies TS) from the Devil's Backbone study site

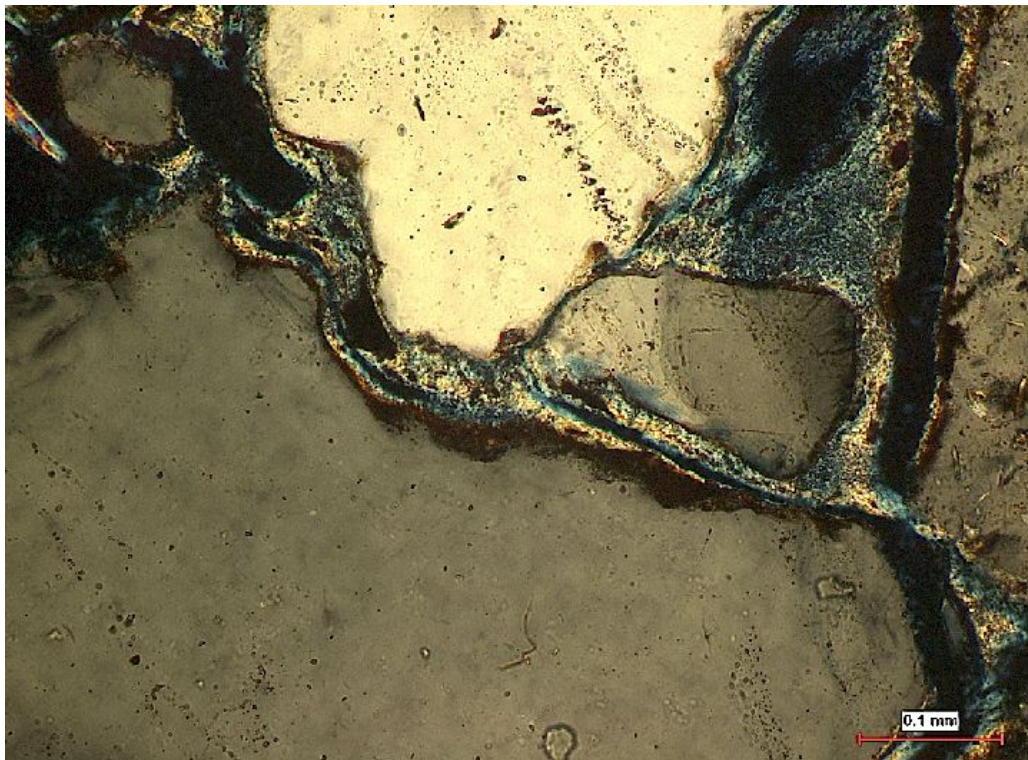


Figure 49. Clay cement filling pore spaces of non-whitened sample D2 (facies CSM) from the Dixon Cove study site. Note that hematite cement coats grains and clay cement coats hematite

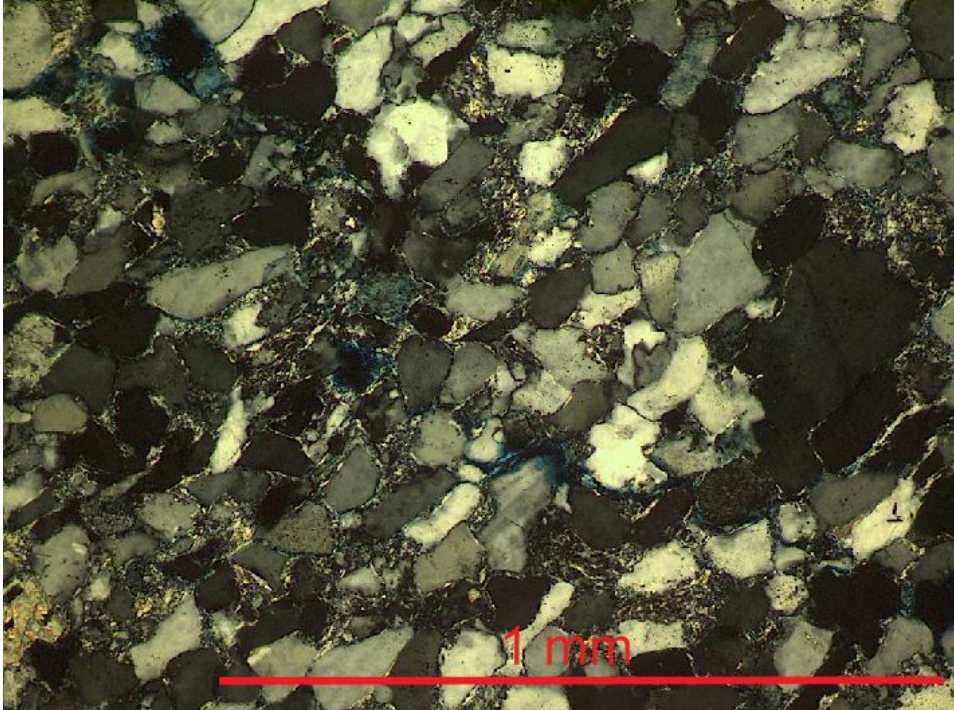


Figure 50. Clay cement in whitened sample A3 (facies VFS) from the Hall Ranch study site

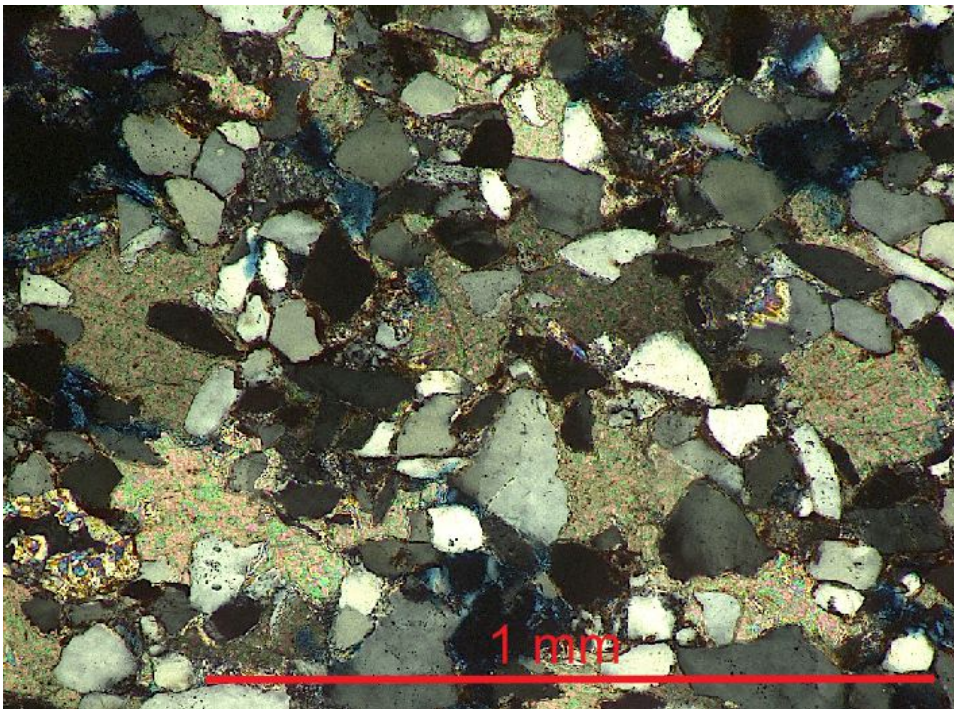


Figure 51. Dolomite cement in non-whitened sample A4 (facies VFS) from the Hall Ranch study site. This sample was taken from the same bed as the sample shown above in Fig. 50 but the bed changed laterally from white to red. The samples were less than twenty feet apart but major differences exist in the compaction, cement type, and amount of hematite present

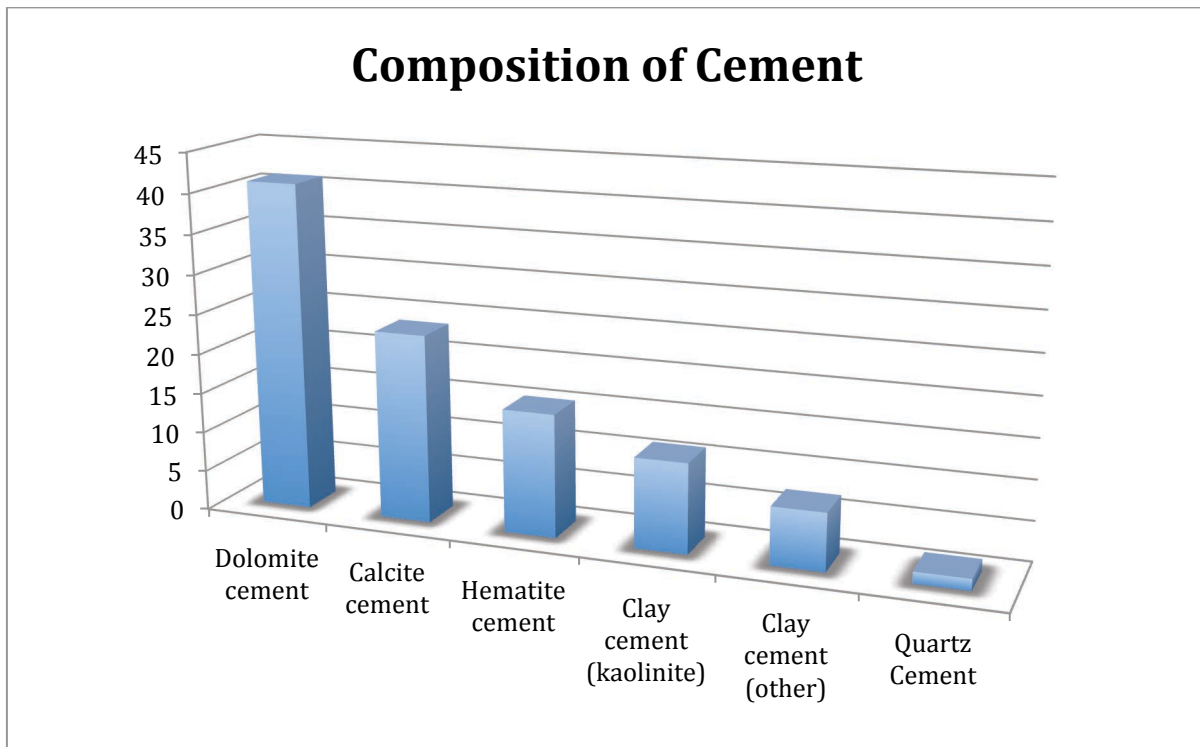


Figure 52. Composition of all cement counted

Table 14. Percentage of each facies composed of cement

Facies	% Cement
SC White	23.7
SC Red	32.5
TS White	20.4
TS White Laminations	23.6
TS Red	31.6
CSM Red	30.3
VFS White	42.0
VFS Red	37.6
MS White	24.2
MS Red	44.8
MUD Red	57.5

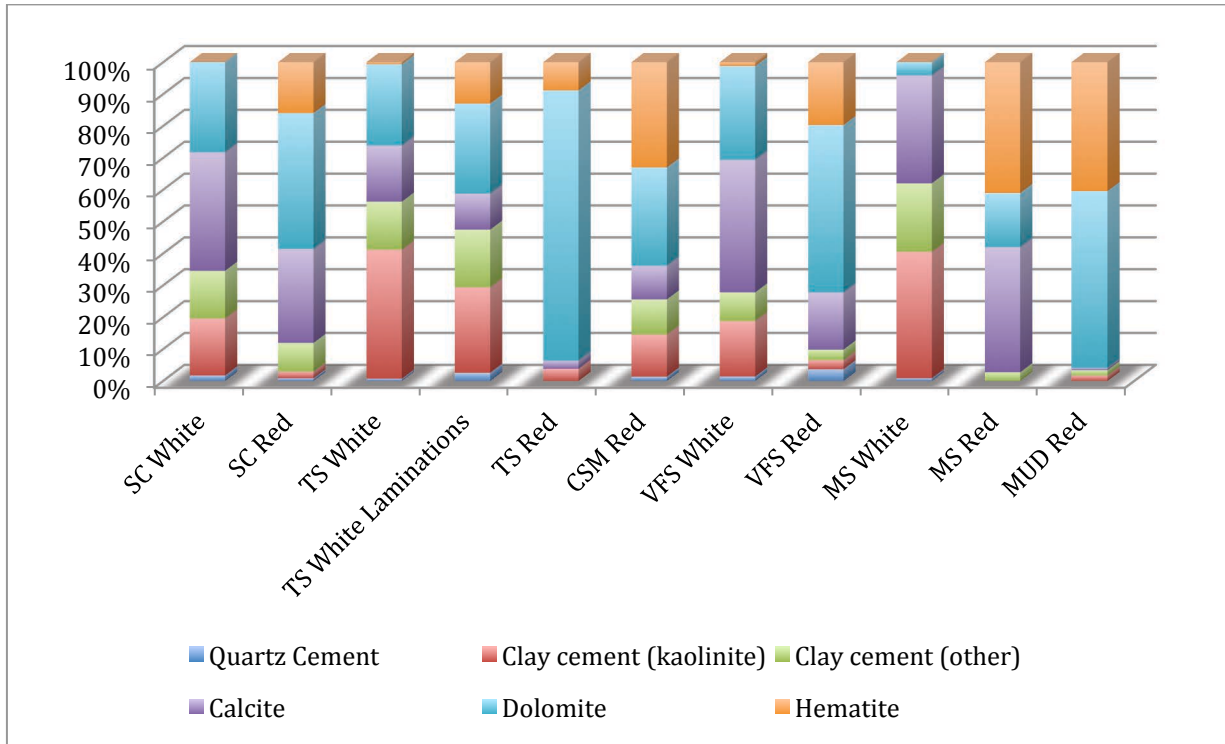


Figure 53. Cement type in each facies

Porosity based on petrographic analysis is an average of 4.7% but is highly variable between facies. Samples from facies SC and TS have the most porosity at 7.1% and 6.6% respectively, samples from facies VFS have an average porosity of 4.1%, and samples from all other facies have less than 3% porosity. Samples from facies MUD only have 0.8% porosity. With the exception of facies VFS, samples of whitened rock have on average slightly higher porosity than samples of non-whitened rock, but the difference is often less than one percent.

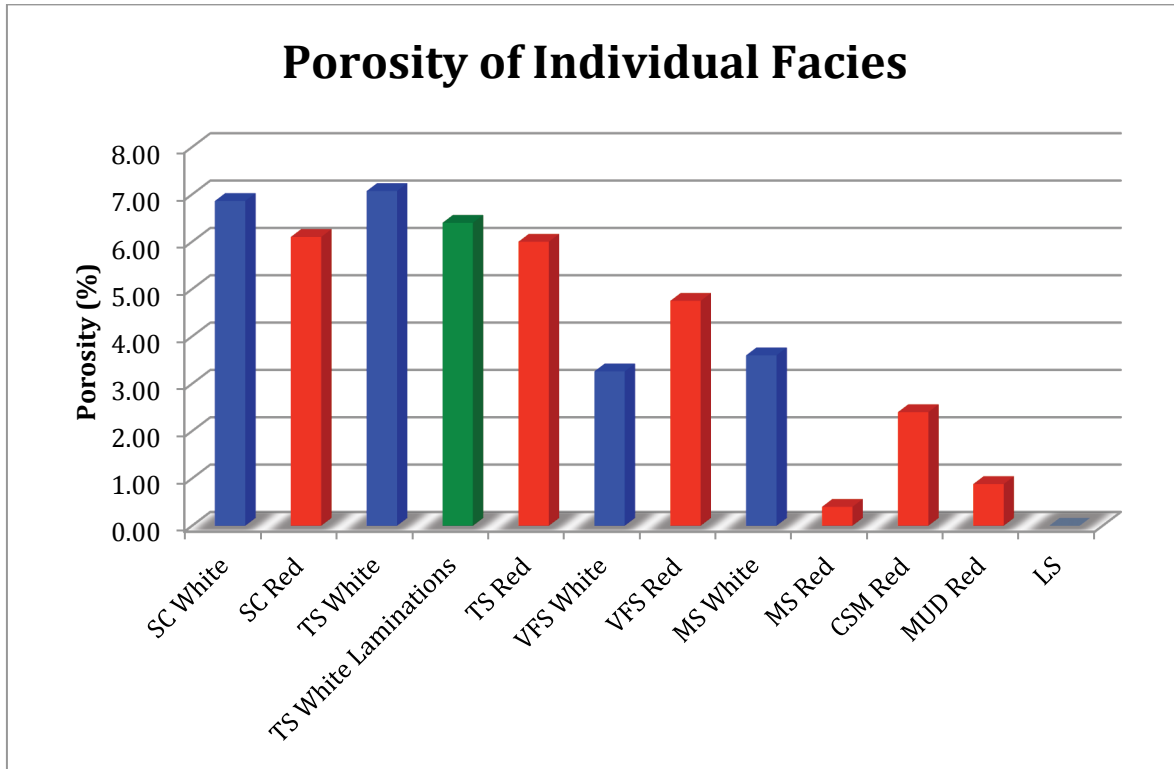


Figure 54. Porosity in various facies

Other minor compositional differences between whitened and non-whitened rock are listed in Table 15. The most apparent is the lower percentage of quartz clasts in non-whitened samples.

Table 15. Mineralogical differences in whitened and non-whitened samples

Mineral	White Samples	Samples with White Laminations	Non-whitened Samples
% Anhydrite	0.2	0.0	0.2
% Biotite	0.8	0.8	2.0
% Calcite	11.1	2.9	5.6
% Chlorite	1.0	0.3	0.1
% Dolomite	8.9	7.2	20.5
% Gypsum	0.1	0.0	0.0
% Hematite	0.2	3.3	11.5
% Kaolinite	7.6	7.2	1.6
% Lithics	2.9	4.3	3.3
% Muscovite	1.1	1.0	1.0
% Opaque minerals	0.2	0.2	0.7
% Other clays	4.3	5.8	2.3
% Plagioclase Feldspar	1.0	1.2	0.7
% Potassium Feldspar	12.7	17.4	10.7
% Quartz	47.9	48.3	40.2
% Zircon	0.1	0.0	0.1

Mineralogical variations exist geographically among outcrops. Feldspar alteration is fairly consistent among outcrops with the one exception of the Owl Canyon site where it is over three times more prevalent than the average of the samples from the other four sites. The amount of kaolinite cement at this site is also roughly three times higher than the average of the other sites. The degree of calcite and dolomite cement also differs from site to site and is shown in table 16 below.

Table 16. Mineralogical differences between outcrops

Site	Altered/Unaltered Feldspar	% Kaolinite	% Calcite	% Dolomite	n
Hall Ranch	2.6	3.8	0.2	8.8	11
Devil's Backbone	2	5	1.4	16.9	8
Blue Sky	3.1	3.4	21.4	0.9	7
Dixon Cove	4.2	1.4	25	12.3	5
Owl Canyon	10.2	11.7	2.2	14.2	6

3.5 FLUORESCENT MICROSCOPY ANALYSIS

Fluorescent microscopy was used to show that bitumen, organic matter, and hydrocarbon inclusions are present in some samples. Bitumen was observed only in samples from rock that had been whitened or was within several inches of whitened rock. Fluorescent dolomite cement is abundant in samples of whitened rock and fluoresces various shades of light blue and yellow (Fig. 55, 56, 57, 58). Under normal light the fluorescent cement is very dark because of small inclusions of organic matter and is usually associated with bitumen (Fig. 59). The fluorescent dolomite cement is microcrystalline and occasionally fills pore spaces between the blocky carbonate cement. Samples of non-whitened rock that were near whitened rock have some fluorescent dolomite cement but it is less common and the fluorescence is much weaker than that in nearby whitened rock. Fluorescent dolomite cement is more abundant and has stronger fluorescence in samples from the Owl Canyon study site than cement in samples from other sites. There are many inclusion-like features with strong fluorescence in the fluorescent cement but they are generally too small to be identified. One bright fluorescent spot, however, was large enough to be identified as a two-phase hydrocarbon inclusion. This inclusion was in fluorescent dolomite cement and abutted against a quartz grain (Fig. 60, 61, 62, 63).

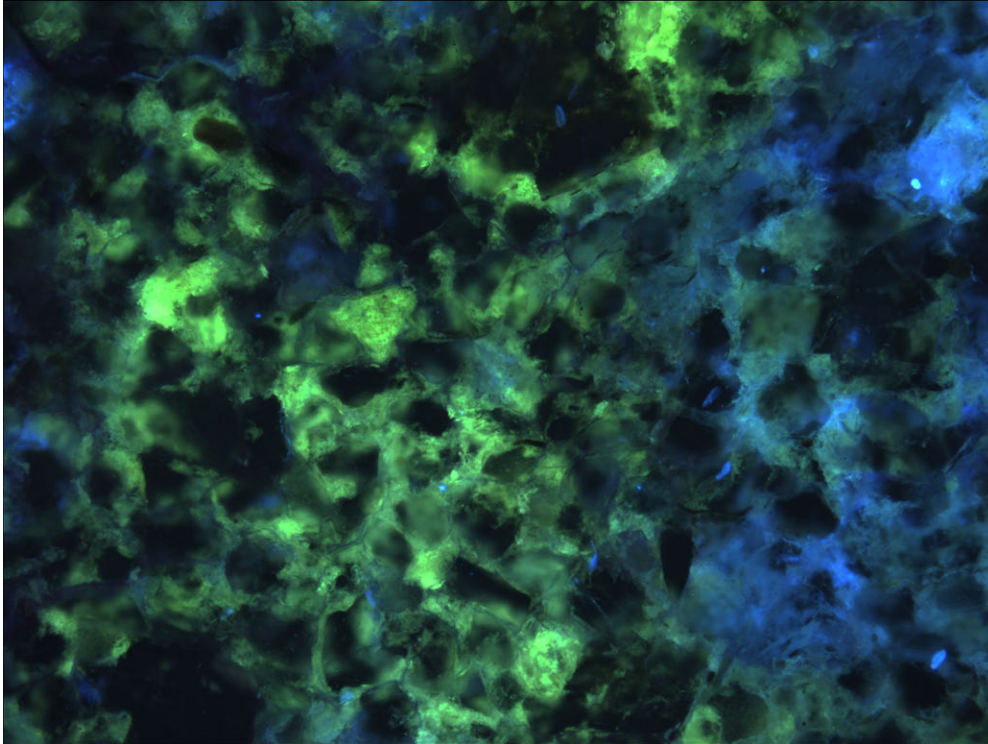


Figure 55. Fluorescent dolomite cement in sample E14 (facies VFS) from the Owl Canyon study site

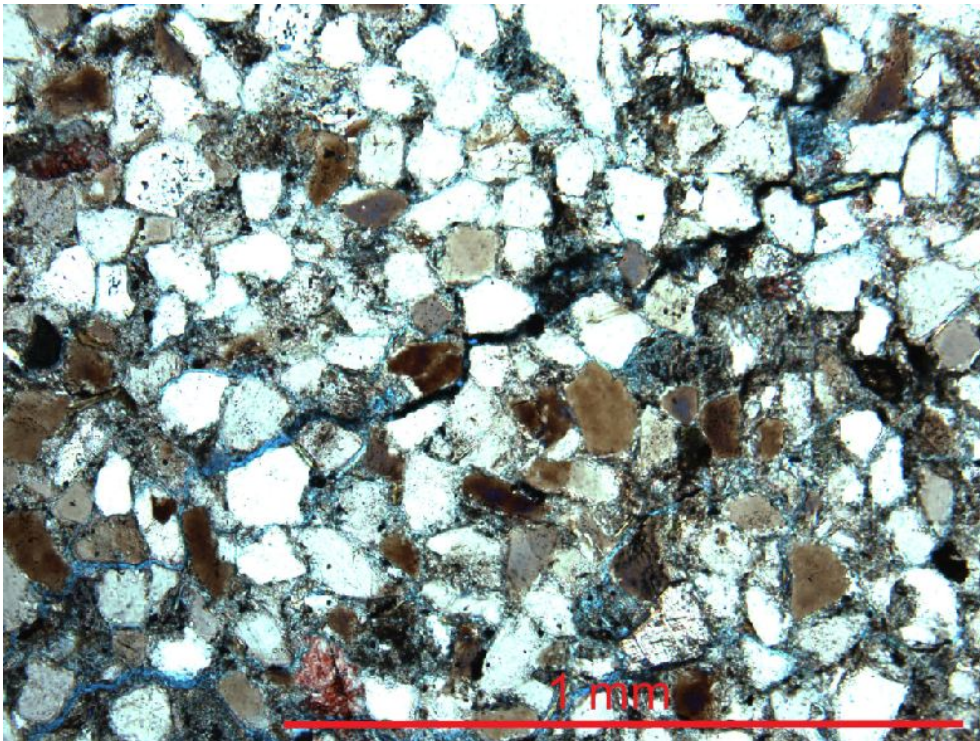


Figure 56. Fluorescent dolomite cement in cross polarized light in sample E14

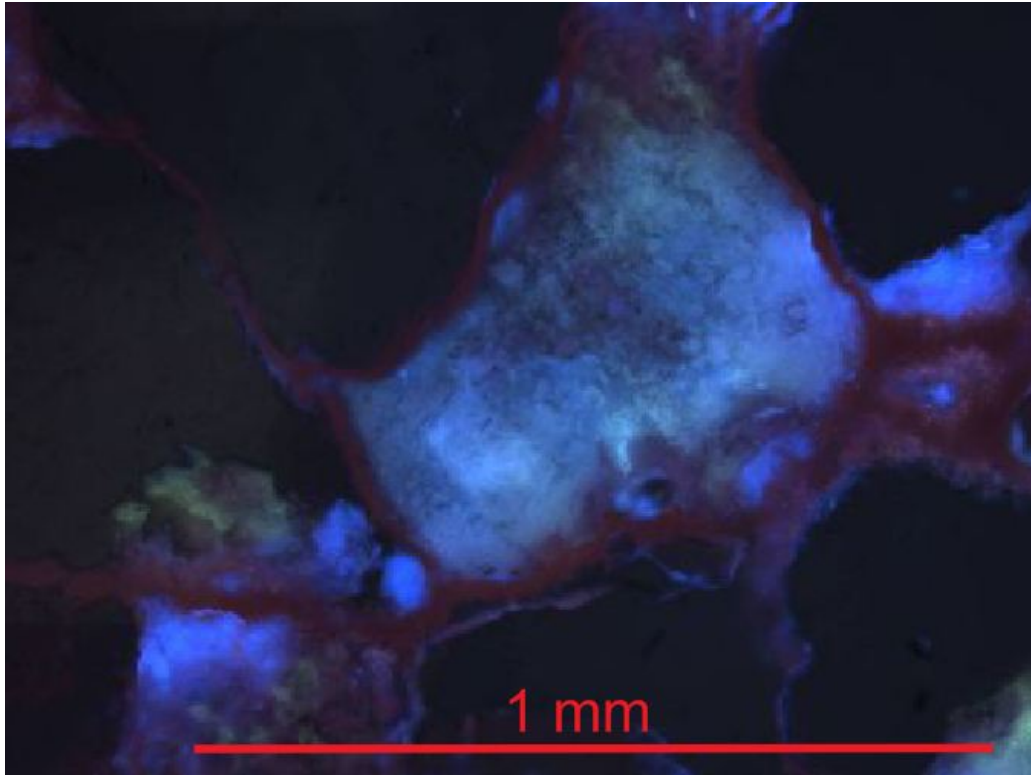


Figure 57. A patch of fluorescent dolomite cement in sample E8 (facies TS) from the Owl Canyon study site

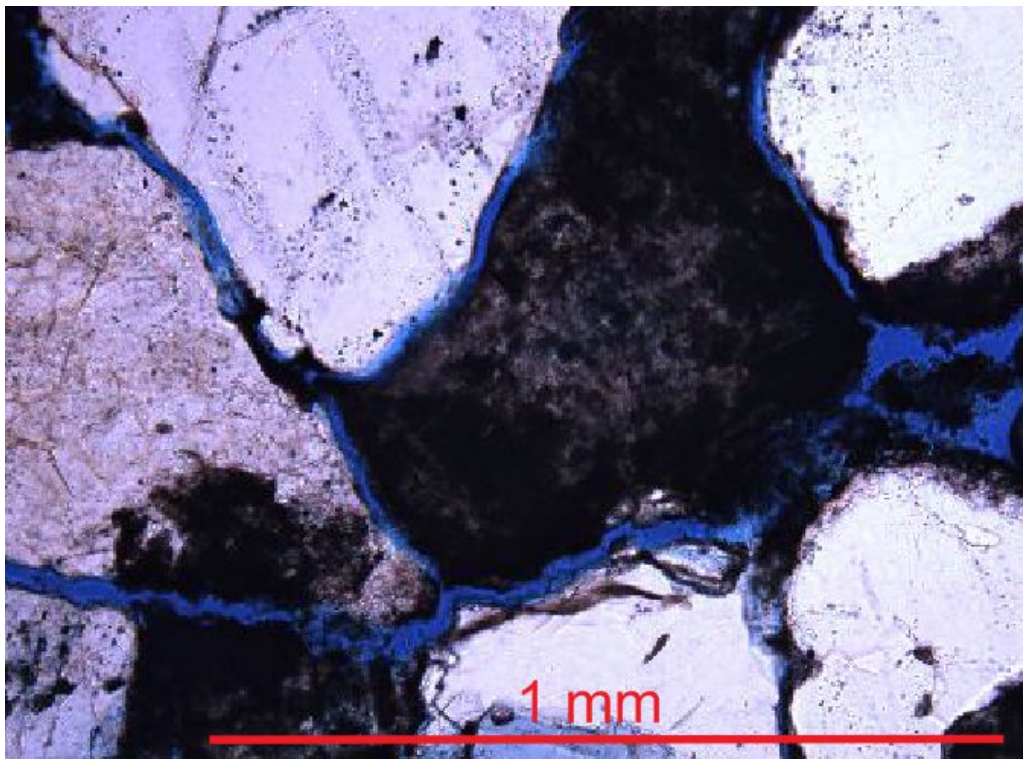


Figure 58. The same patch of fluorescent dolomite cement shown in Fig. 57 in plane polarized light

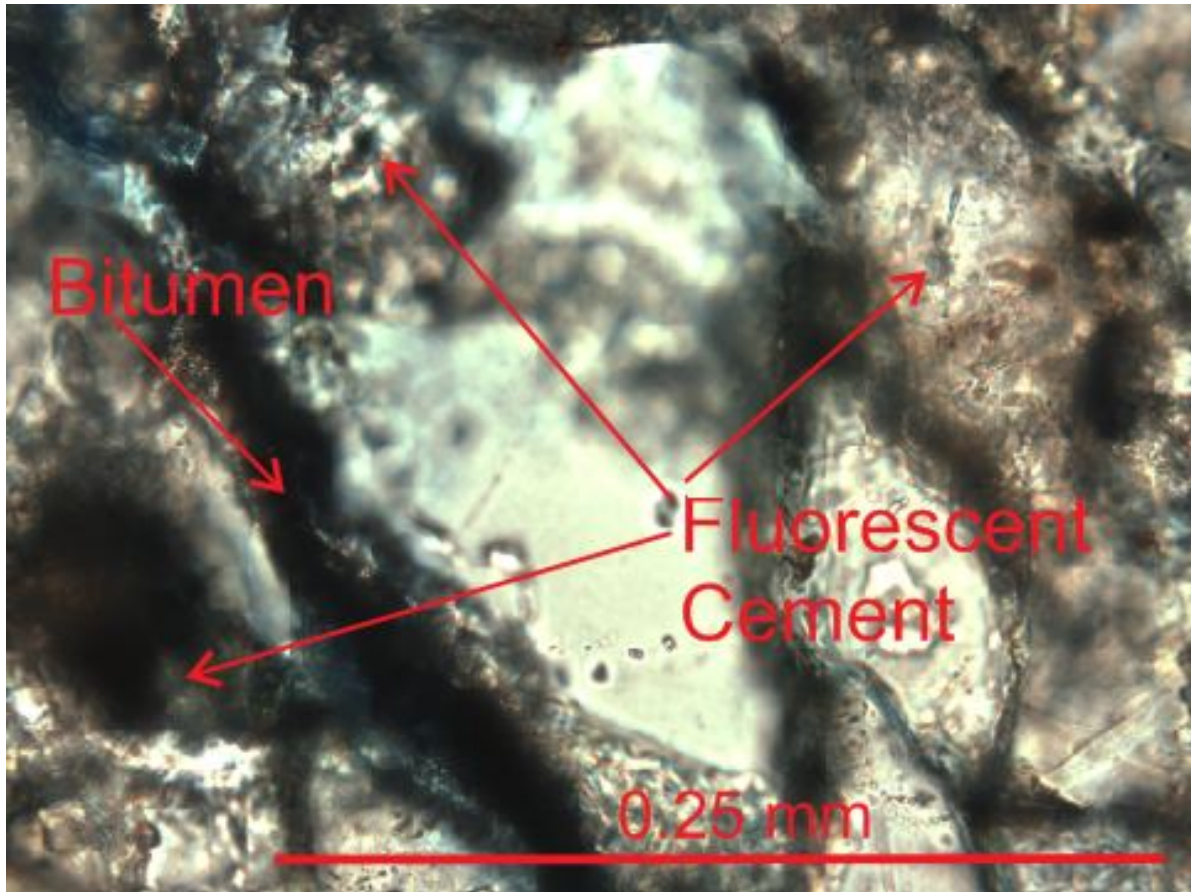


Figure 59. Bitumen and fluorescent dolomite cement in whitened sample D13 (facies MS) from the Dixon Cove study site

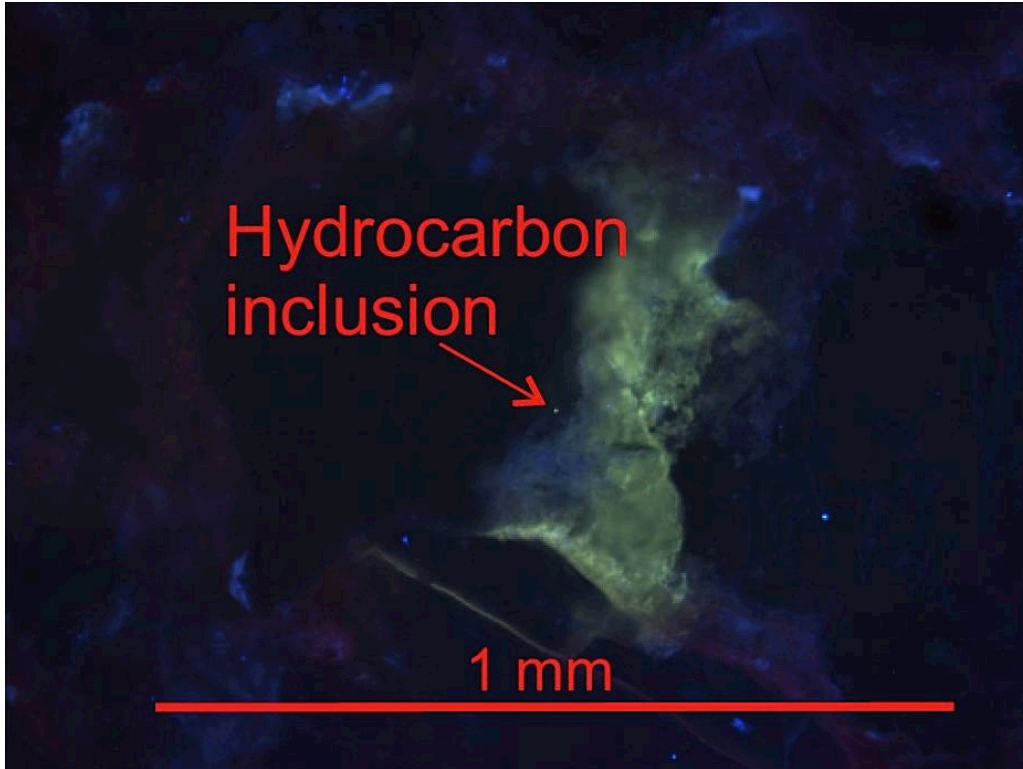


Figure 60. Hydrocarbon inclusion and fluorescent dolomite cement in sample A12 (facies SC) from the Hall Ranch study site

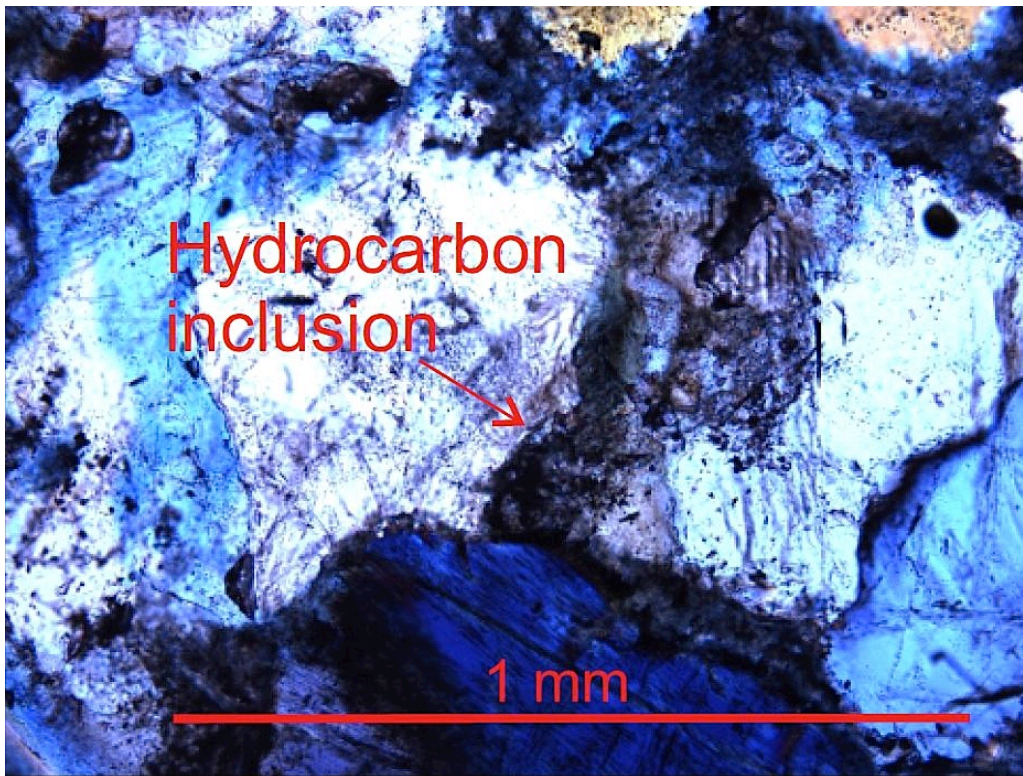


Figure 61. Hydrocarbon inclusion and fluorescent dolomite cement in sample A12 (facies SC) from the Hall Ranch study site in cross polarized light

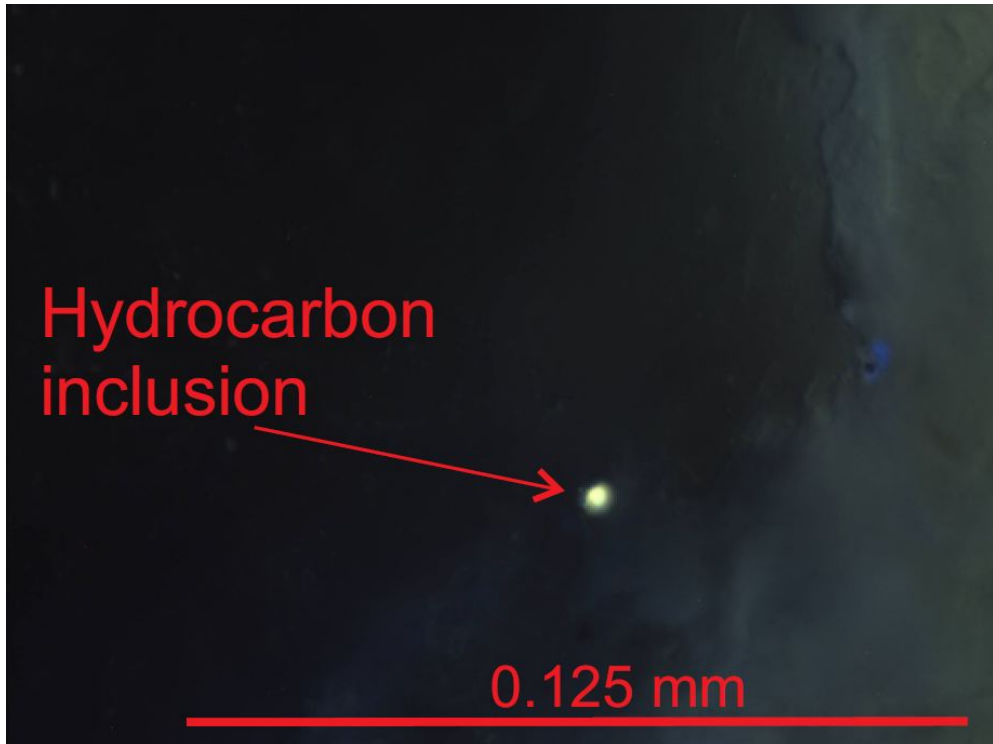


Figure 62. Hydrocarbon inclusion in sample A12 (facies SC) from the Hall Ranch study site

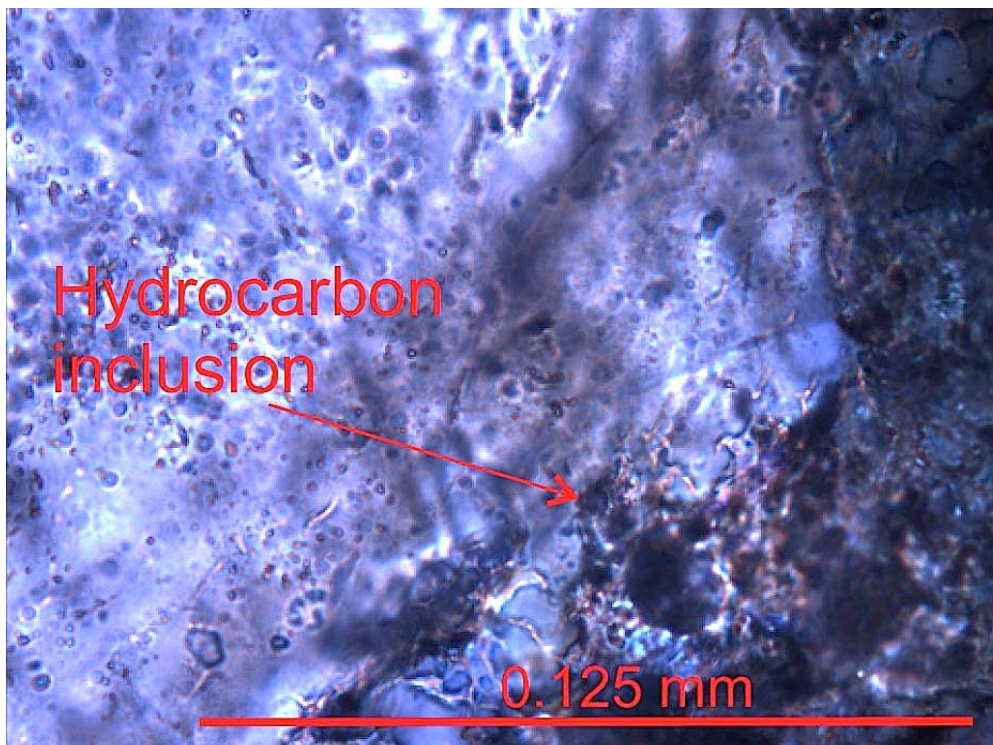


Figure 63. Hydrocarbon inclusion in sample A12 (facies SC) from the Hall Ranch study site in plane polarized light. Inclusion is in fluorescent dolomite cement abutted against the side of a quartz grain

3.6 FLUID INCLUSION ANALYSIS

Fluid inclusions were studied to determine fluid composition, maximum burial temperature, and hence the timing of diagenetic events. Thirteen inclusions in non-fluorescent calcite cement and 64 inclusions in quartz grains were studied. Small flakes of black material were observed in several fluid inclusions, but the material did not fluoresce. Inclusions in calcite cement had a narrow range of homogenization temperatures with the exception of four outliers. Two of these outliers were heated to 200°C and showed no change in bubble size or movement. Inclusions in quartz grains had a very wide range of homogenization temperatures. Inclusion trails in quartz grains varied in orientation and did not cross cut cement or extend to other grains. All results are shown below in Figures 65 through 69.

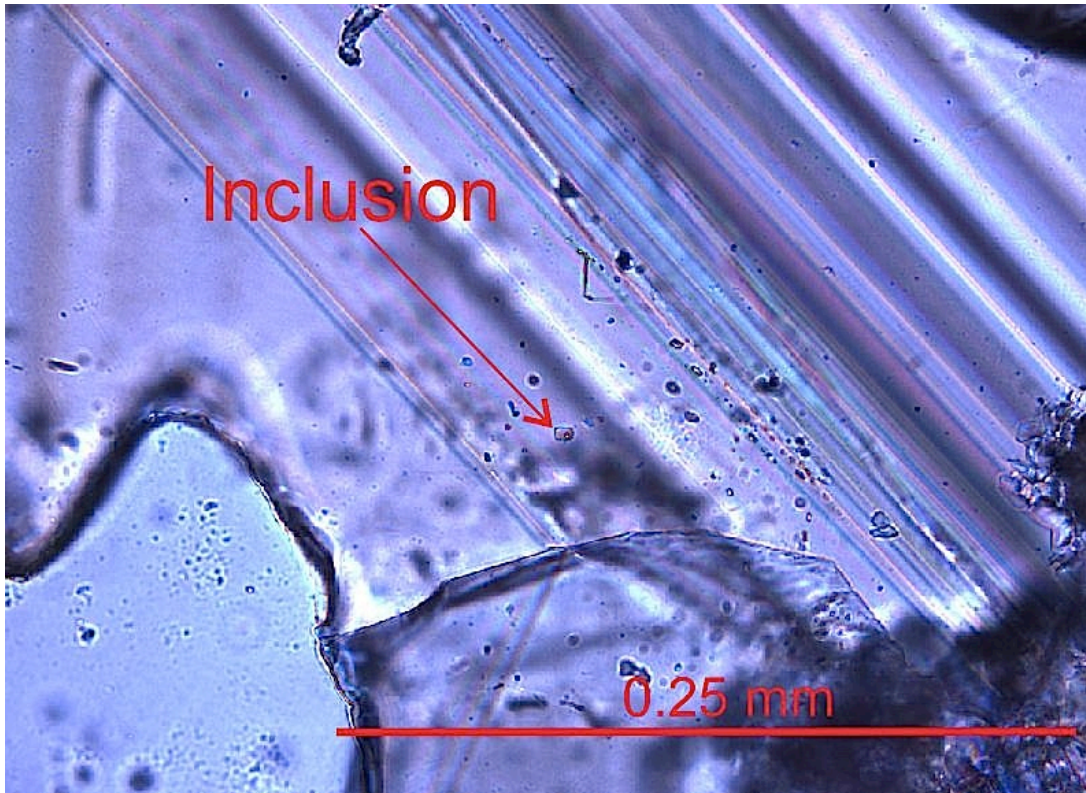


Figure 64. A two phase fluid inclusion in non-fluorescent blocky calcite cement in sample C3 (facies SC) from the Blue Sky Trail study site

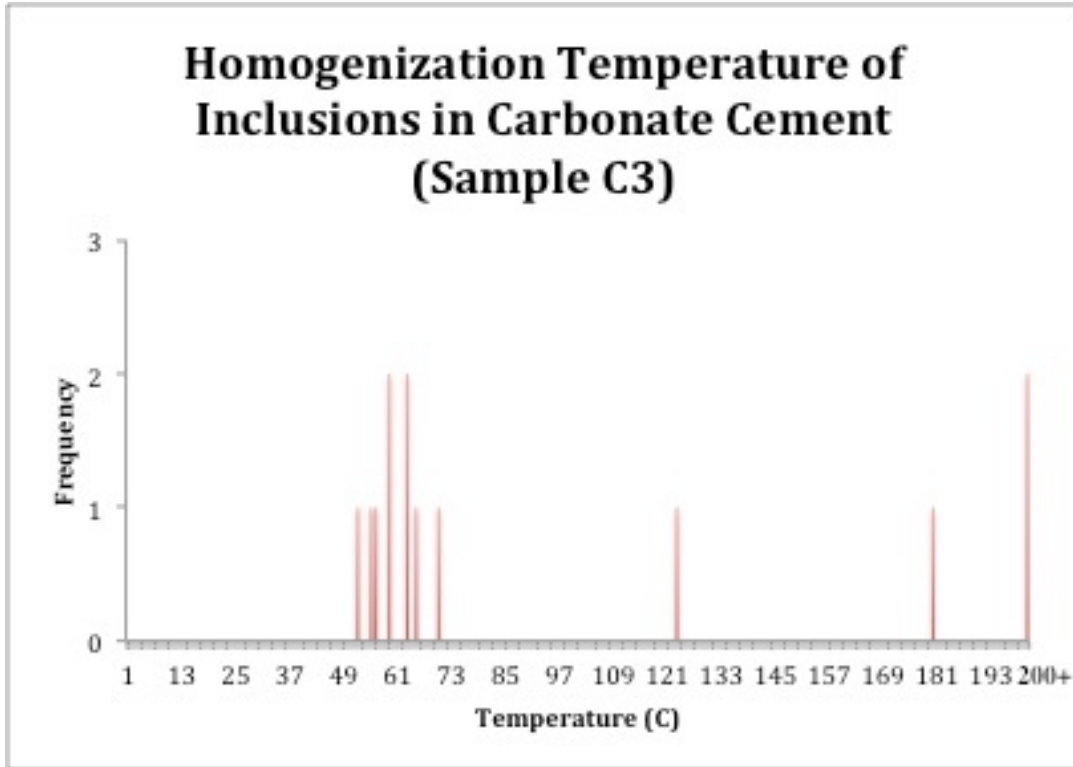


Figure 65. Homogenization temperature of inclusions in calcite cement from sample C3

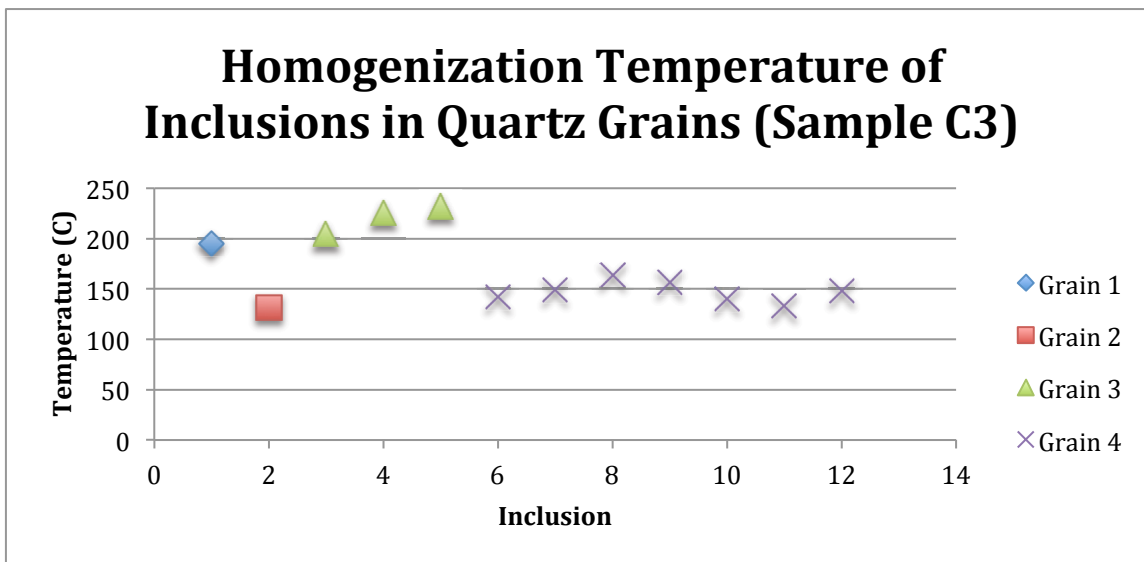


Figure 66. Homogenization temperature of inclusions in quartz grains from sample C3

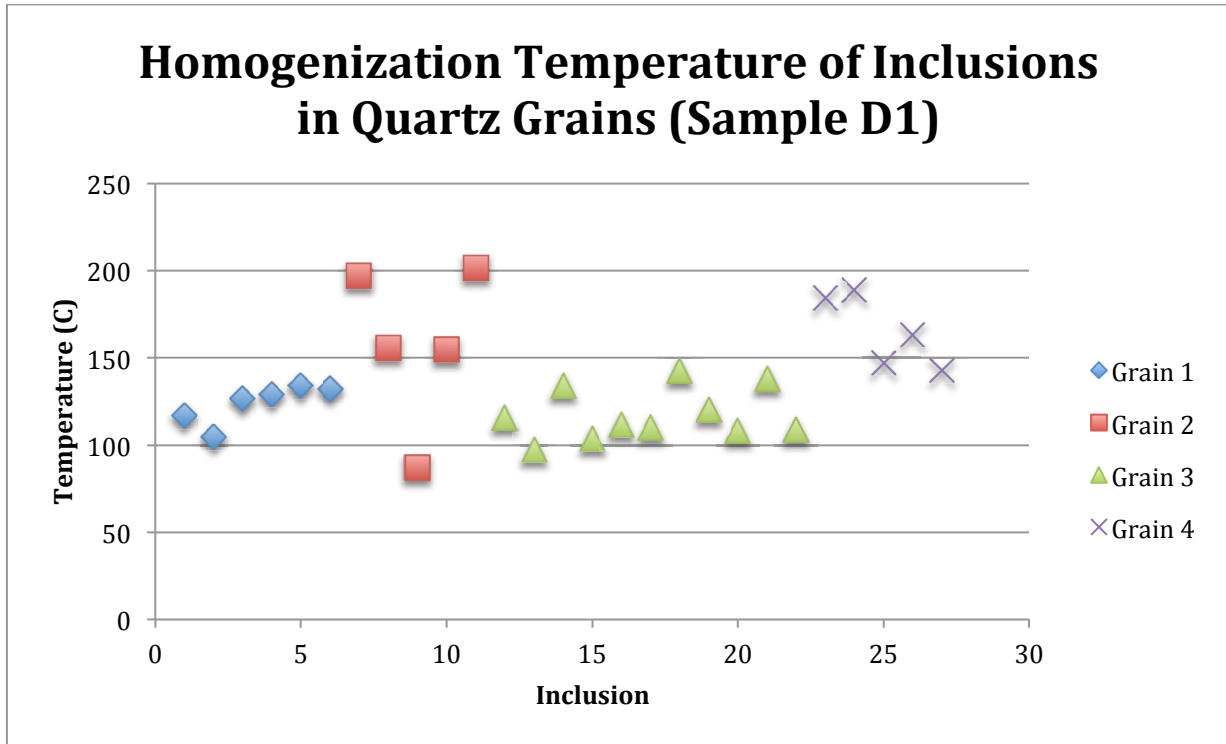


Figure 67. Homogenization temperature of inclusions in quartz grains from sample D1

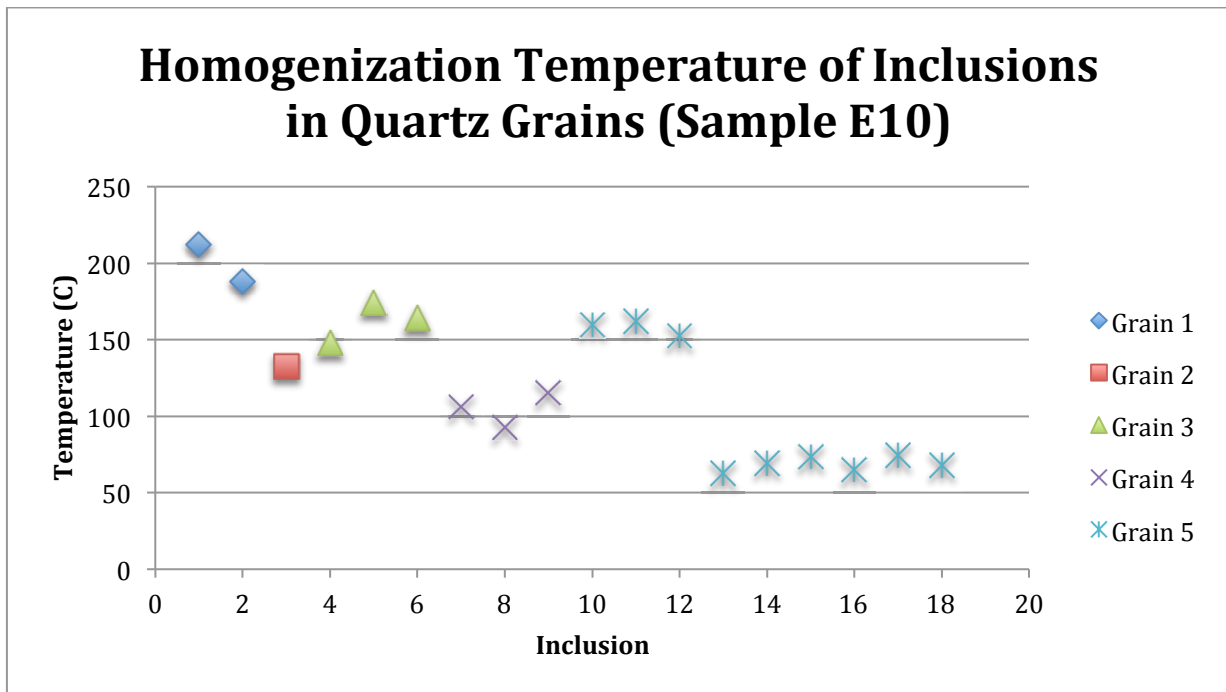


Figure 68. Homogenization temperature of inclusions in quartz grains from sample E10

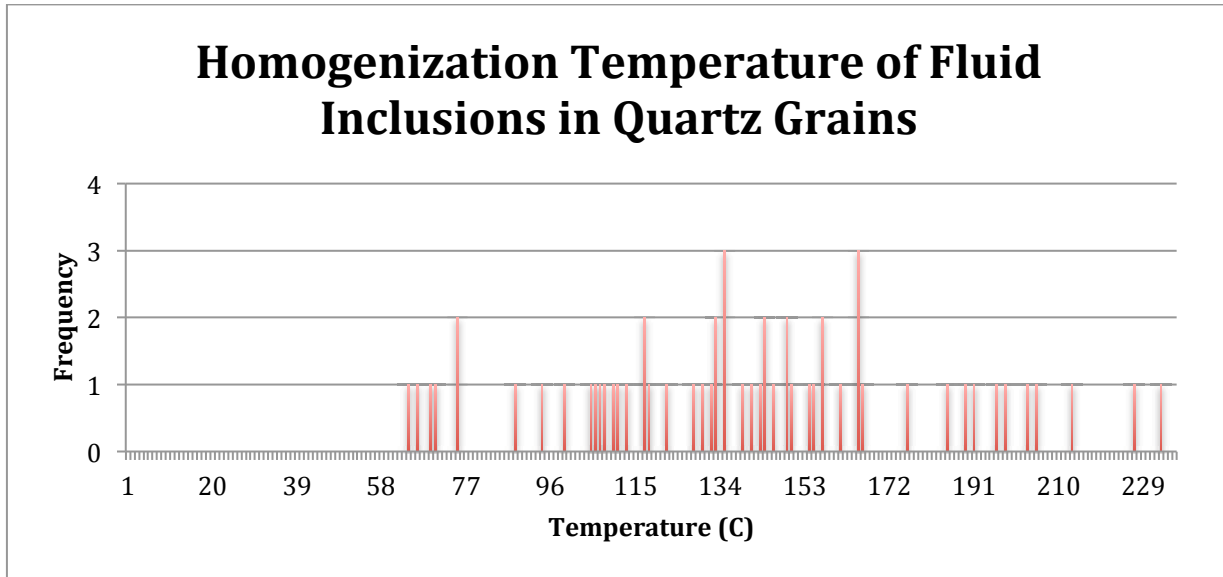


Figure 69. Homogenization temperature of inclusions in quartz grains from samples C3, D1 and E10

The final melting temperature of frozen inclusions in calcite cement was variable (Table 17). Two inclusions had a final melting temperature slightly below 0°C. The other three had a final melting temperature between 12.9° and 16.1°C, most probably indicating the presence of methane hydrates. The final melting temperature of inclusions in quartz grains was variable and is shown in Tables 17 through 20. Only inclusions that could be used for final melting temperature data are shown below.

Table 17. Data from inclusions in calcite cement in sample C3

Inclusion	Final Melting Temperature (°C)	Homogenization Temperature (°C)
1	-0.7	54.1
4	13.7	69.2
6	-1.2	55.1
9	16.1	58.7
11	12.9	>200

Table 18. Data from inclusions in quartz grains in sample C3

Inclusion	Final Melting Temperature (°C)	Homogenization Temperature (°C)
3	-7.2	205
5	0.6	232
6	-8.2	142
10	-2.1	139.9
11	-0.8	133

Table 19. Data from inclusions in quartz grains in sample D1

Inclusion	Final Melting Temperature (°C)	Homogenization Temperature (°C)
1	-0.3	116.7
5	1.4	133.9
6	0.6	132.1
7	-0.7	197.1
8	-0.1	155.8
9	14.1	87.2
17	-3.3	110
18	-2.4	112.1
20	-3.1	134.5
23	-1.7	184.2
26	16.2	163.2
27	-5.4	143

Table 20. Data from inclusions in quartz grains in sample E10

Inclusion	Final Melting Temperature (°C)	Homogenization Temperature (°C)
1	-5.5	212.4
2	-4.7	188
9	-4	115.5
13	14.6	62.8
14	17	69.2
15	12.3	73.5
16	-1.8	164
17	-0.5	152.6

CHAPTER 4

DISCUSSION

4.1 STRATIGRAPHY

4.1.1 FINING UPWARD SEQUENCES

The Fountain Formation is composed of many vertically stacked fining upward sequences. The shifting of fluvial channels and migration of bars produces this style of deposition (Miall, 1996). Sequences begin with an erosive base caused by scour in river channels and end with paleosol mudstones representing floodplain deposits and soil development and may have the other fluvial facies described in section 3.2 in between. The next sequence begins and the pattern repeats, representing shifting lateral movement of river and stream systems. Commonly, the fining upward sequences end mid-sequence and do not evolve to the mudstone facies. They are instead truncated by facies SC and the start of the next sequence. This indicates that either lateral movement of channels occurred before the development of whole sequences or channel incision was deep enough to erode the upper portion of the fining upward sequence. There is significant lateral change in facies within beds and intertonguing of facies is common over short distances of only tens to hundreds of feet. This is common in deposits of fluvial systems that had rapid lateral movement such as braided streams (Miall, 1977).

4.1.2 SANDSTONES AND CONGLOMERATES

The Fountain Formation is composed mostly of sandstones and conglomerates. Of the seven sections measured, 90.7% of strata were sandstone and conglomerates. Quartz and potassium feldspars make up a bulk of the sand grains and carbonate, clay, and hematite cement is abundant. Clay in sandstones appears to be from diagenetic alteration and possibly from modern weathering of feldspars. With the exception of cement types the mineralogy of sandstones is consistent throughout the study area.

4.1.3 SANDSTONE AND CONGLOMERATE FACIES

Structureless Conglomerate (Facies SC): This facies marks the beginning of a fining upward sequence. It has an erosive basal surface that represents the scouring of underlying sediment in stream channels during high-energy floods. In the scours were large clasts including quartz and feldspar fragments, lithic fragments, and rip up clasts that were likely only transported by the strongest floodwaters. Many of the conglomerates in this facies are clast supported indicating that the sand matrix filtered into the depressions following deposition of the larger clasts (Miall, 1977).



Figure 70. Clast supported conglomerate in facies SC representing channel lag deposits

Trough Cross-Bedded Sandstone (Facies TS): Based on the trough cross bedding, this is a channel fill deposit. Trough cross bedding is caused by the migration of ripples and dunes (Boggs, 2012). Miall (1977) also describes shallow angle cross bedding similar to that seen in the Fountain Formation in modern braided streams and attributes it to migrating dunes. Bed thickness in this facies is on the order of feet to several inches indicating that water depth was highly variable. The grain size, bed thickness, and angle of cross bedding in units of this facies all decrease upward within a fining upward unit and indicate a decrease in water depth over time. This facies represents migrating subaqueous dunes in a stream channel and the pattern of decreasing grain and bed size represents a dissipation of channel energy caused by the transition from flood stage to normal discharge or the switching of the channel position.



Figure 71. Paleo-channel consisting of facies SC and TS that truncates facies VFS

Coarse Sandstone with Mud Drapes (Facies CSM): The coarse to medium grain sandstone beds separated by very thin mud drapes probably represent a continuation of the decreasing energy represented in the underlying trough cross-bedded sandstone facies. The presence of mud drapes is evidence that deposition took place in very slow moving or stagnant water. It is possible that this facies represents seasonal variability in which water levels dropped enough to create isolated pools or it may represent the shifting of channel position that resulted in pools or areas of very slow moving water.

Very Fine Sandstone (Facies VFS): This facies probably represents the movement of bars in the channel during low flow stages and thin sand sheets in shallow water depths. Rust (1972) describes horizontally laminated sands forming in longitudinal bars in braided rivers. Longitudinal bars develop by vertical accretion on bar tops and migration downstream. Smith (1971) describes horizontally laminated sand sheets forming in very shallow water of less than one inch on the Platte River. The sands described by Smith alternate between very fine grained and coarse grained laminations and form in low flow regimes by sorting at the foreset of a thin sand sheet. Many of the sandstones in this facies in the Fountain Formation fit the description of the shallow water sand sheet deposits that Smith describes. Smith (1972) also describes planar cross-bedded sandstones formed by the downstream migration of transverse bars in braided river systems. The rare planar cross-bedded units in some of the VFS facies likely represent transverse bar deposits and the more common horizontally laminated sandstones represent longitudinal bars and sand sheets.



Figure 72. Horizontally laminated beds in facies VFS representing shallow migrating bars and sand sheets

Massive Sandstone (Facies MS): This facies may represent many of the other facies that have been subjected to bioturbation and soil development, which destroyed any previous sedimentary structures. This would explain why this facies is so variable in terms of grain size, color, and position in sequence packages.

4.2 PETROGRAPHIC AND FLUID INCLUSION INTERPRETATIONS FROM SANDSTONE SAMPLES

Sandstones in the Fountain Formation contain abundant quartz grains. Most quartz is monocrystalline and the angular and subangular monocrystalline quartz was likely derived from the erosion of granitic basement from the nearby Ancestral Rocky Mountains. Subrounded, monocrystalline quartz grains may have a more complicated history and are discussed later in this section. There is also a small amount of polycrystalline quartz, and a possible source of these grains is the Sawatch Formation, a Cambrian quartzite. This formation is not present in the Fort Collins area but is

exposed about 130 miles to the south in the Manitou Springs area. During uplift of the Ancestral Rockies the Sawatch formation may have been completely removed in the Fort Collins area.

Fluid inclusion homogenization temperatures in quartz grains from sandstones were highly variable and ranged from 62.8° to 232.0°C. The geothermal gradient in the Denver Basin is unusually high and near Fort Collins is about 40°C per kilometer (Berkman and Watterson, 2010). It is possible that some of the lower temperature inclusions may have formed after burial within the Denver Basin, which before exhumation of the Fountain in the Late Cretaceous to early Eocene was buried to a depth of at least 1,575 meters (Braddock et al., 1989). The high temperature inclusions cannot be explained by burial in the basin at these depths. The highest temperature inclusions could not have formed in the basin even at depths twice that of which the Fountain was buried too. Inclusion trails in quartz grains do not cut across grain boundaries or extend into cement, and inclusion trails in grains near one another are not oriented in the same directions. If the inclusions formed in the Denver Basin after burial, inclusion trails would have formed in similar orientations because the stresses on grains would have been similar. In general one would expect high temperature inclusions to have formed after lithification and inclusion trails would thus cut across grain boundaries. The high temperature of the inclusions, absence of trails that cut across grain boundaries, and chaotic orientation of inclusion trails indicate that these inclusions formed somewhere else before incorporation in the Fountain sediment. Two scenarios are discussed below.

The first scenario is that these inclusions formed in the source terrain and are of metamorphic origin. Secondary inclusions commonly form in healed fractures of metamorphic rocks, especially quartz (Roedder, 1984). Fluid inclusion trails in quartz grains derived from metamorphic rocks would have wide ranges of orientations because they were not caused by burial stresses and they would not cut across grain boundaries. Sources of these grains may be the Sawatch quartzite or the Proterozoic basement.

Another scenario is that some of these grains, particularly the subround monocrystalline grains, are extrabasinal. In this scenario high temperature inclusions formed when the grains were buried in a distant deep basin that was exhumed before or during deposition of the Fountain and the grains were then transported into the Denver Basin. This scenario does not explain the angular and sub-angular grains or the polycrystalline grains. Neither scenario fully explains the variety of high temperature quartz grains in the Fountain Formation although they are similar in the respect that inclusions predate incorporation of the host grains in the Fountain Formation. It is possible that quartz grains with high temperature inclusions were derived from a combination of both of these scenarios.

Potassium feldspar grains are also common in the Fountain Formation. Most potassium feldspar grains have well developed tartan plaid twinning patterns that formed from slow cooling at low temperatures and is characteristic of microcline. Although granitic rocks such as the ones that likely made up the Ancestral Rockies

commonly contain slightly more potassium feldspar than plagioclase feldspar, the discrepancy between the two abundances of the feldspars cannot be explained by source alone. The Permian Cutler Formation of central Colorado is Fountain equivalent and was also formed from erosion of the Ancestral Rockies. It has a plagioclase feldspar composition close to five percent and a potassium feldspar content of about six percent (Suttner and Dutta, 1986). The Pennsylvanian-Permian Sangre de Cristo Formation is another Fountain equivalent with the same source and contains about equal percentages of potassium and plagioclase feldspars (Lindsey, 2000). Napp and Ethridge (1985) and Van de Kamp and Leake (1994) reported high ratios of potassium feldspar to plagioclase feldspar in the Fountain Formation. This is most likely due to dissolution of plagioclase during diagenesis.

Feldspar alteration is very common in the Fountain Formation rocks considered in this study. Altered feldspars are over four times more common in whitened rock than non-whitened rock. Feldspar dissolution is favored in acidic environments and the fact that alteration is so much more prevalent in whitened strata suggests that an acidic fluid flowed through those volumes. Whether the feldspar-altering paleo-fluid was the same fluid that reduced and removed hematite cement cannot be determined. Plagioclase feldspars seem to have been affected much more than potassium feldspars and are more heavily altered, usually to the point that they are barely recognizable. The low percent of plagioclase feldspars in both whitened and non-whitened strata in the Fountain is probably the result of many of these grains being completely altered to clays. Many patches of clay are clearly grains that have been altered but the original

mineral is beyond recognition. Van de Kamp and Leake (1994) also reported that most plagioclase in the Fountain Formation has been nearly completely altered to clay.

Lithic fragments are also present in the Fountain sandstones and are mostly of plutonic and clastic sedimentary origins. The plutonic grains are likely detritus from the erosion of the Ancestral Rockies and clastic grains are rip up clasts. Biotite and muscovite are common accessory minerals and are common products of the erosion of granitic rocks.

4.3 MUDSTONES

Siltstone/Mudstone (Facies MUD): This facies makes up the top of fining upward sequences and represents floodplain deposits and paleosols. The numerous root traces, soil horizons, and calcareous nodules found within this facies support these interpretations. The wide range in colors may be due to varying paleosol horizons being present. The reduction spots in this facies are likely the result of early reduction of organic material. Calcareous nodules likely formed as caliche. Caliche forms up to several feet below the soil surface due to leaching of minerals or the decay of organic matter in the presence of calcium and begins as beds of carbonate nodules (Reeves, 1976; Schlesinger, 1985). The variable lateral extent of this facies suggests two depositional environments. The wedge-shaped bodies less than ten feet wide likely represent muds that filled abandoned channels. The other beds, with fairly uniform bases and which extend for hundreds of feet, were probably valley wide floodplain

deposits. The large size of roots, well-developed caliche, and thickness of the deposits suggest that some of these paleosols were environmentally stable for at least decades.



Figure 73. Carbonate nodules in facies MUD representing caliche

4.4 LIMESTONES

Limestone (Facies LS): This rare facies represents well-developed caliche or lacustrine deposits. The development of caliche usually forms beds of carbonate nodules, but if development continues and precipitation of carbonate is extensive, thick beds of solid carbonate may form (Reeves, 1976). This may be the cause of some of the limestone beds found in the Fountain. A bed at the Blue Sky Trail, however, contains numerous fossils, which suggest that this bed was deposited in a lacustrine setting (Fig. 74). Another bed at Dixon Cove contains numerous carbonate intraclasts

and oscillation ripples, which also suggests deposition in a lacustrine setting (Fig. 75). This facies, when present, is at the top of sequences so as a new sequence began with erosion of a stream channel the limestone deposits would have been the first to be eroded. The limestone beds and limestone fragments that were eroded and redeposited within younger units may have supplied some of the calcium carbonate that was required for such large volumes of carbonate cement. Some sandstones contain numerous rounded carbonate clasts that may be from eroded limestone beds (Fig. 76).

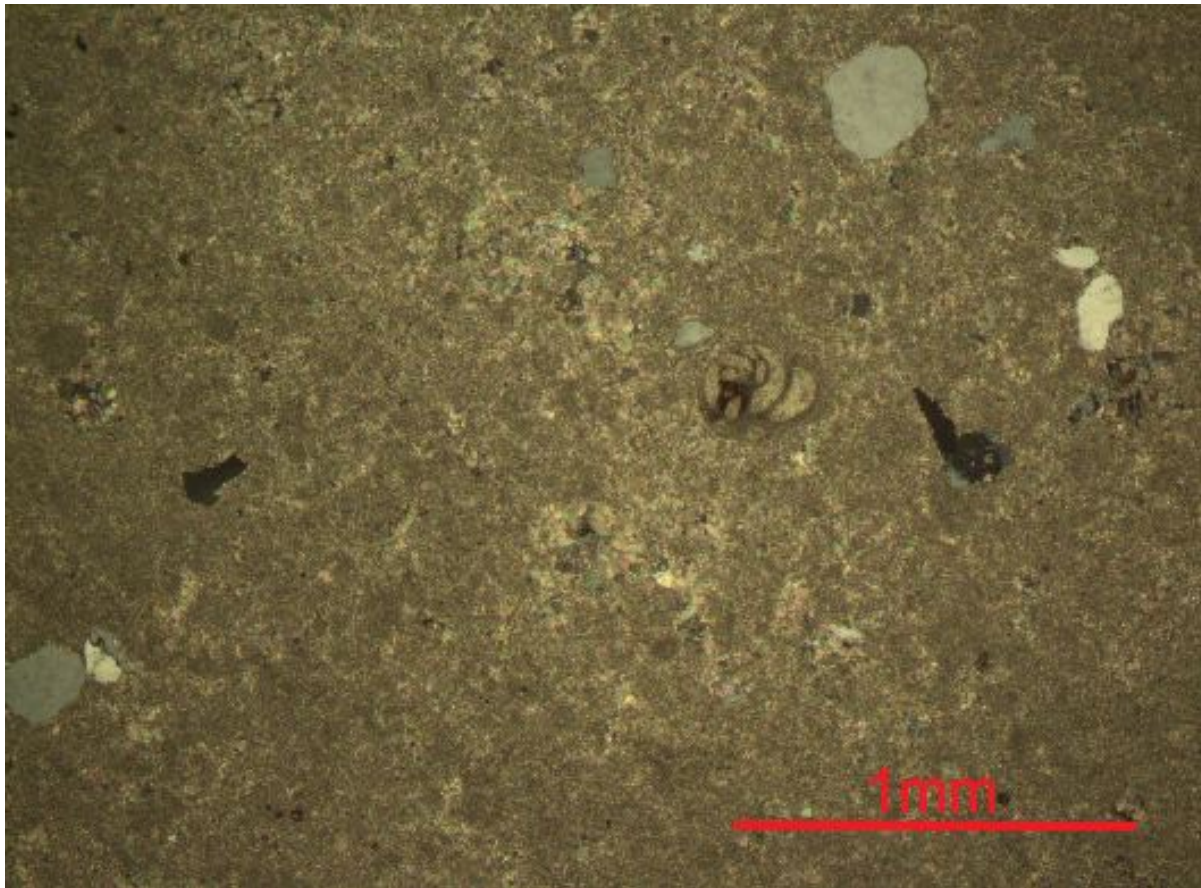


Figure 74. Gastropod and shell fragments in sample C11 (facies LS) from the Blue Sky field site

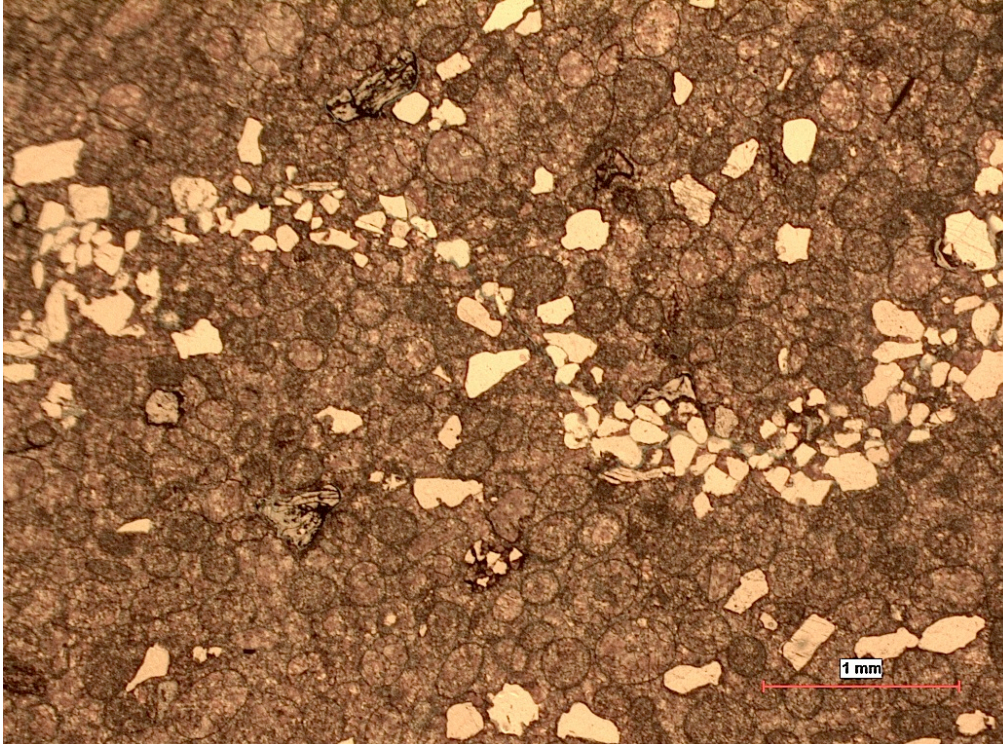


Figure 75. Carbonate intraclasts and an oscillation ripple in sand laminae in sample D4 (facies LS) from the Dixon Cove study site

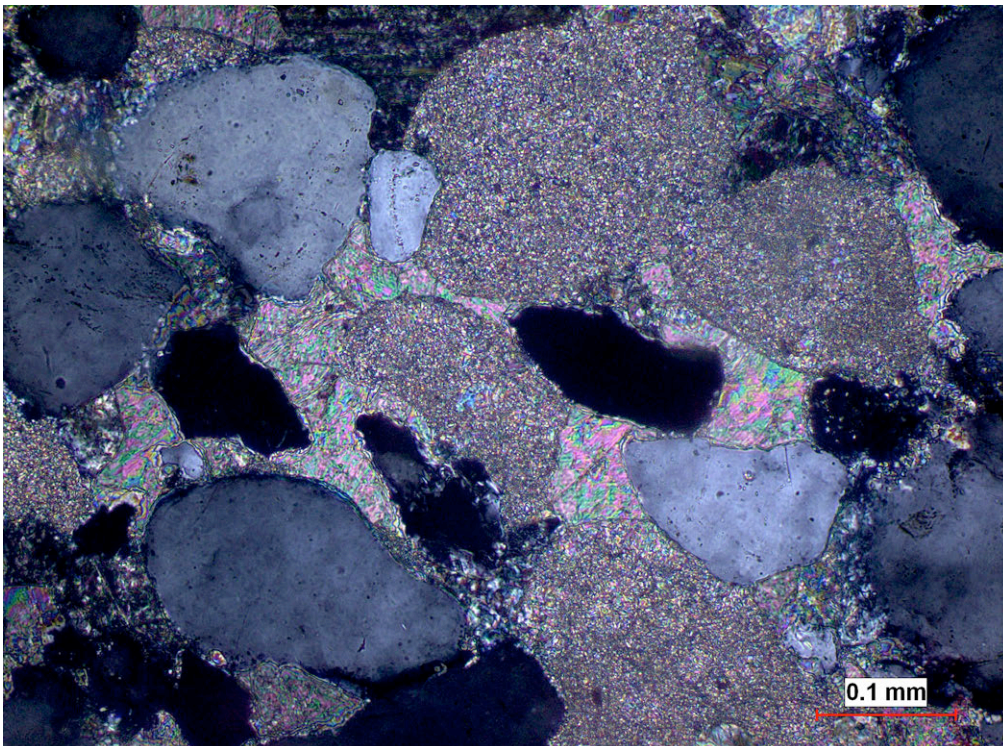


Figure 76. Numerous lithic sedimentary carbonate clasts in sample C9 (facies VFS) from the Blue Sky Trail study site

4.5 DIAGENESIS IN THE FOUNTAIN FORMATION

Most sandstone in the Fountain hosts multiple episodes of cementation. The most common cements are calcite and dolomite, various clays, and hematite. Hematite cement began precipitating very early in the formation's history, but after deposition. Evidence that hematite precipitation occurred after deposition includes hematite filling pore spaces and rare hematite cement coating and filling irregularities in crystallographic boundaries of early carbonate cement (Fig. 78). Hematite cement in compacted sandstones is present between grains that display grain-to-grain contact. This is evidence that hematite precipitation began before compaction.

A poikilotopic dolomite cement is interpreted to have precipitated very early. This cement surrounds grains that show no sign of significant compaction. These grains must not have been compacted for this cement to precipitate between them. This cement probably protected them from stresses caused by grain-to-grain contact during burial, which may be why fracturing and contact dissolution was not observed in these grains. This cement precipitated at the same time or possibly even before the precipitation of hematite cement. In samples with hematite cementation, grains that are near the center of the poikilotopic patches of dolomite cement are not stained with hematite, while grains near the edges and outside of the cement patches are stained with hematite (Fig. 42, 43). This probably indicates that this cement precipitated first and shielded the grains from hematite staining. An alternative is that this cement was precipitated as the hematite was being removed, but this does not explain why grains on the outer margins of the cement patches still have hematite cement rims.

The second stage of carbonate cementation is represented by blocky cement that varies regionally from calcite to dolomite. It is the most common carbonate cement. This cement fills fractures in clastic grains indicating that it precipitated during or after deep burial. Homogenization temperatures of fluid inclusions within this cement from a sample at the Blue Sky Trail study site cluster between 51° to 69°C. This cement replaces clastic grains in many samples. Evidence of this includes partially replaced grains and ghosts of grains (Fig. 79). The ghosts are of grains that were once coated with hematite cement and all that remains in the large patches of calcite and dolomite cement are grain shaped rings of hematite. In some samples the amount of replacement is so great that remaining clastic grains float in carbonate cement. In rare cases hematite cement is present on the outer boundaries of blocky carbonate cement and indicates that hematite precipitated continuously or in stages bracketing the blocky carbonate precipitation.

The third stage of carbonate cementation is a replacement calcite cement. It is not very common. It replaces the outer margins or in some cases completely replaces blocky dolomite cement. In rare cases it forms acicular needles around dolomite cement if the dolomite crystals are not tightly packed, otherwise it simply replaces dolomite rhombs, overprinting cleavage (Fig. 80).

The fourth stage of carbonate cementation is fluorescent dolomite cement that is very dark and replaces blocky dolomite and carbonate cement. The third and fourth

stages of cement were not observed in the same samples, so the temporal relationship between them is not clear. The fluorescent dolomite is microcrystalline, is very dark because of organic matter, contains hydrocarbon inclusions, and is associated with pore filling bitumen. The dark material in the cement that causes it to fluoresce may be degraded hydrocarbons but this cannot be confirmed. This cement probably precipitated from the paleo-fluid that caused the whitening in the Fountain Formation. It is only found in samples of rock that have been whitened or in samples that are within a few inches of whitened rock. In non-whitened rock in close proximity to whitened rock the cement is much less abundant. Many other fluorescent inclusion-like features are in this cement and may be hydrocarbon inclusions that are too small to identify. This cement contains hydrocarbon inclusions and is associated with bitumen, which indicate oil was present. The cement likely precipitated from an aqueous fluid that was in the presence of oil. The hydrocarbons associated with the aqueous fluid would have caused it to be reducing and is likely responsible for the reduction and removal of hematite in the whitened strata of the Fountain Formation. The fluorescent dolomite appears to be the last cement to have precipitated. Although its timing cannot be completely constrained, this fluorescent dolomite cement postdates the blocky cement that has evidence of precipitation at temperatures of up to 69.2°C. This shows that the migration of immiscible oil and water that likely whitened the Fountain Formation probably occurred late in the formation's cementation history.

Other common cements in the formation include various clays. Most clay cements are in sandstones that are compacted and show grain-to-grain contact,

indicating that most clay cement precipitation probably took place during or after compaction (Fig. 81). Clay cement composed mostly of illite and minor amounts of kaolinite is present in non-whitened sandstones. It fills pore spaces around hematite coated grains and seems to replace some feldspar grains. This cement formed after hematite precipitation but is otherwise not well constrained in terms of its timing. Some of the clay may also have formed during modern weathering. Another clay cement composed of kaolinite is common in whitened strata. It fills pore spaces and replaces many of the feldspar grains in samples from whitened rock. Some of the replaced grains also have small patches of calcite, which indicates that those grains were at least partially replaced during diagenesis and not modern weathering. Kaolinite precipitation is favored by low pH, so its presence suggests that an acidic fluid flowed through the permeable sections of the formation. Many patches of this cement fluoresce slightly, indicating the presence of organic matter. Organic matter can adsorb to clay mineral surfaces (Margulies et al., 1988; Kennedy et al., 2002), which will cause them to fluoresce. This is evidence that the kaolinite cement was at some point in contact with an organic rich fluid. The Fountain Formation has a complex diagenetic history and a summary of the sequence of diagenetic events is given in Figure 82.

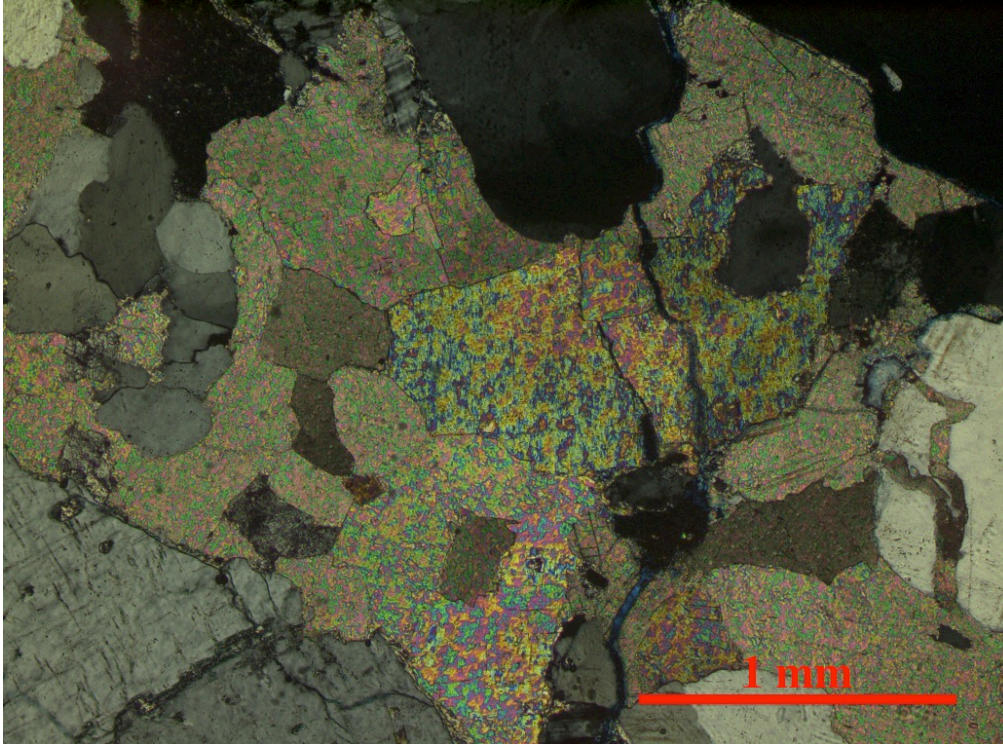


Figure 77. Carbonate cement in sample A8 (facies SC) from the Hall Ranch study site makes up a majority of the sample

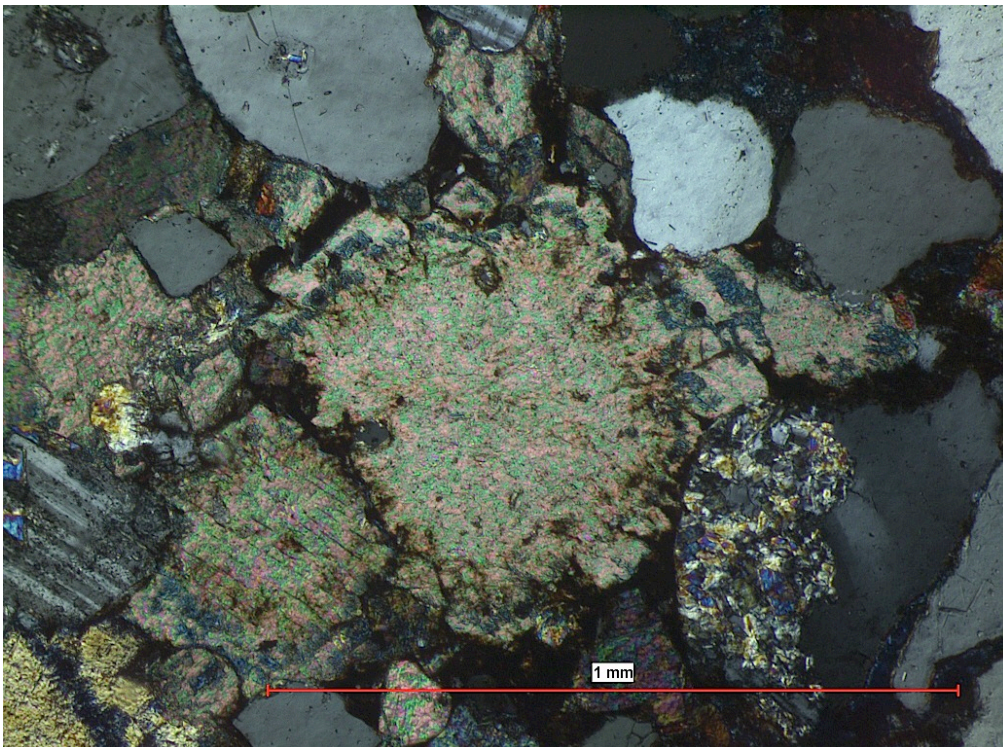


Figure 78. Early dolomite cement with hematite staining around the edges in sample D15 (facies TS) from the Dixon Cove study site

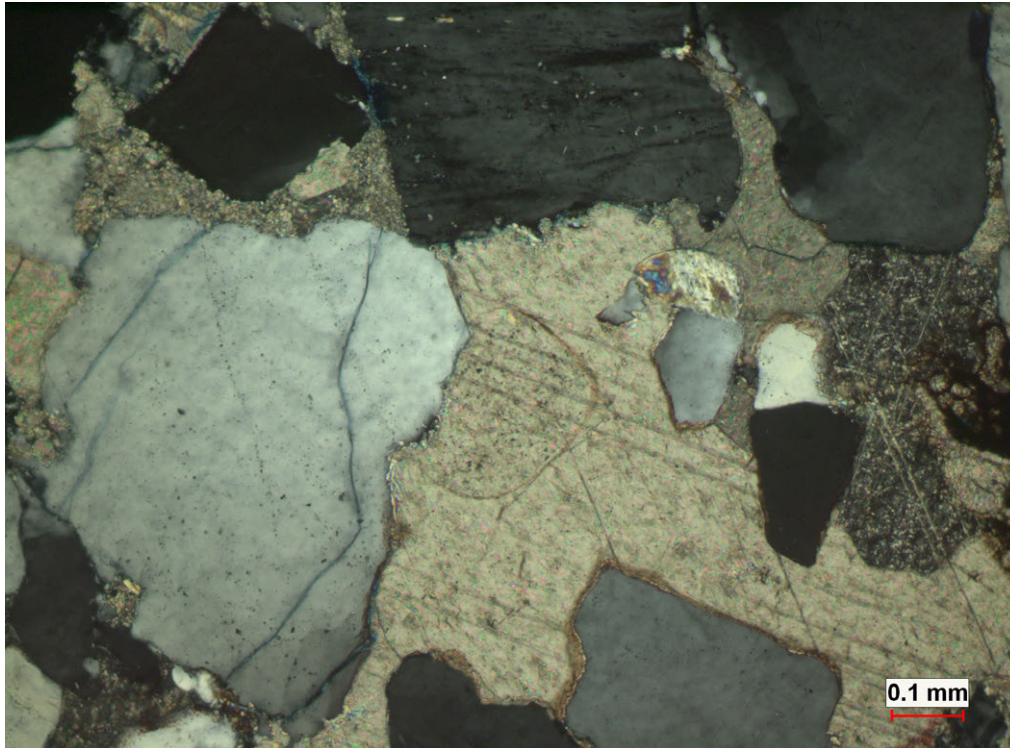


Figure 79. Complete replacement of a grain by dolomite cement in sample C7 (facies VFS) from the Blue Sky Trial study site. The ghost of the grain is in center of the photomicrograph and has a light ring of hematite around it

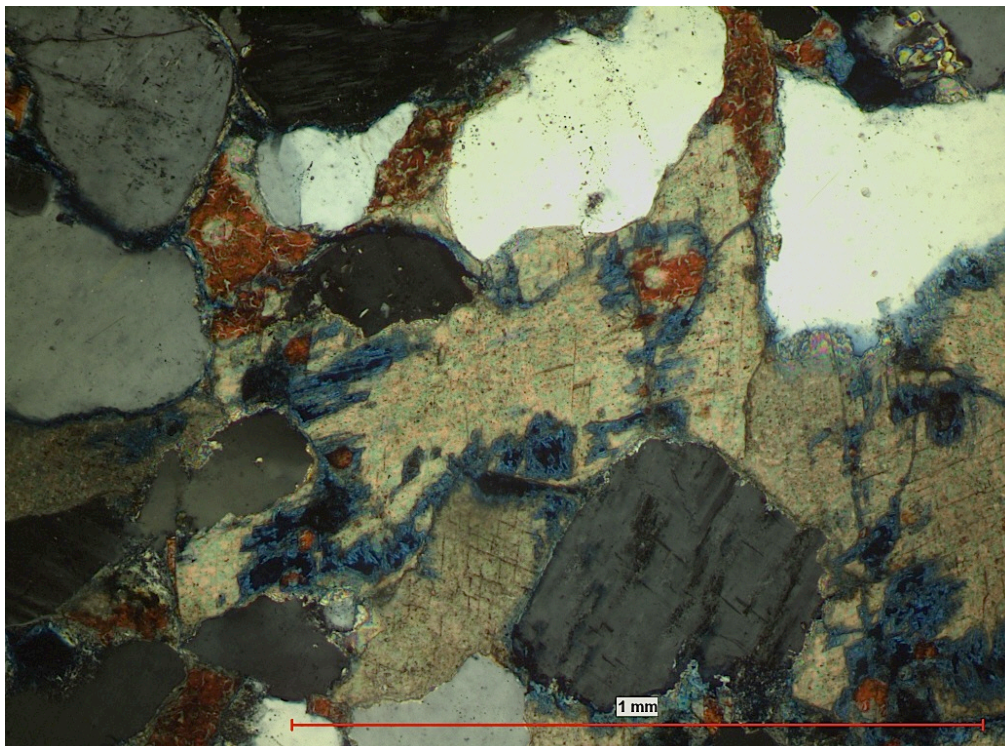


Figure 80. Calcite cement replacing blocky dolomite cement in sample D14 (facies SC) from the Dixon Cove study site

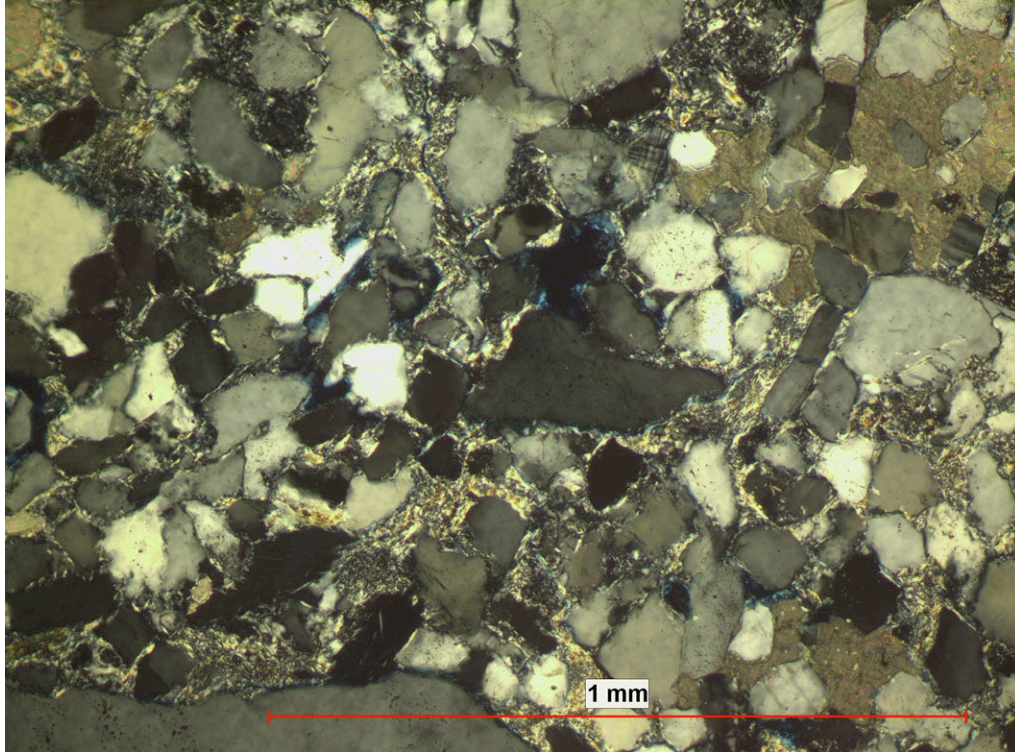


Figure 81. Clay cement filling pore spaces around compacted grains in sample B9 (facies TS) from the Devil's Backbone site. Note that grains within poikilotopic dolomite cement in right top corner were not compacted

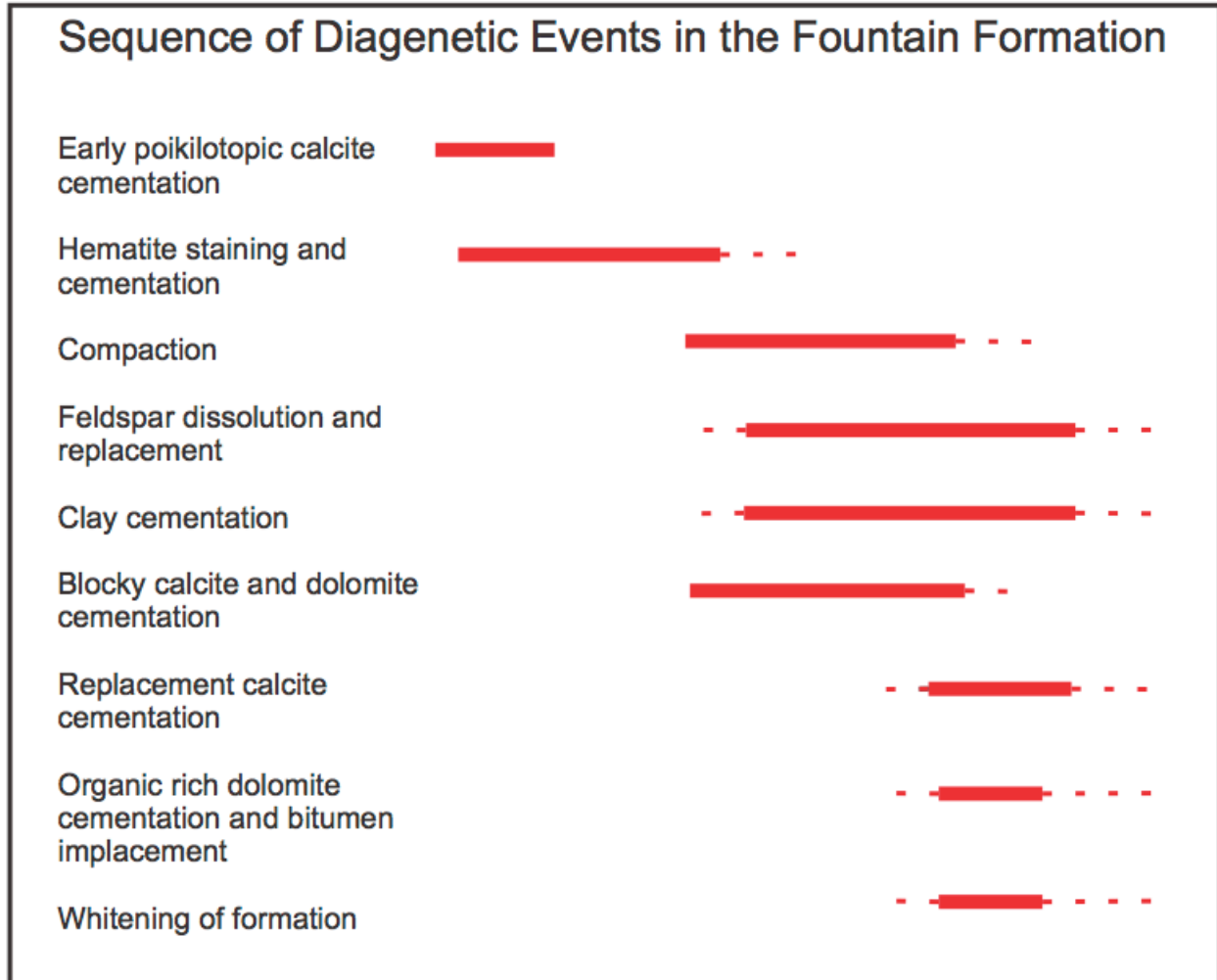


Figure 82. Sequence of diagenetic events in the Fountain Formation near Fort Collins based on observations of 75 thin sections

4.6 FLUORESCENT MICROSCOPY

Fluorescent dolomite cement and fluorescent clay cement are present in many of the samples of whitened rock. The dolomite is very dark in color, indicating that it contains numerous impurities. The strong fluorescence of the dolomite demonstrates that the impurities are organic matter or hydrocarbons (Dravis and Yurewicz, 1985; Russo et al., 1997). The presence of hydrocarbon inclusions in this cement is direct evidence that hydrocarbons were present when the cement was being precipitated.

Bitumen is also found exclusively in samples of whitened rock that contain the fluorescent cements and may be from degraded oil. The hydrocarbons would have caused the paleo-solution to be reducing so it is likely that the fluorescent cement was precipitated from the same fluids that reduced and removed hematite cement causing whitening in the Fountain Formation.

4.7 FLUID INCLUSIONS AND BURIAL TEMPERATURES

Quartz grain fluid inclusion temperature data are extremely variable. This is likely the result of inclusions forming before incorporation of the clasts into the sediment of the Denver Basin or in metamorphic rocks. Fluid inclusion data from the calcite cement are less variable. Most of the homogenization temperatures are within several degrees of one another. Two inclusions in calcite had anomalously high temperatures, which may be due to the inclusion being leaky or stretched. Calcite inclusions are notorious for being leaky for various reasons including deformation in the subsurface or overheating in the lab, and leaks will result in high homogenization temperatures (Goldstein, 2001). Another two inclusions were heated to 200°C and appeared to have no change in bubble size at high temperatures. The bubble in the inclusion is a space filled by gas or water vapor that forms when the fluid in the inclusion cools and condenses. When heated the fluid expands and returns to its original single phase. If, however, the bubble is methane gas that was present during formation of the inclusion it will remain even when the inclusions is heated to temperatures exceeding 200°C (Goldstein and Reynolds, 1994). This may be the case for the two inclusions that appeared to have no change in bubble size at high temperatures. The fact that

methane hydrates were detected in one of the two, as well as in other inclusions in the calcite cement, strengthens this argument (Table 17).

The highest homogenization temperature in the calcite cement was 69.2°C and is used to constrain the maximum burial temperature. A surface temperature of 18°C during the Cretaceous is assumed (Royer et al., 2004). The Denver Basin currently has an abnormally high geothermal gradient and in the Fort Collins area it is about 40°C per km. At this geothermal gradient if 69.2°C represented the maximum burial temperature, the Fountain Formation would have a maximum burial depth of roughly 1.3 km. This coincides well with the known modern thickness of overlying Permian through Late Cretaceous formations in the study area. The known thickness of these sediments is 1.42 km (Braddock et al., 1989). A stratigraphic column of the formations that would have overlain the Fountain before exhumation in the Late Cretaceous is shown below (Fig. 83). The column shows current thickness of the formations in the study area.

The geothermal gradient, however, may not have been as high in the Paleozoic and Mesozoic as it is currently. The current high geothermal gradient is associated with magma at depth and probably began in the Cenozoic (Elliott et al., 1996). Near Cameron Pass to the west of the Fort Collins area are outcrops of basalt and rhyolite that may belong to Eocene and Oligocene volcanism (Corbett, 1966). South Table Mountain to the west of Denver contains basalts that were Ar-Ar dated at 64 million years (Obradovich, 2002). Other volcanic rocks in the Colorado region are younger and belong to Late Oligocene and Miocene volcanism (Bove et al., 2001). All known volcanism took place after the Late Cretaceous, which suggests that the high

geothermal gradient may have developed too late to affect the Fountain rocks because they were no longer buried or were in the process of being exhumed. If a normal geothermal gradient of 25°-30°C per kilometer is used instead of the current geothermal gradient, the maximum burial depth would be roughly 1.7 to 2.0 kilometers. More research into the cause of the high geothermal gradient in the Denver Basin, timing of volcanism in northern Colorado, and degree of erosion at unconformities in Pennsylvanian through Late Cretaceous sediments along the Front Range would be needed to constrain the historic geothermal gradient. Without more information, a maximum burial depth ranging from 1.3 to 2.0 km can be inferred for the Fountain Formation.

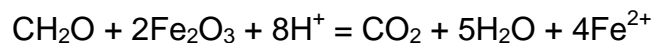
Era	Period	Formation	Thickness	
Mesozoic	Cretaceous	Pierre Shale	580 m	
		Niobrara	107 m	
		Benton	148 m	
		Dakota Group	88 m	
		Lytle	24 m	
	Jurassic	Morrison	98 m	
		Sundance	60 m	
	Triassic	Lykins	183 m	
	Paleozoic	Permian	Lyons	15 m
			Owl Canyon	61 m
Ingleside			46-53 m	
Pennsylvanian		Fountain	224-268 m	
Precambrian Basement				

Figure 83. Stratigraphic column of the formations and their modern thicknesses in the study area that were above the Fountain prior to the onset of exhumation (modified from Braddock, 1989)

4.8 WHITENING OF THE FOUNTAIN FORMATION

The Fountain Formation is a classic red bed deposit and its color is attributed to hematite cement and grain coatings. Hematite cement probably formed shortly after burial by the alteration of goethite or ferromagnesian silicates in contact with oxygenated groundwater. The source of the iron is unknown but may have come from the breakdown of ferromagnesian silicates. The Fountain Formation is composed mostly of detritus from the Ancestral Rocky Mountains, and these mountains likely contained abundant ferromagnesian silicates such as hornblende. No such minerals, however, are found in the Fountain samples. It is possible that this is because they have been altered to hematite and other byproducts early in the formation's history or that they weathered during or prior to transport.

Whitening of strata in the Fountain Formation was likely caused by the reduction and removal of hematite cement by the movement of fluids through the formation. The fluid was reducing and evidence of this is hematite removal along apparent fluid pathways. The following reaction illustrates how a fluid containing hydrocarbons would reduce hematite (Chan et al., 2000).



Once in a reduced state, the iron becomes soluble and can be removed by the fluids (Chan et al., 2000; Beitler, 2005). The fluorescent dolomite cement, hydrocarbon inclusions, and bitumen in strata that the fluid passed through indicate that the reducing

fluid was a combination of immiscible oil and water. The migration of this fluid through the Fountain occurred late in the formation's diagenetic history; the cements that precipitated from this fluid postdate cement that had fluid inclusions with homogenization temperatures of up to 69°C. These fluid inclusions indicate that fluid migration and whitening of the Fountain happened after the formation was buried to at least 1.3km, which would have been in the Late Cretaceous or later. Whitening of strata in the Fountain can be seen throughout the exposed western flank of the Denver Basin, indicating that this was a very large-scale event. A burial depth of 1.3km would not put the Fountain into the oil window at the location of the study sites so the fact that hydrocarbon inclusions and bitumen were present indicate that fluid migrated from deeper in the basin or that burial depth exceeded 1.3km after deposition of the blocky carbonate cement. Fountain equivalents to the east of the study area are composed of marine shales and carbonates. Clayton et al. (1992) describe numerous Pennsylvanian black shales in the northern Denver Basin. These sediments were rapidly buried to hydrocarbon generating temperatures during the latest Cretaceous as the Denver Basin subsided (Lee and Bethke, 1994). During that time, the Fountain along the Front Range was uplifted and tilted, which would have allowed for updip migration of hydrocarbons.

Lee and Bethke (1994) speculate that the fluids that reduced hematite and caused grey colored sandstones in the overlying Lyons Formation were expelled from the Fountain. The grey colored sandstones are characteristic of the hydrocarbon reservoirs in the Lyons. The Black Hollow, Lake Canal, and Pierce fields in Larimer and Weld Counties have produced about 26 million barrels of oil from the Lyons Formation

as of 2007 (Higley and Cox, 2007). Although there is production, no source rock has been identified for these hydrocarbons (Clayton and Swetland, 1980). Some of the oil that migrated through the Fountain may have moved upwards and charged the Lyons.

Whitening in the Fountain Formation can be assigned to three different categories. The first is complete whitening of strata and represents lateral movement of reducing fluids. This was observed mostly at the base of fining upward sequences in channel fill facies such as SC and TS that are bounded at the bottom by the MUD facies of the previous sequence. Complete whitening of strata was also observed near the top of fining upward sequences in somewhat porous facies such as VFS and MS, but only when bounded above by the MUD facies. Units of completely whitened strata are commonly laterally continuous for several tens of feet, although a few of the completely whitened units have little lateral continuity and are wedge-shaped. Wedge-shaped units probably represent a channel fill deposit surrounded by less porous sand or mud and may be continuous out of the plane of the exposed outcrop. Another category of whitening is whitening of individual laminae in beds. This is most common in facies TS, although it also occurs in facies VFS. Laminae whitening usually occurs directly above completely whitened strata and probably represents an extension of that fluid movement into a less porous or permeable facies. Sand in whitened laminae is usually coarser than sand in the surrounding red laminae, which may be why fluids moved through them. Fluorescent dolomite cement that likely precipitated from fluids associated with hydrocarbons that whitened the Fountain is present in both completely whitened strata and in and around whitened laminae. Feldspar alteration and the abundance of

kaolinite cement are greater in completely whitened strata and along whitened laminae than in non-whitened strata. This is further evidence that whitening in these categories is the result of migrating reducing fluids. The third category of whitening consists of white reduction spots and whitening of root traces and occurs randomly in outcrop. This type makes up less than one percent of whitening and was probably caused by early reduction near organic material in bioturbated areas and along root traces. Reduction spots are probably unrelated to the reducing fluid flow event and commonly form by reduction during anaerobic decomposition of organic matter shortly after burial (Retallack, 1997).

4.8.1 PREFERENTIAL FLUID-FLOW PATHWAYS

Cross cutting relationships in outcrop and cement stratigraphy indicate that whitened strata in the Fountain Formation were caused by diagenetic events long after burial. Fluorescent cement, bitumen, and hydrocarbon inclusions in whitened strata provide evidence that whitening was likely the result of the migration of reducing aqueous fluids and oil and therefore represents paleo-fluid migration pathways. The fluids migrated laterally through the Fountain as stringers that took up less than 15% of the formation's total volume. Whitened strata are much more common in some facies than others, especially facies SC and TS. It is not surprising that most whitening is in these facies as they have the highest porosity, and studies have shown that channel fill sandstones such as these commonly constitute the migration pathway of fluids (Barker and Tellam, 2006; Schatzinger and Jordan, 1999). While the position of porous and permeable facies, such as SC and TS, played a major role in determining the path of

fluid flow, facies MUD seems to have played an equally important role. Facies MUD was likely impermeable because of the very small grain size, abundance of cements (Table 14), and lack of porosity (Figure 54). Within facies SC and TS the bulk of whitening occurs at the bases of the facies, especially if they are in contact with a paleosol mudstone from the previous sequence. Coarse channel sandstones stratigraphically separated from mudstones are far less likely to be whitened than those in direct contact with mudstones. Whitening of facies VFS and MS makes up the remainder of the whitening in the formation. These very fine grained sandstones that are rarely whitened elsewhere are almost always whitened when in contact with mudstones. The mudstones therefore played a very important role in controlling the path of fluid flow. Paleosol mudstones only make up nine percent of the measured section, yet 64% of whitened strata are concentrated directly above and below this impermeable facies. Sixty three percent of strata above and within one foot of paleosol mudstones are whitened, 40% of strata below and within one foot of paleosol mudstones are whitened, and 7% of strata greater than one foot from paleosol mudstones are whitened. Fluids in the adjacent facies likely concentrated and flowed laterally along the paleosol mudstones.



Figure 84. Whitening above and below a paleosol. The lower unit is facies VFS and the upper unit includes facies SC and TS. Whitening was observed laterally along this paleosol for nearly half a mile. This mudstone facies probably acted as a major barrier to paleo-fluid flow and controlled the pathway of fluid migration.

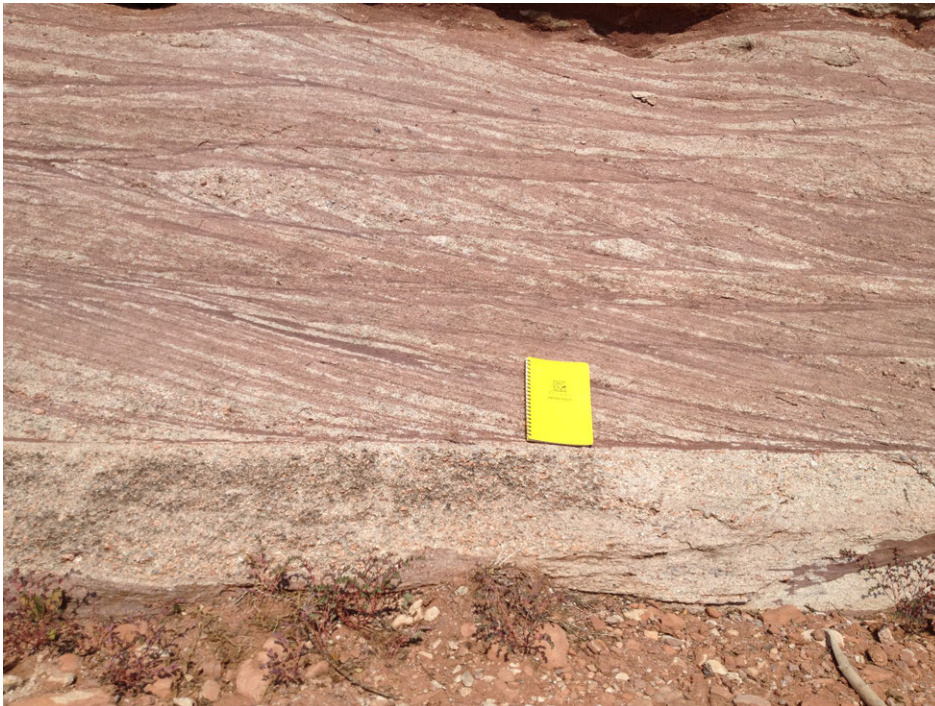


Figure 85. Complete whitening of facies SC and whitening within laminations of TS. Laminations get shallower near the top of the trough bedded unit and transitions into facies CSM where the whitening ends.



Figure 86. Whitening within facies TS ends abruptly at facies CSM. CSM is muddy and probably acted as a local barrier to fluid flow.

4.8.2 GEOGRAPHIC VARIABILITY TRENDS OF WHITENING

Whitening in the Fountain Formation follows a geographical trend for which there are multiple possible explanations. Whitening is more prevalent in the southern section of the study area and decreases to the north. This might be due to the higher percentage of channel fill sandstones in outcrops to the south. Facies SC and TS were probably the main conduits of fluid flow in the subsurface and are therefore the facies that contain most of the whitened strata. As these facies decrease in abundance to the north so does the amount of whitened strata (Fig. 87). If the prevalence of facies SC and TS in the southern sites allowed the higher percentage of whitening at those sites, the geographic trend of whitened strata ultimately comes down to changes in the

environment of deposition that favored higher energy deposition and a source of coarser material to the south.

Howard (1966) used over 1,000 paleocurrent readings to plot eleven alluvial fan deposits radiating out from the Ancestral Rockies along the Front Range. Figure 88 shows the location of the study sites overlain on the fans plotted by Howard. The closer the study site is to the apex of a fan, the more that study site's strata are the coarser, higher energy deposits represented by facies SC and TS. The southernmost study site, Hall Ranch, is estimated to be about 10 miles from an apex of a fan and contains the highest percentage of facies SC and TS at 65.8%. The northern most study site, Owl Canyon, is estimated to be about 27 miles from an apex of a fan and contains the lowest percentage of facies SC and TS at 15.6%. The middle clustered study sites, Devil's Backbone, Bobcat Ridge, Blue Sky Trail, Hwy 38 Roadcut, and Dixon Cove, sit between 14 to 19 miles from an apex of a fan and contain between 40.0 to 61.4 percent facies SC and TS, with an average of 48.2%.

Another possibility is that the direction of paleo-fluid flow caused this geographic trend in the proportion of strata whitened. The study area is northwest of the basin depo-center where sediment was buried deepest. If the paleo fluids that caused whitening were hydrocarbons there may have been more generation in the deepest portions of the basin, which are to the southeast near Denver (Matuszczak, 1973). In this situation, more hydrocarbon-bearing fluids may have been moving up dip in the southern portion of the study site. This, however, is probably not the case. The

northern-most study site has the least amount of whitened strata but the strata that was whitened there has about three times more feldspar alteration and kaolinite cement than whitened strata in other sites (Table 16). The northern site also has more fluorescent dolomite cement and it has a stronger fluorescence indicating that it may have had higher concentrations of organic matter or hydrocarbons. It is possible that just as much fluid flowed through the Owl Canyon strata as elsewhere, but a smaller percentage of permeable beds caused the fluids to focus more. This would have increased the amount of fluid through a given volume of permeable rock and increased the degree of feldspar alteration. Although the depth of the basin was not as deep due east of Owl Canyon as it is in Denver, it was likely still deep enough to produce temperatures needed for hydrocarbon generation (Matuszczak, 1973). These hydrocarbons could have migrated updip in the Fountain and passed through the Owl Canyon site.

Amount of Whitened Strata vs. Amount of Channel Sandstone Facies at Study Sites

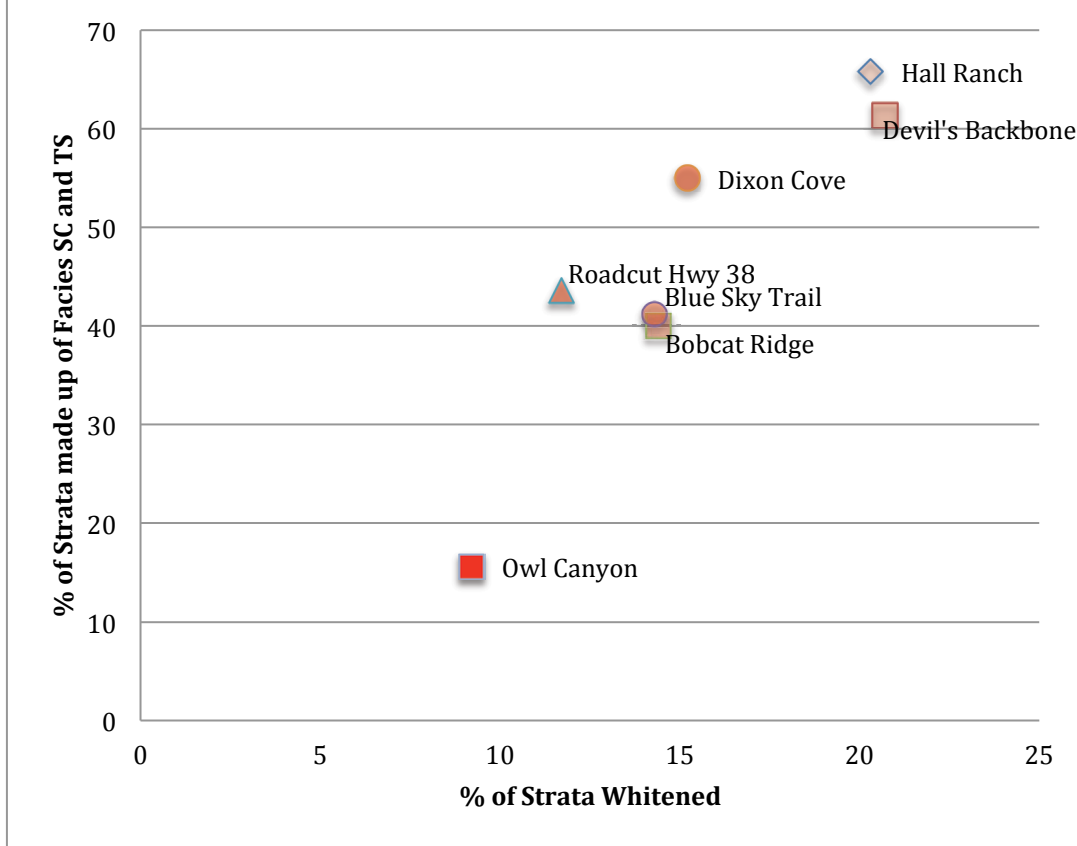


Figure 87. The decrease in whitened strata northward in the study area may be due to a decrease in facies SC and TS in the northern study sites. The amount of whitened strata follows a linear relationship with the amount of facies SC and TS present in each outcrop. Degree of transparency indicates location of outcrop with most transparent furthest south

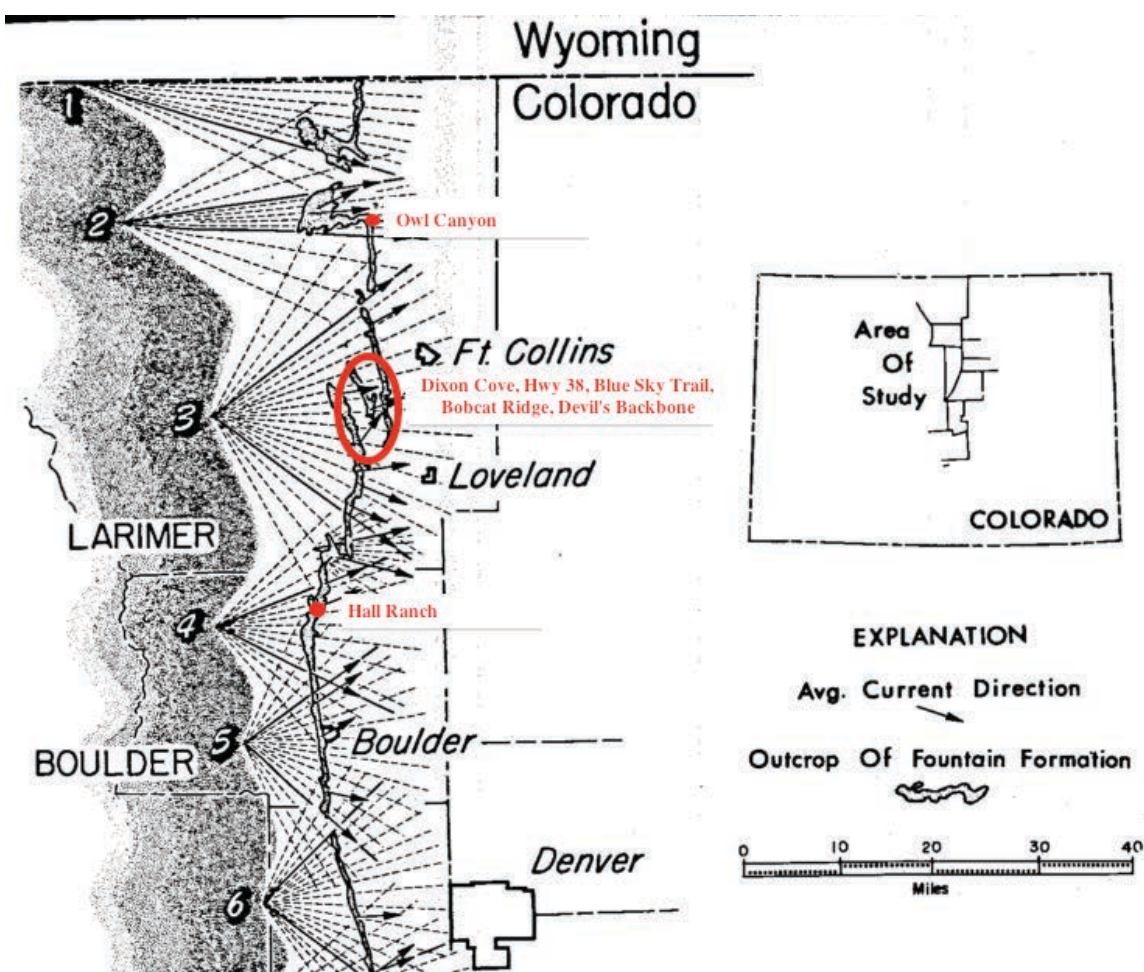


Figure 88. Locations of study sites overlain on Pennsylvanian-Permian alluvial fans radiating off of the Ancestral Rockies (after Howard, 1966). The closer a study site is to the apex of a fan the higher the percentage of facies SC and TS in outcrop at that site.

CHAPTER 5

CONCLUSIONS

The Fountain Formation was deposited in alluvial fan and fluvial environments that developed along the eastern edge of the Ancestral Rockies during the Pennsylvanian to early Permian. In the study area the formation was exposed by uplift during the Laramide orogeny. The formation dips steeply to the east into the Denver Basin where it is covered by nearly 4,000 meters of sediment. In the study area about 90% of the formation consists of subarkosic to arkosic sandstones and conglomerates. Thin mudstones and rare limestones make up the remaining 10% of strata. The formation consists of multiple fining upward sequences and within these sequences seven facies were identified, described, and classified. These include structureless conglomerates, trough cross-bedded sandstones, sandstones with thin interbedded mud drapes, very fine grain sandstones with horizontal laminations, massive sandstones, mudstones, and limestones. These facies are interpreted as channel lag, channel dunes, pools in abandoned channels, migrating bars and sand sheets, bioturbated sands, paleosols, and lacustrine deposits.

The Fountain Formation is a classic redbed deposit and owes its red and pink hues to hematite cement that was precipitated shortly after burial. The formation has a complex diagenetic history. About 15% of strata in the study area have been whitened and this was most likely caused by the reduction and removal of hematite cement by migrating aqueous fluids and oil late in the formation's diagenetic history. Evidence of

diagenetic alteration caused by fluid movement includes geographically widespread whitening of the Fountain, reported whitening in both non-marine and marine facies (McLaughlin, 1947; Garner, 1963), whitened strata cross cutting depositional features, and the confinement of late stage organic rich dolomite cement, bitumen, and hydrocarbon inclusions to whitened strata. Whitened strata therefore likely represent fluid migration pathways and are found mostly in coarse channel sandstones and are especially common when the channel sandstones are adjacent to laterally continuous paleosol mudstones. The reducing paleo-fluid probably concentrated along impermeable mudstones and moved laterally along them in the coarse channel sandstones. Some laterally continuous mudstones that are interpreted as valley wide paleosols may have acted as major barriers to fluid flow, controlling the spatial distribution of migration pathways in the formation.

Petrographic and fluorescent light microscopy provides evidence that reducing paleo-fluids that whitened sections of the Fountain Formation contained hydrocarbons. Fluorescent microcrystalline dolomite cement that likely precipitated from a reducing paleo-fluid contains high concentrations of organic matter and hydrocarbon inclusions. It is also associated with bitumen that may have been oil that was degraded upon uplift and exposure in outcrop.

Evidence from fluid inclusions indicates that fluid migration that caused whitening in the Fountain occurred sometime after the formation was buried to depths that exposed the formation to temperatures of at least 69°C. Using this burial temperature,

a depth of 1.3 to 2.0 km can be derived depending upon the paleo-geothermal gradient. Therefore, the fluid migration has a maximum age of Late Cretaceous, as this amount of sediment would not have been present until then. This would have been when Laramide deformation and uplift was beginning and strengthens the case that fluid migration occurred after this time. A complete sequence of events is shown in Figure 89. The Laramide orogeny caused the uplift of the Front Range block, which eventually exposed the Fountain on the western flank of the basin but buried it beneath increasing amounts of sediment to the east. Deposition of the Pierre Shale in the Late Cretaceous had buried sediments in the center of the basin to depths deep enough to produce the temperatures needed for hydrocarbon generation (Lee and Bethke, 1994) and the Laramide Orogeny in the Late Cretaceous to Eocene tilted the Fountain beds allowing for up dip migration of hydrocarbons. The depth to which the Fountain at the study sites was buried may not have been enough to generate temperatures to produce hydrocarbons, so the fact that hydrocarbon inclusions and bitumen is present indicates migration of oil from a deeper source. The source may have been Fountain equivalents consisting of marine shales and carbonates further east in the basin. The formation consists of coarse clastic material on the western side of the basin, which provided good conduits to fluid flow. Some migrated oil may have either escaped at the surface or concentrated in sediment that has since been eroded during exhumation. Some of the hydrocarbons that migrated through the Fountain Formation may have helped charge the overlying Lyons Formation. Although there does not seem to be much potential for petroleum exploration in the Fountain in this area, the whitened strata in the formation may be a good analog for hydrocarbon migration pathways in basins with

similar histories and lithologies that have not been exhumed. The way in which fluids move in the subsurface is an important component in understanding petroleum systems. In the Fountain Formation, hydrocarbon-bearing fluids probably migrated as stringers through the channel sandstones and took up less than 15% of the total volume of rock in the formation.

The amount of whitened strata decreases to the north and is probably related to the decrease in coarse channel sandstones to the north, specifically facies SC and TS. The decrease in coarse channel sandstones correlates with an increasing distance from the location of paleo-alluvial fans that came off of the Ancestral Rockies. Although the amount of whitened strata decreases, the increasing degree of feldspar alteration suggests that the volume of paleo-fluid that flowed through the northern sites may not have been much different from that which flowed through strata in the southern sites.

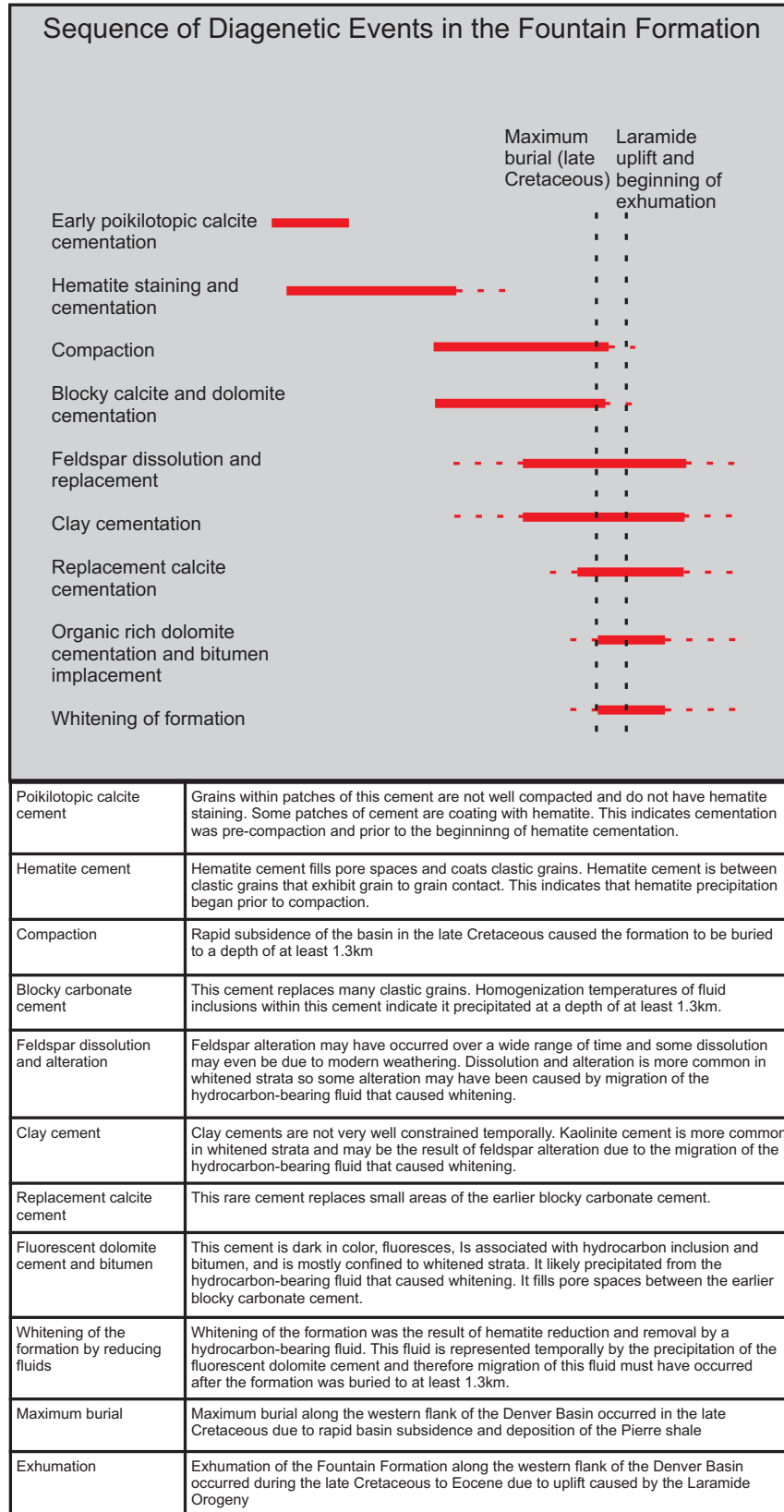


Figure 89. Complete list of sequence of diagenetic events with time constraints

LIST OF REFERENCES

- Barker, R., & Tellam, J. (2006). Fluid flow and solute movement in sandstones; the onshore UK Permo-Triassic red bed sequence. *Geological Society Special Publications*, 263
- Blakey, R. (2011). Paleogeography and Geologic Evolution of North America. *Paleogeography*. Retrieved October 1, 2012 from <http://www2.nau.edu/rcb7/index.html>
- Beitler, B. (2005). Fingerprints of Fluid Flow: Chemical Diagenetic History of the Jurassic Navajo Sandstone, Southern Utah, U.S.A. *Journal of Sedimentary Research*, 75(4), 547-561.
- Berkman, F., & Watterson, N. (2010). Interpretive Geothermal Gradient Map of Colorado. Colorado Geological Survey. Retrieved February 19, 2013 from http://geosurvey.state.co.us/SiteCollectionDocuments/EnergyResources/Geothermal/Plate_1_Interpretive_Geothermal_Gradient_Map_of_Colorado.pdf
- Berner, R. A. (1969). Goethite stability and the origin of red beds. *Geochimica Et Cosmochimica Acta*, 33(2), 267-273.
- Boggs, S. Jr. (2012) *Principles of Sedimentology and Stratigraphy*. Pearson Prentice Hall: Upper Saddle River, NJ.
- Bove, D. J., Hon, K., Budding, K. E., Slack, J. F., Snee, L. W., & Yeoman, R. A. (2001). Geochronology and geology of late Oligocene through Miocene volcanism and mineralization in the western San Juan Mountains, Colorado. *U. S. Geological Survey Professional Paper*
- Braddock, W., Calvert, R., O'Connor, J., Swann, G. (1989). *Geologic Map of the Horsetooth Reservoir Quadrangle, Larimer County, Colorado* (map). 1:24,000. Washington D.C.: USGS
- Budnik, R. T. (1986). Left-lateral intraplate deformation along the ancestral Rock Mountains; implications for late Paleozoic plate motions. *Tectonophysics*, 132(1-3), 195-214
- Chan, M. A., Parry, W. T., & Bowman, J. R. (2000). Diagenetic hematite and manganese oxides and fault-related fluid flow in Jurassic sandstones, southeastern Utah. *AAPG Bulletin*, 84(9), 1281-1310
- Clayton, J. L., & Swetland, P. J. (1980). Petroleum generation and migration in the Denver Basin. *AAPG Bulletin*, 64(10), 1613-1633

- Cole, J. C., & Braddock, W. A. (2009). Geologic map of the Estes Park 30' X 60' quadrangle, north-central Colorado. *Scientific Investigations Map*
- Cole, J., Trexler, J., Cashman, P., Miller, I., Shroba, R., Cosca, M., Workman, J. (2010). Beyond Colorado's Front Range – A new look at Laramie basin subsidence, sedimentation, and deformation in north-central Colorado. *GSA Field Guide*: 18. Geological Society of America
- Corbett, M. K. (1966). The geology and structure of the Mount Richthofen-Iron Mount region, north central Colorado. *Mountain Geologist*, 3(1), 3-21
- Cross, C. (1894). Pikes Peak, Colorado. *Geological Atlas Folio*
- Dembicki, H. (1989). Secondary Migration of Oil; Experiments Supporting Efficient Movement of Separate, Buoyant Oil Phase Along Limited Conduits. *AAPG Bulletin*, 73(8), 1018
- Denver Core Research Center (2013). U.S. Geological Survey. Core Library Number E053. <http://my.usgs.gov/crcwc/core/report/11788>
- Dickinson, W. R., & Lawton, T. F. (2003). Sequential intercontinental suturing as the ultimate control for Pennsylvanian ancestral Rocky Mountains deformation. *Geology*, 31(7), 609-612
- Dravis, J. J., & Yurewicz, D. A. (1985). Enhanced carbonate petrography using fluorescence microscopy. *Journal Of Sedimentary Petrology*, 55(6), 795-804
- El-Banna, M. (1993). Paleosols, provenance, and diagenesis of the Fountain Formation, NE Colorado and SE Wyoming. Colorado State University, Fort Collins, CO., M.S. Thesis
- Elliott, W., Roden-Tice, M. K., & Higley, D. K. (1996). Thermal history of the Denver Basin 'hot spot'. *Annual Meeting Expanded Abstracts - American Association Of Petroleum Geologists*, 541-42.
- Friend, P. (1966). Clay fractions and colours of some Devonian red beds in the Catskill Mountains, U.S.A. *Quarterly Journal Of The Geological Society Of London*, 122, Part 3273-288
- Garbarini, G., & Veal, H. K. (1968). Potential of Denver Basin for disposal of liquid wastes, subsurface disposal in geologic basins—a study of reservoir strata: *American Association of Petroleum Geologists Memoir*, p. 165–185
- Garden, I. R. (2001). An exhumed paleo-hydrocarbon migration fairway in a faulted carrier system, Entrada Sandstone of SE Utah, USA. *Geofluids*, 195-213.

- Garner, H. (1963). Fountain Formation, Colorado: A Discussion. *New York*, (October), 1299-1301.
- Goldstein, R. H., & Reynolds, T. (1994). Systematics of fluid inclusions in diagenetic minerals. *SEPM Short Course Notes*, 31
- Goldstein, R. H. (2001). Fluid Inclusions: Phase Relationships - Methods - Applications. Fluid inclusions in sedimentary and diagenetic systems. *Lithos*. 55(1-4).
- Higley, D. K., & Cox, D. O. (2007). Oil and gas exploration and development along the front range in the Denver Basin of Colorado, Nebraska, and Wyoming. *U. S. Geological Survey Digital Data Series DDS-69-P*
- Higley, D., Pollastro, R., & Clayton, J. (1995) USGS National Oil and Gas Assessment, Denver Basin Province (039).
- Howard, J. (1966). Patterns of sediment dispersal in the Fountain Formation of Colorado. *The Mountain Geologist*, 3(4), 147.
- Hoy, R. G., & Ridgway, K. D. (2002). Syndepositional thrust-related deformation and sedimentation in an ancestral Rocky Mountains basin, Central Colorado Trough, Colorado, USA. *Geological Society Of America Bulletin*, 114(7), 804-828
- Hubert, J. F. (1960). Syngenetic Bleached Borders on Detrital Red Beds of the Fountain Formation, Front Range, Colorado. *Geological Society of America Bulletin*, 71(1), 95.
- Kennedy, M. J., Pevear, D. R., & Hill, R. J. (2002). Mineral surface control of organic carbon in black shale. *Science*, 295(5555), 657-660
- Kluth, C. F., & Coney, P. J. (1981). Plate tectonics of the ancestral Rocky Mountains. *Geology*, 9(1), 10-15
- Kluth, C. F., Ye, H., Royden, L. H., Burchfiel, C., & Schuepbach, M. (1998). Late Paleozoic deformation of interior North America; the greater ancestral Rocky Mountains; discussion and reply. *AAPG Bulletin*, 82(12), 2272-2279
- Kluth, C. F., & McCreary, J. A. (2006). Reinterpretation of the geometry and orientation of the late Paleozoic Frontrange Uplift. *Abstracts With Programs - Geological Society Of America*, 38(6), 29
- Knight, S. (1929). The Fountain and the Casper Formations of the Laramie Basin; a Study on Genesis of Sediments. *Wyoming Univ. Pub. Sci. Geology*, 1(1), 1-.
- Larter, S., Bowler, B., Chen, M., Brincat, D., Bennett, B., Noke, K., Donohoe, P. (1996). Molecular Indicators of Secondary Oil Migration Distances. *Nature*, 383(17).

- Lee, M. & Bethke, C. (1994). Groundwater Flow, Late Cementation, and Petroleum Accumulation in the Permian Lyons Sandstone, Denver Basin. *AAPG Bulletin*, 78(2), 221-241.
- Levandowski, D. W., Kaley, M. E., Silverman, S. R., & Smalley, R. G. (1973). Cementation in Lyons Sandstone and its Role in Oil Accumulation, Denver Basin, Colorado. *AAPG Bulletin*, 57(11), 2217-2244
- Lindsey, D. (2000). Petrology of arkosic sandstones, Pennsylvanian Minturn Formation and Pennsylvanian and Permian Sangre de Cristo Formation, Sangre de Cristo Range, Colorado - data and preliminary interpretations. *USGS open file report*, 474
- Maples, C. G., & Suttner, L. J. (1990). Trace Fossils and Marine-Nonmarine Cyclicity in the Fountain Formation (Pennsylvanian : Morrowan / Atokan) Near Manitou Springs, Colorado. *Journal of Paleontology*, 64(6).
- Margulies, L. L., Rozen, H. H., & Nir, S. S. (1988). Model for competitive adsorption of organic cations on clays. *Clays And Clay Minerals*, 36(3), 270-276.
- Matuszczak, R. A. (1973). Wattenberg Field, Denver Basin, Colorado. *Mountain Geologist*, 10(3), 99-105.
- Maughan, E.K., and Ahlbrandt, T.S., (1985). Pennsylvanian and Permian rocks, northern Front Range, Colorado. *SEPM Field Trip Guide: American Association of Petroleum Geology Rocky Mountain Section*, p. 99- 113.
- Maughan, E. K., & Wilson, R. F. (1963). Permian and Pennsylvanian strata in southern Wyoming and northern Colorado. *Rocky Mountain Association of Geologists* 95-104.
- McKee, J. W., Jones, N. W., & Anderson, T. H. (1988). Las Delicias Basin; a record of late Paleozoic arc volcanism in northeastern Mexico. *Geology*, 16(1), 37-40
- McLaughlin, K. P. (1947). Pennsylvanian stratigraphy of the Colorado Springs Quadrangle, Colorado. *Bulletin Of The American Association Of Petroleum Geologists*
- Meyer, A. J. (2007). Variations Among Paleosol Characteristics In Relation to Fluvial Deposits, Pennsylvanian Fountain Formation, Northern Colorado Front Range. Colorado State University, Fort Collins, CO., M.S. Thesis
- Miall, A. D. (1977). A review of the braided-river depositional environment. *Earth-Science Reviews*, 13(1), 1-62.

- Miall, A. D. (1996). *The geology of fluvial deposits; sedimentary facies, basin analysis, and petroleum geology*. Federal Republic of Germany: Springer-Verlag : Berlin, Federal Republic of Germany.
- Napp, K., Ethridge, F. (1985) Depositional Systems of Fountain Formation and its Basinal Equivalents, Northwest Denver Basin, Colorado. Colorado State University, Fort Collins, CO., Ph.D. Dissertation
- Obradovich, J. D. (2002). Geochronology of Laramide synorogenic strata in the Denver Basin, Colorado. *Rocky Mountain Geology*, 37(2), 165-171.
- Parry, W. T., & Blamey, N. J. F. (2010). Fault fluid composition from fluid inclusion measurements, Laramide age Uinta thrust fault, Utah. *Chemical Geology*, 278(1-2), 105-119.
- Parry, W. T., Chan, M. a., & Beitler, B. (2004). Chemical bleaching indicates episodes of fluid flow in deformation bands in sandstone. *AAPG Bulletin*, 88(2), 175-191.
- Rall, E. P. (1996). *Influence of highstands and lowstands on Virgil and Wolfcamp paleogeography in the Denver Embayment, eastern Colorado*. (pp. 321-334). Society for Sedimentary Geology, Rocky Mountain Section, United States.
- Reeves, C. (1976). *Caliche; origin, classification, morphology and uses*. Estacado Books. Lubbock, Texas, United States.
- Retallack, G. (1997). *A Colour Guide to Paleosols*. John Wiley & Sons Ltd. West Sussex, England.
- Roedder, E. (1984) *Fluid Inclusions. Reviews in Mineralogy Volume 12*. Mineralogical Society of America. Book Crafters, Inc. Chelsea, Michigan, United States.
- Royer, D. L., Berner, R. A., Montanez, I. P., Tabor, N. J., & Beerling, D. J. (2004). CO₂ (sub 2) as a primary driver of Phanerozoic climate. *GSA Today*, 14(3), 4-10
- Russo, F., Neri, C., Mastandrea, A., & Baracca, A. (1997). The mud mound nature of the Cassian platform margins of the Dolomites; a case history; the Cipit boulders from Punta Grohmann (Sasso Piatto Massif, northern Italy). *Facies*, 3625-36
- Rust, B. R. (1972). Structure and process in a braided river. *Sedimentology*, 18(3-4), 221-245.
- Schatzinger, R., & Jordan, J. (1999). Reservoir characterization; recent advances. *AAPG Memoir*, 71
- Schlesinger, W. (1985). The formation of caliche in soils of the Mojave Desert, California. *Geochimica et Cosmochimica Acta*. 49 (1), 57-66

- Smith, N. D. (1971). Pseudo-planar stratification produced by very low amplitude sand waves. *Journal Of Sedimentary Petrology*, 41(1), 69-73.
- Smith, N. D. (1972). Some sedimentological aspects of planar cross-stratification in a sandy braided river. *Journal Of Sedimentary Petrology*, 42(3), 624-634.
- Soreghan, G. S., & Gilbert, M. (2006). The end of the ancestral Rocky Mountains. *Abstracts With Programs - Geological Society Of America*, 38(1), 36
- Soreghan, G. S., Keller, G., Gilbert, M., Chase, C. G., & Sweet, D. E. (2012). Load-induced subsidence of the ancestral Rocky Mountains recorded by preservation of Permian landscapes. *Geosphere*, 8(3), 654-668
- Suttner, L. J., & Dutta, P. K. (1986). Alluvial sandstone composition and paleoclimate; I, Framework mineralogy. *Journal Of Sedimentary Petrology*, 56(3), 329-345.
- Suttner, L., Langford, R., Shultz, A. (1984). *Sedimentology of the Fountain Fan-Delta Complex near Manitou Springs and Canon City, Colorado*. SEPM : Tulsa, OK, United States
- Sutton, S. J., Ethridge, F. G., Almon, W. R., Dawson, W. C., & Edwards, K. K. (2004). Textural and sequence-stratigraphic controls on sealing capacity of Lower and Upper Cretaceous shales, Denver Basin, Colorado. *AAPG Bulletin*, 88(8), 1185-1206.
- Sweet, D. E., & Soreghan, G. S. (2009). Late Paleozoic tectonics and paleogeography of the ancestral Front Range: Structural, stratigraphic, and sedimentologic evidence from the Fountain Formation (Manitou Springs, Colorado). *Geological Society of America Bulletin*, 122(3-4), 575-594.
- Thomas, W. A. (1983). Continental margins, orogenic belts, and intracratonic structures. *Geology*, 11(5), 270-272
- Turner, P. (1980). *Continental Red Beds*. Amsterdam. Elsevier Scientific Publishing Company.
- Van de Kamp, P. C., & Leake, B. E. (1994). Petrology, geochemistry, provenance, and alteration of Pennsylvanian-Permian arkose, Colorado and Utah; with Suppl. Data 9448. *Geological Society Of America Bulletin*, 106(12), 1571-1582
- Walker, T. R. (1967). Formation of red beds in modern and ancient deserts. *Geological Society Of America Bulletin*, 78(3), 353-368.
- Wilson, D.W., (2002). Petrographic provenance analysis of Kiowa Core sand- stone samples, Denver Basin, Colorado: *Rocky Mountain Geology*, v. 37, p. 173-187.

Wolfe, J. A. (1953). Geology of the Masonville Mining District, Larimer County, Colorado. Colorado School of Mines, Golden, Colo., M.S. Thesis

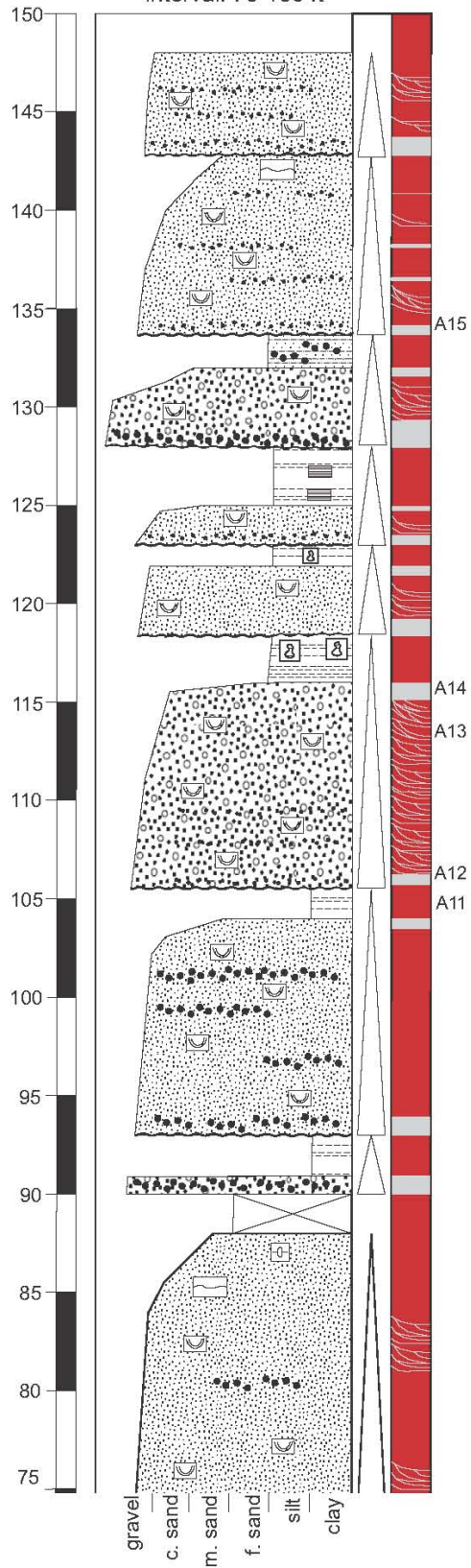
Ye, H., Royden, L., Burchfiel, C., & Schuepbach, M. (1996). Late Paleozoic deformation of interior North America; the greater ancestral Rocky Mountains. *AAPG Bulletin*, 80(9), 1397-1432

APPENDIX

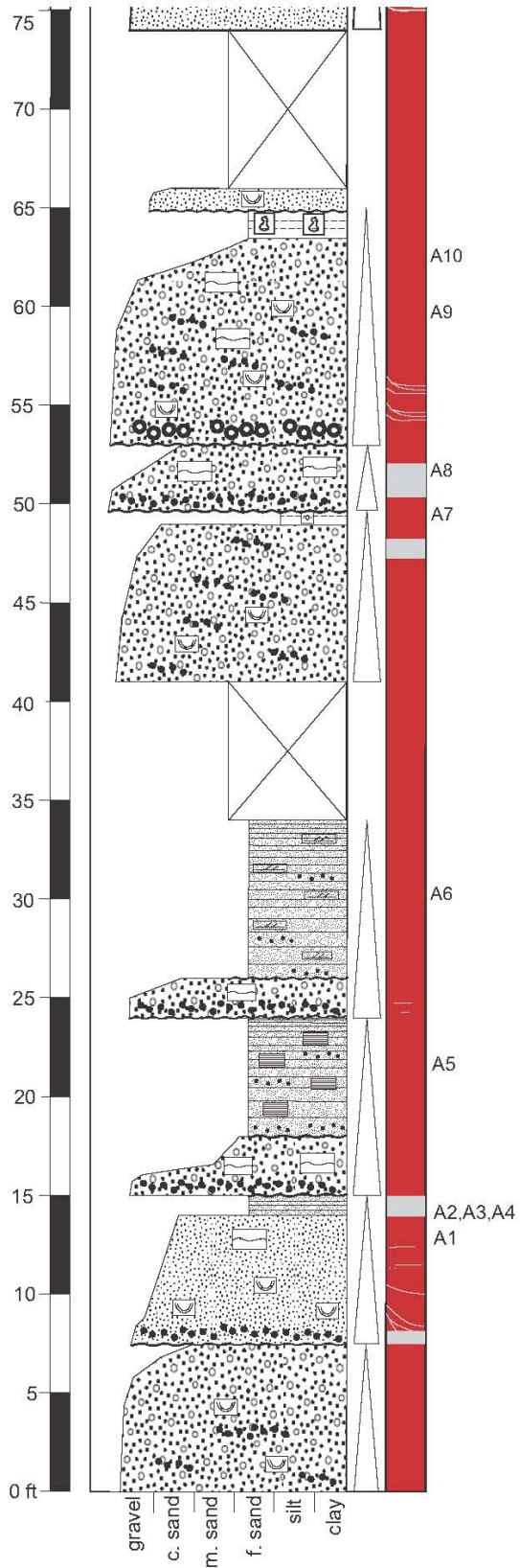
Symbols for Stratigraphic Columns

-  Trough cross bedding
-  Planar cross bedding
-  Horizontal lamination
-  Sand with mud drapes
-  Load casts
-  Pedogenic nodules
-  Imbricated clasts
-  Bioturbation
-  Granules
-  Pebbles
-  Cobbles
-  Erosional Surface
- A1 Sample location
-  Whitened strata
-  Whitened laminations only

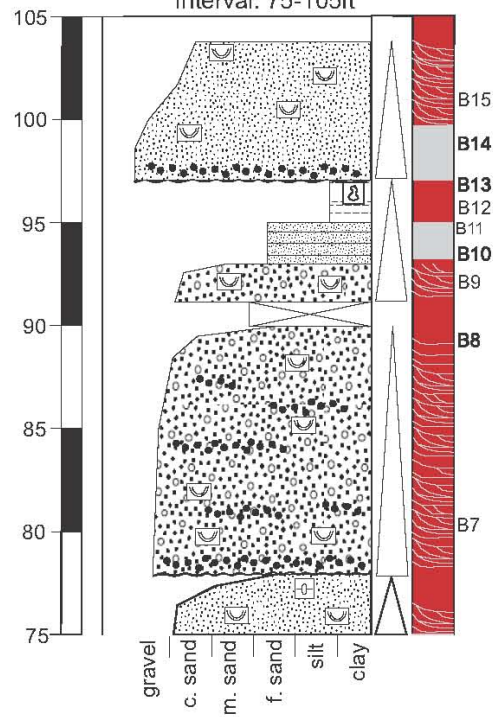
Location: Hall Ranch
Interval: 75-150 ft



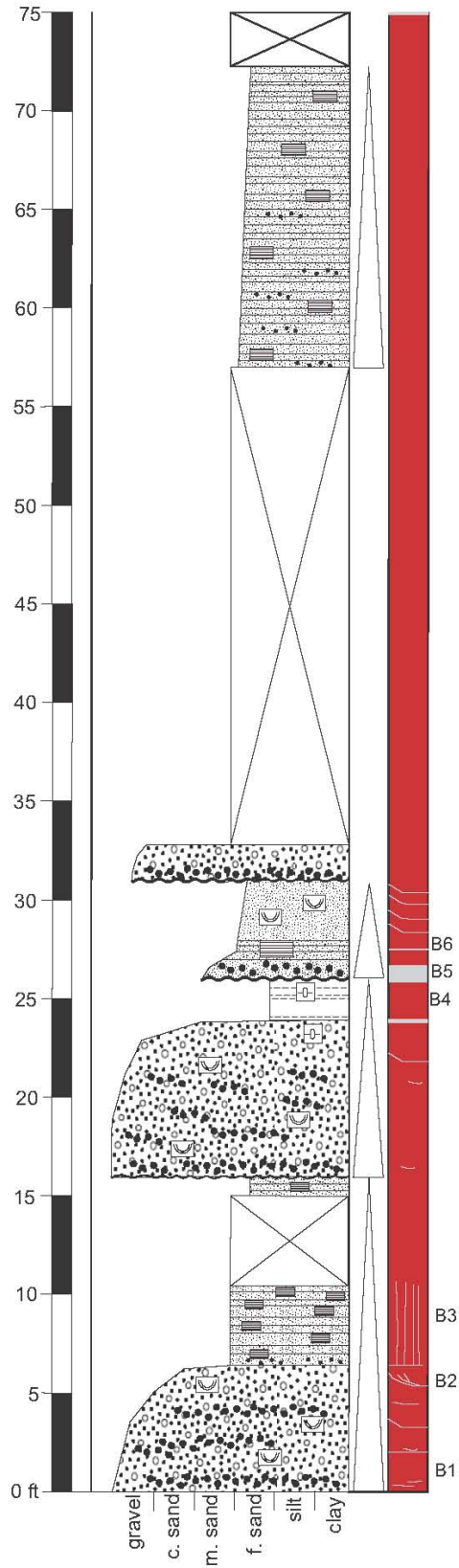
Location: Hall Ranch
Interval: 0-75ft



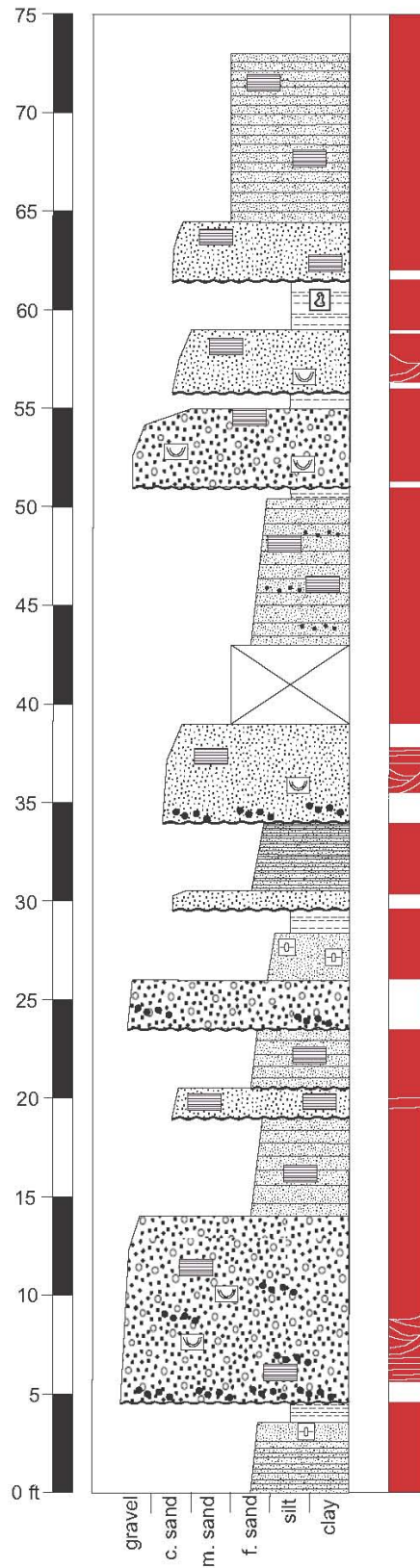
Location: Devil's Backbone
Interval: 75-105ft



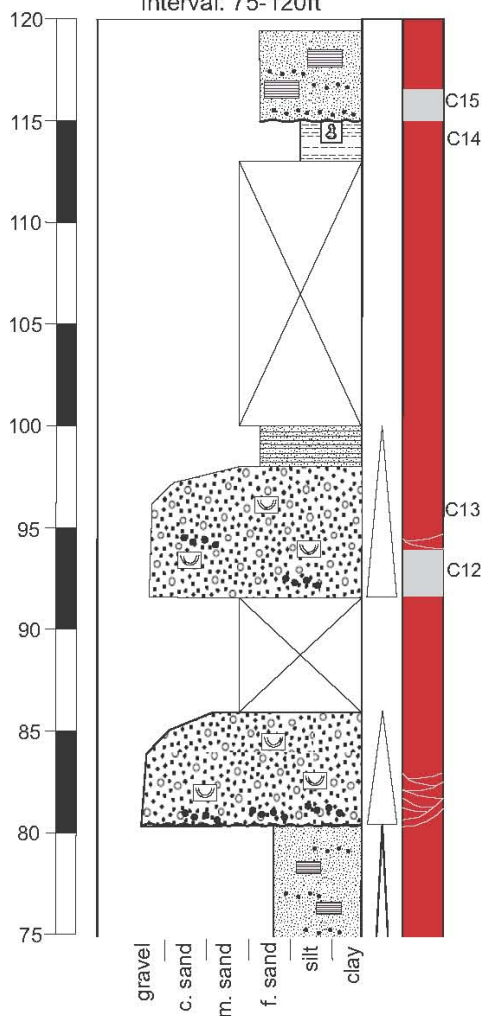
Location: Devil's Backbone
Interval: 0-75ft



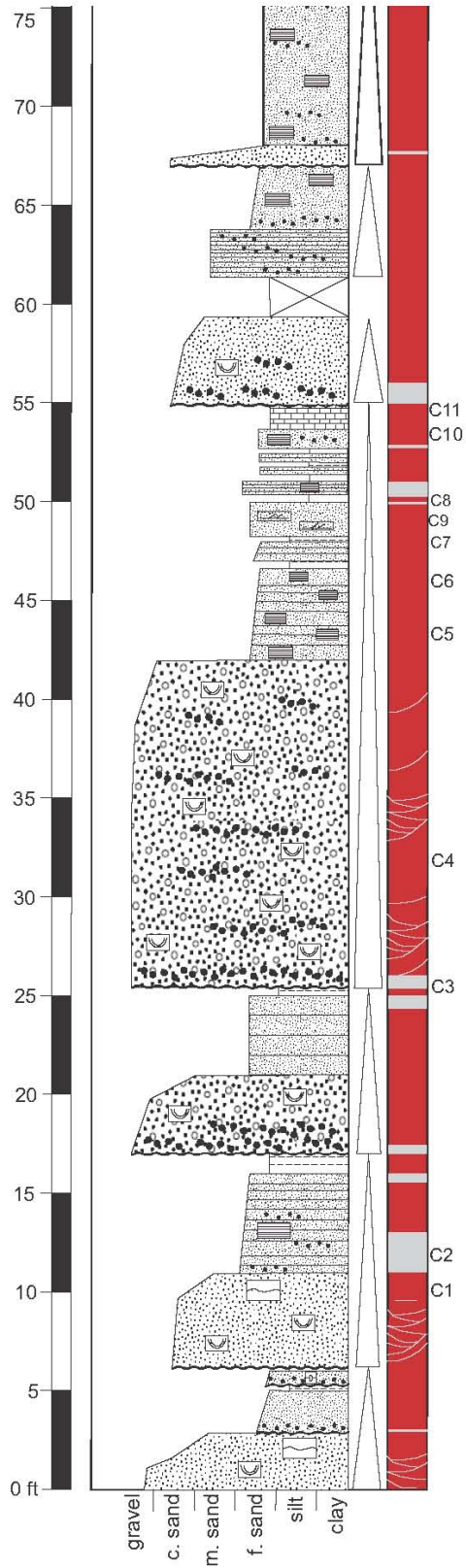
Location: Bobcat Ridge
Interval: 0-75ft



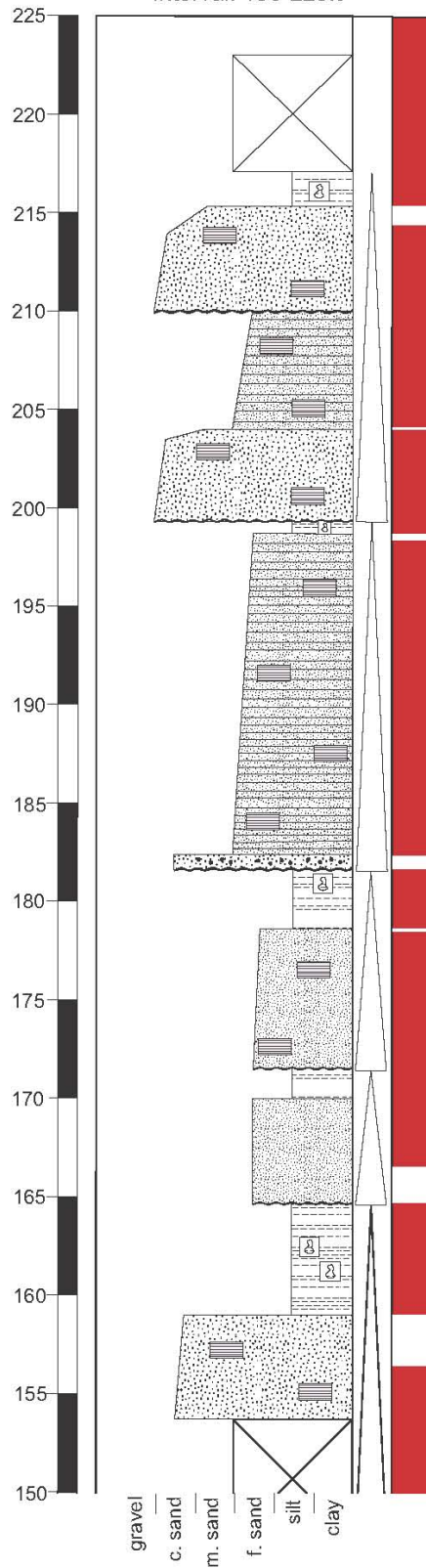
Location: Blue Sky Trail
Interval: 75-120ft



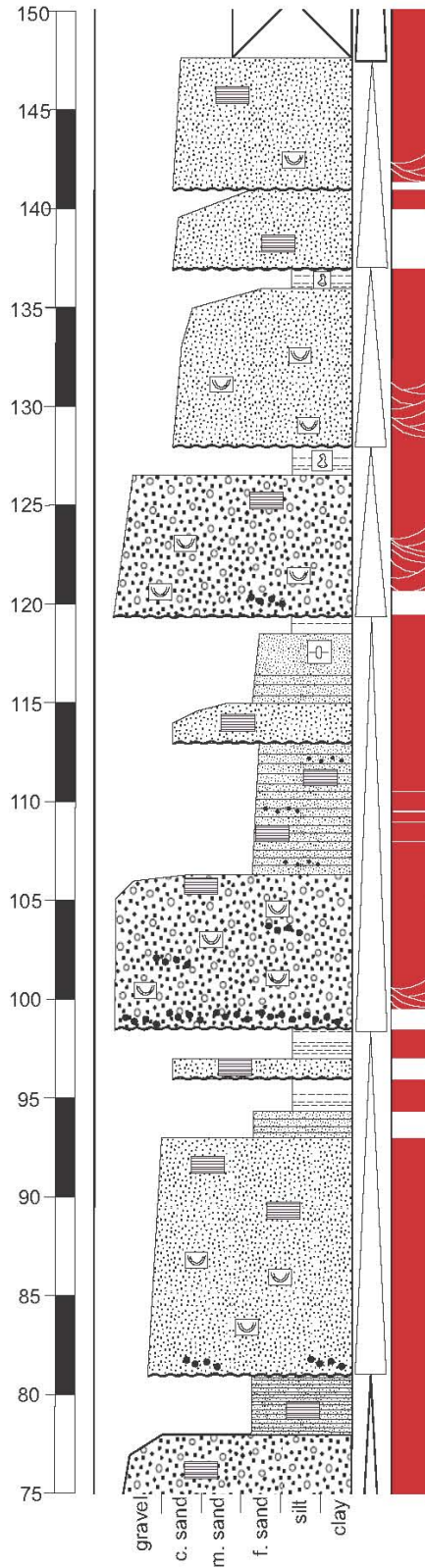
Location: Blue Sky Trail
Interval: 0-75ft



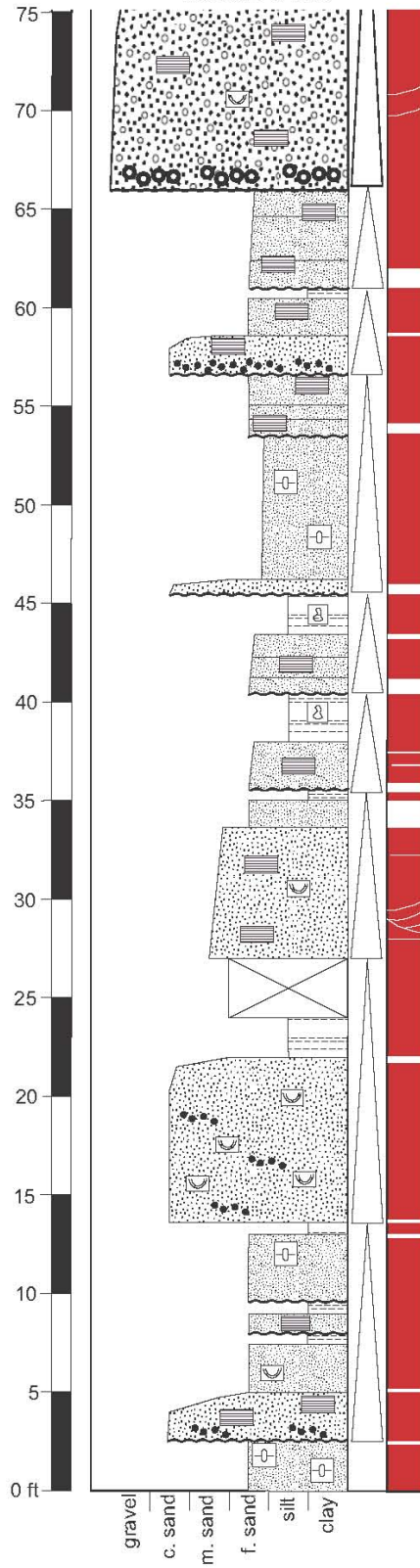
Location: Hwy 38 Roadcut
Interval: 150-225ft



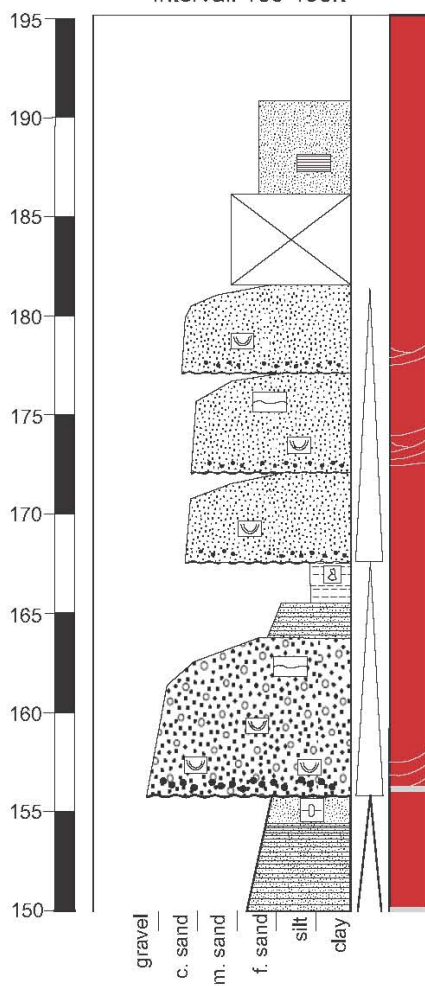
Location: Hwy 38 Roadcut
Interval: 75-150ft



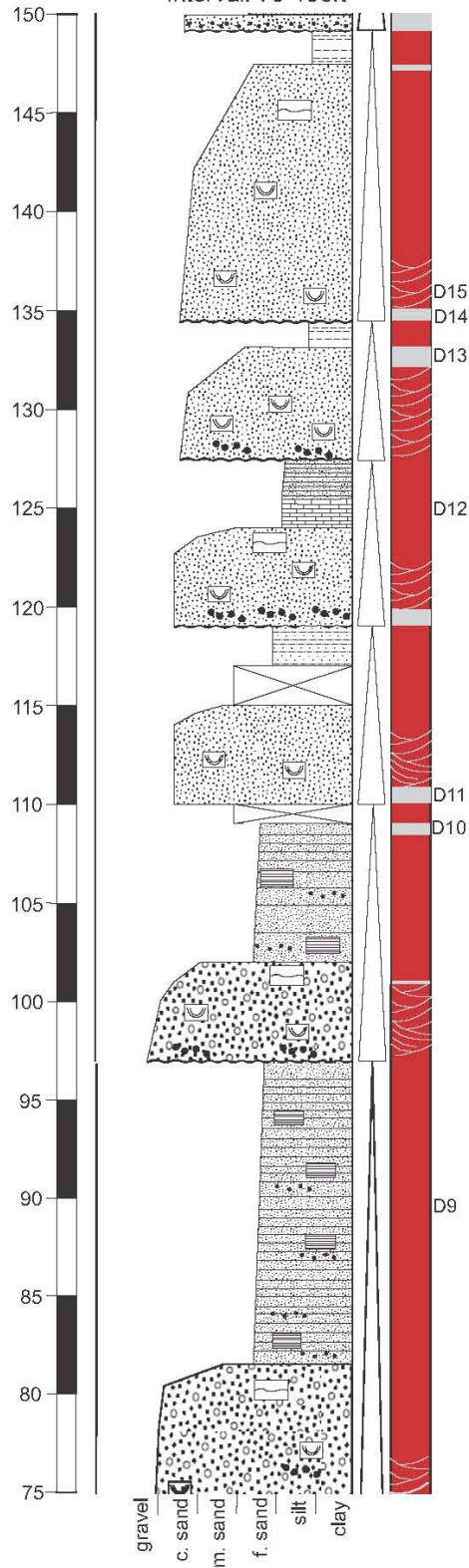
Location: Hwy 38 Roadcut
Interval: 0-75ft



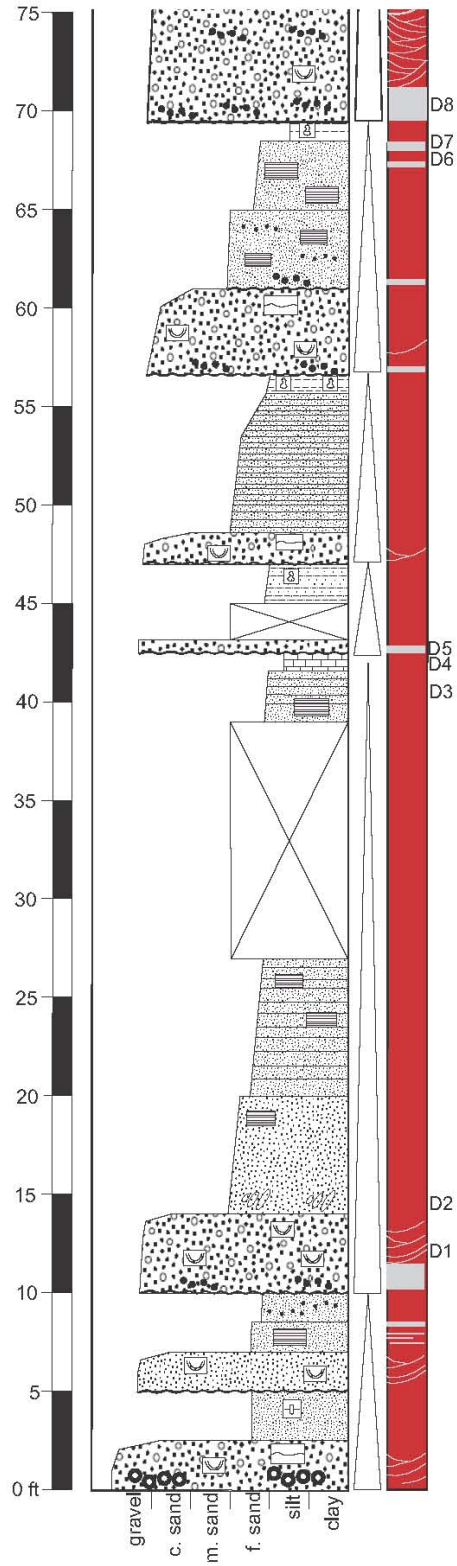
Location: Dixon Cove
Interval: 150-195ft



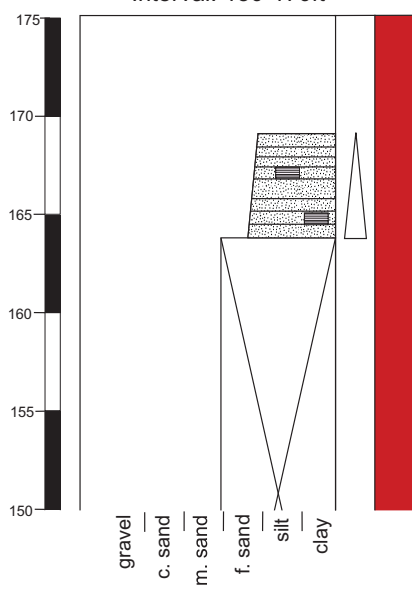
Location: Dixon Cove
Interval: 75-150ft



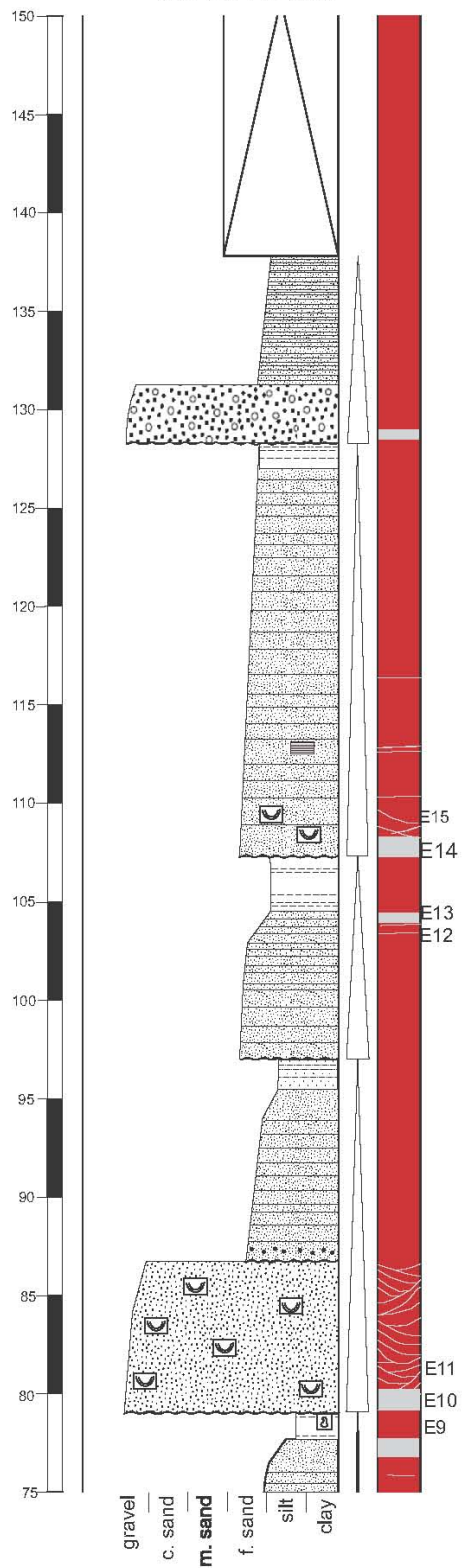
Location: Dixon Cove
Interval: 0-75ft



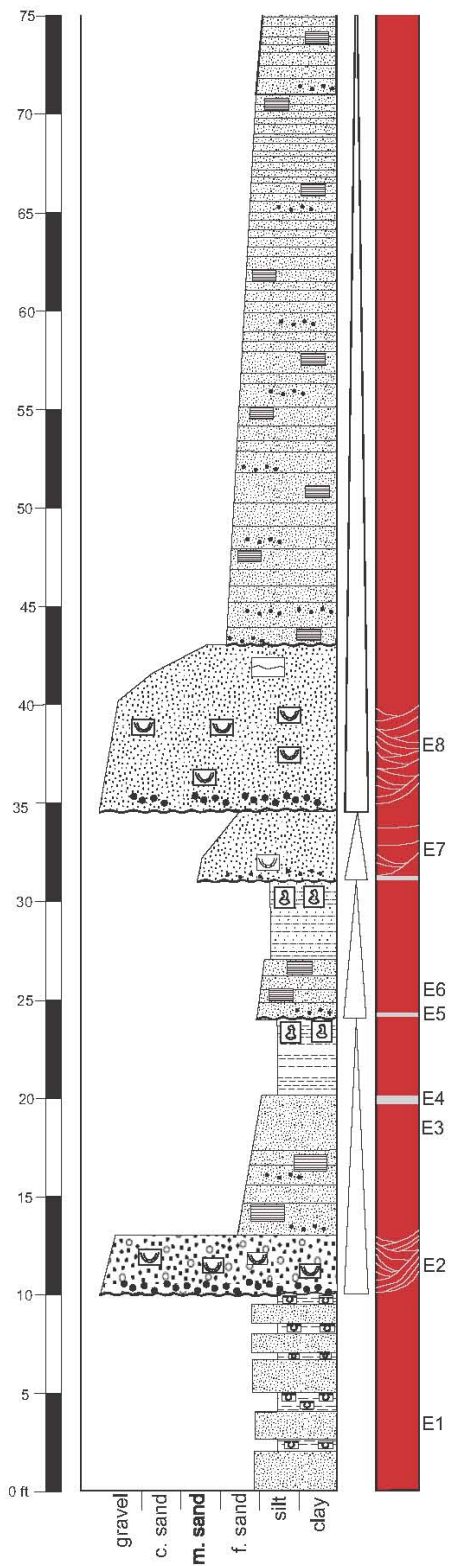
Location: Owl Canyon
Interval: 150-170ft



Location: Owl Canyon
Interval: 75-150ft



Location: Owl Canyon
Interval: 0-75ft



Measured Units Hall Ranch

Unit	Lithology	Classification	Total (ft)	Complete White (ft)	Laminations White (ft)	Hand Sample	Thin Section
1	cong ss	SC/TS	7.5	0	0		
2	cong ss	SC/TS/CSM	6.1	0.5	2	1,4	A1
3	vf ss	VFS	0.8	0.8	0	2,3,5,6,A, B,C	A2,A3,A4
4	cong ss	SC/CSM	2.3	0	0		
5	vf ss	VFS	6	0	0	7,23	A5
6	cong ss	SC/CSM	1.8	0	0.18		
7	vf ss	VFS	8	0	0	18	
8	cong ss	SC/TS	8	0.25	1		
9	mudstone	MUD	0.5	0	0	8	A7
10	cong ss	SC	1.2	1.2	0	9	A8
11	c ss	CSM	2.2	0	0		
12	cong ss	SC/TS/CSM	10.5	0.17	0	10,11	A9,A10
13	siltstone	MUD	1	0	0	12	
14	c ss	TS	1.3	0	0		
15	c ss	SC/TS/CSM/MS	14	0	3.5		
16	cong ss	SC	1	1	0		
17	claystone	MUD	1.8	0	0		
18	cong ss	SC/TS	11	1.8	0	13	
19	claystone	MUD	1.5	0	0	14	A11
20	cong ss	SC/TS	11	2	9	15,16,17	A12,A13, A14
21	siltstone	MUD	2.5	0	0		
22	c ss	TS	3.1	1.97	0.25		
23	siltstone	MUD	1.1	0	0		
24	c ss	SC/TS	2	0.8	0.1		
25	silty ss	MUD	2.5	0	0		
26	cong ss	SC/TS	3.9	1.33	2.57		
27	silty ss	MS	1	0	0		
28	vc ss	SC/TS/CSM	7	0.58	3	25	A15
29	c ss	SC/TS	5	1.2	3.8		
					25.4 x 0.44		
	Total		125.6	13.6	11.938		

Measured Units Hall Ranch

Unit	Remarks
1	gravel, poor sort
2	white in x-beds, at bottom
3	all white at study area but fades orange to east
4	erosional scour at base
5	bi modal grain size horizontal laminations
6	few white streaks in middle
7	strike and dip taken here: N20E, 14E
8	white top, some white streaks
9	root traces. paleosol
10	all white. Good sort
11	mud streaks
12	floating clasts >5cm at base
13	carbonate nodules. paleosol
14	thin ss bed
15	some white in laminations
16	all white
17	paleosol
18	bottom and top white. several stacked channel
19	paleosol
20	bottom and top white, white in laminations
21	lots of carbonate nodules. paleosol
22	white top and bottom, some white streaks
23	carbonate nodules. paleosol
24	white top and bottom, some white streaks
25	silty laminated ss
26	cobbles at base. white top and bottom, white in laminations
27	cobbles floating in silt/sand
28	white bottom, some white streaks. muddy top
29	white bottom, white in laminations. clastic dykes to SE

Measured Units Devil's Backbone

Unit	Lithology	Classification	Total (ft)	Complete White (ft)	Laminations White (ft)	Hand Sample	Thin Section
1	cong ss	SC/TS	7	0.17	1	B1,B2	B1,B2
2	f ss	VFS	3.7	0.08	0	B3	B3
3	f ss	VFS	0.8	0	0		
4	cong ss	SC/TS	8	0.17	0	B4,B5	
5	siltstone	MUD	2.3	0	0	B6	B4
6	f ss	SC/TS	5.5	0.75	0.5	B7,B8	B5,B6
7	cong ss	SC	2.7	0	0		
8	f ss	VFS	14	0.08	0	B9	
9	c ss	TS/MS	2.8	0.17	1	B10	
10	cong ss	SC/TS	12	0	12	B11,B12	B7,B8
11	cong ss	TS	3.1	0.08	3	B15	B9
12	vf ss	VFS	2	1.8	0	B13,B14	B10,B11
13	mudstone	MUD	2.5	0	0	B16,B17,B18	B12,B13
14	cong ss	SC/TS	8	2.5	3	B19,B20	B14,B15
					20.5 x 0.44		
	Total		74.4	5.8	9.6		

Unit	Remarks
1	a few white streaks in laminations
2	some white in vertical fractures. horizontal laminations
3	continuation of unit 2?
4	white at top
5	roots. Paleosol
6	white base and top, few white streaks
7	erosive base
8	bimodal grain size horizontal laminations
9	white streaks in bottom half
10	white in laminations
11	white in laminations
12	all white. at some lateral locations white extends down into unit 11
13	paleosol. many carbonate nodules. laterally extensive over 2,500 ft
14	white bottom and in laminations

Measured Units Bobcat Ridge

Unit	Lithology	Classification	Total (ft)	Complete White (ft)	Laminations White (ft)
1	vf sand	VFS/MS	3.4		
2	mudstone	MUD	0.8		
3	cong	SC/TS/CSM	9.1	1	1.91
4	vf sand	VFS	5.1		
5	c sand	CSM	1.5		0.18
6	vf sand	VFS	3		
7	cong	SC/MS	2.5	2.5	
8	vf sand	MS	2.1		
9	mudstone	MUD	1.1		
10	c sand	MS	0.9	0.5	
11	f sand	VFS	3.6		
12	c sand	SC/TS/CSM	5.2	2.3	2.9
13	f/vf sand	VFS	7.2		
14	mudstone	MUD	0.5		
15	cong	TS/CSM	4	0.25	
16	mudstone	MUD	0.8		
17	c sand	TS/CSM	3.2	0.33	0.32
18	mudstone	MUD	2.4		
19	c sand	TS	3	0.42	
20	m sand	VFS	8.5		
					5.31 x 0.44
	Total		67.9	7.3	2.5

Measured Units Bobcat Ridge

Unit	Remarks
1	some bioturbation near top
2	platy soil horizon. paleosol
3	white at base, in lower laminations
4	strike and dip N5W,7E
5	partial whitening within a small clastic dyke
6	horizontal laminations
7	completely whitened
8	massive, some indications of bioturbation
9	platy soil horizon. paleosol
10	completely whitened
11	thin beds < 3 inches
12	white base and top and in laminations
13	bimodal horizontal laminations
14	thin mudstone, possible channel fill
15	white base
16	thin mudstone
17	white base and top
18	thick paleosol unit. lots of carbonate concretions
19	white base
20	possibly Ingleside, no clastic dykes to mark contact

Measured Units Blue Sky Trail

Unit	Lithology	Classification	Total (ft)	Complete White (ft)	Laminations White (ft)	Hand Sample	Thin Section
1	c ss	TS/CSM	3.1	0	1.5		
2	vf ss	MS	2.3	0.08	0		
3	vf ss	MS	1	0	0		
4	c ss	TS/CSM	5	0	2.5	C25	C1
5	f ss	VFS	5.4	2.25	0	C24,C23	C2
6	silt/ss	MUD	1.2	0	0		
7	cong ss	SC/TS	3.9	0.25	0		
8	vf ss	VFS	4.4	0.5	0	C22,C21	
9	silt	MUD	0.25	0	0		
10	cong ss	SC/TS	16.9	0.5	4	C20,C19, C18	C3, C4
11	vf ss	VFS	5.5	0	0	C17	C5,C6
12	vf ss	VFS	0.75	0	0	C16	C7
13	vf ss	VFS	2.3	0.08	0	C15,C14	C8,C9
14	f ss	VFS	3	0.5	0	C13,C12	
15	vf ss	VFS	1.6	0.19	0	C11	C10
16	ls	LS	0.9	0	0		C11
17	c ss	SC/TS	4.8	1	0		
18	f ss	VFS	2.5	0	0		
19	f ss	VFS	4	0	0	C10	
20	c ss	MS	1.3	0.08	0	C9	
21	vf ss	VFS	12	0	0	C8	
22	cong ss	SC/TS	5.6	0	3		
23	cong ss	SC/TS	7	2.2	1	C7,C6	C12, C13
24	c ss	VFS	1.7	0	0	C5	
25	mudstone	MUD	2	0	0	C4,C3	C14
26	f ss	VFS	4.2	1.5	0	C2,C1	C15
27					12 x 0.44		
	Total		102.6	9.13	5.6		

Measured Units Blue Sky Trail

Unit	Remarks
1	white in bottom laminations, grades into poorly sorted muddy ss
2	massive
3	massive, some bioturbation, bounded by thin mud beds
4	similar to unit 1
5	white in bottom and top
6	platy mudstone. paleosol
7	white base
8	top white is discontinuous
9	very thin mudstone, local barrier to fluid flow?
10	bottom white is discontinuous
11	liesegang bands
12	liesegang bands
13	planar cross beds angles between 20-30 degrees
14	alternating thin mud and sand layers, whitened ss
15	bi modal grain size, horizontal laminations
16	blocky limestone, gastropod and shell fragments
17	erosive base, white base
18	very thin beds <3 inches
19	
20	white streak where it nears top
21	bi modal horizontal laminations
22	white laminations
23	white base
24	
25	thick paleosol, lots of carbonate nodules. laterally continuous >2,000 ft
26	white base. whitening across some clastic dykes

Measured Units Hwy 38 Roadcut

Unit	Lithology	Classification	Total (ft)	Complete White (ft)	Laminations White (ft)	Hand Sample
1	vf ss	MS	2.3	0.17		
2	c ss	CSM	2.6			
3	vf ss	VFS	8.5	0.33		
4	c ss	SC/TS/CSM	11	0.25		
5	mudstone	MUD	2			
6	m ss	TS	6.8		1	
7	vf ss	VFS	1.3	1.3		
8	mudstone	MUD	0.4			
9	vf ss	VFS	2.7	0.33	0.14	G1
10	mudstone	MUD	2.4			
11	vf ss	VFS	3	0.83		G2
12	mudstone	MUD	2			
13	c ss	MS	1.2	0.42		
14	vf ss/siltstone	MS	7			
15	vf ss	VFS/MS	3.1	0.66		
16	c ss	TS/CSM	1.8			
17	vf ss	VFS	2	0.17		
18	mudstone	MUD	0.5			
19	vf ss	VFS	4.9	1		
20	cong ss	SC/TS/CSM	12		0.12	
21	vf ss	VFS	3			
22	c ss	TS/CSM	12			
23	vf ss	VFS	1.2	1.2		
24	mudstone	MUD	2			
25	c ss	MS	1	1		
26	mudstone	MUD	1.6			
27	cong ss	SC/TS/CSM	8	1	0.5	
28	vf ss	VFS	7		0.7	
29	c ss	TS	2.1			
30	vf ss	VFS/MS	3.7	0.33		
31	mudstone	MUD	0.9			
32	cong ss	SC/TS/CSM	7.1	1.58	2.8	
33	mudstone	MUD	1.2			
34	c ss	TS	8		2	
35	mudstone	MUD	1.1			
36	c ss	TS	3.8	3		G3
37	c ss	TS/CSM	6.6	0.25	1.3	
38	c ss	TS	5.5	2.6		

39	mudstone	MUD	5.8			
40	vf ss	MS	5.2	1.8		
41	mudstone	MUD	1.3			
42	vf ss	VFS	7	0.09		
43	mudstone	MUD	2.8			
44	c ss	SC	0.8	0.8		
45	f ss	VFS	16	0.25		
46	mudstone	MUD	0.3			
47	c ss	TS/CSM	4.8	0.09		
48	vf ss	VFS	6.1			
49	c ss	TS	4	0.9		
50	mudstone	MUD	1.2			
					8.56 x 0.44	
	Total		208.6	20.35		4

Measured Units Hwy 38 Roadcut

Unit	Remarks
1	paleosol. many white reduction spots and roots
2	floating gravel clasts at bottom
3	thick sand beds seperated by thin mudstone layers. Top is bioturbated and contains roots >1.5in in diameter
4	white at base and top, several channel deposits
5	thick mudstone
6	white in laminations
7	completely whitened
8	thin mudstone layer
9	white base. calcite crystals 1-2mm
10	thick paleosol mudstone. carbonate nodules
11	lots of biotite and chlorite
12	thick paleosol mudstone. carbonate nodules
13	white
14	massive with some areas of bioturbation
15	white base horizontal laminations
16	erosive base
17	
18	thin mudstone layer
19	white base
20	cobbles at base >4cm

21	thin beds >3in
22	
23	completely whitened
24	thick mudstone
25	completely whitened
26	thick mudstone
27	white base, white laminations at bottom
28	bi modal horizontal laminations
29	horizontal laminations
30	bioturbated at top
31	
32	white base, grades into white laminations
33	paleosol, lots of carbonate nodules
34	white laminations at base
35	paleosol, lots of carbonate nodules
36	grey color
37	white base, grades into white laminations
38	white top
39	very thick paleosol, two layers of carbonate nodules
40	white base, massive
41	
42	
43	thick paleosol, carbonate nodules
44	completely whitened
45	thick unit of thin bedded ss with horizontal laminations, white top
46	paleosol, carbonate nodules
47	
48	
49	white top
50	paleosol, carbonate nodules

Measured Units Dixon Cove

Unit	Lithology	Classification	Total (ft)	Complete White (ft)	Laminations White (ft)	Hand Sample	Thin Section
1	cong ss	SC/TS/CSM	2.5	0	0.8	D1,D2	
2	vf ss		3.1	0	0		
3	c ss	TS	2.4	0	1.2		
4	vf ss	VFS	1.5	0.33	0.5		
5	vf ss/silt		1.5	0	0		
6	cong ss	SC/TS	3.7	1.2	1.25	D3	D1
7	vf ss	MS	6	0	0	D4	D2
8	vf ss	VFS	6.7	0	0		
9	vf ss	VFS	2.3	0	0	D6	D3
10	ls	LS	0.9	0.9	0	D7	D4
11	cong ss	SC/CSM	0.5	0.25	0	D8	D5
12	vf ss/silt	MUD	2	0	0		
13	cong ss	TS/CSM	1.8	0	0.3		
14	vf ss	VFS	7.5	0	0		
15	silt	MUD	1	0	0		
16	cong ss/c ss	SC/TS/CSM	4.3	0.17	0.1		
17	f ss	VFS	3.8	0.17	0		
18	vf ss	VFS, MS	3.5	0.75	1.8	D9,D10	D6,D7
19	mudstone	MUD	1.1	0	0		
20	cong ss	SC/TS/CSM	12	1.3	6	D11	D8
21	vf ss	VFS	15	0	0	D12	D9
22	cong ss	SC/TS/CSM	4.5	0.08	3.5		
23	f ss	VFS	6.7	1	0	D13	D10
24	c ss	TS	4.5	0.8	3.7	D14	D11
25	siltstone	MUD	2.2	0	0		
26	c ss	SC/TS/CSM	5	1.2	2		
27	ls	LS	1.5	0	0	D19	D12
28	silty ss		2	0	0		
29	c ss	SC/TS	5.6	1	4.6	D15	D13
30	mudstone	MUD	1.5	0	0		
31	c ss	TS/CSM	13	0.75	2	D16, D17	D14,D15
32	clay	MUD	1.5	0	0		
33	c ss	SC	0.8	0.8	0		
34	m/f ss	VFS	5.6	0.25	0		
35	cong ss	SC/TS/CSM	8	0.17	1		
36	silty ss	VFS	2	0	0		
37	mudstone	MUD	2.2	0	0		

38	c ss	TS	4.5	0	0		
39	c ss	TS/CSM	5	0.08	2	D18	
40	c ss	TS	4.3	0	0.21		
41	f ss	VFS	5.5	0	0		
					30.96 x 0.44		
	Total		169	11.2	14.6		

Measured Units Dixon Cove

Unit	Remarks
1	irregular white spots and streaks
2	bioturbation
3	white in lower trough bedded part of unit
4	some white streaks
5	strike and dip N1W,24E
6	white base grades into white laminations
7	large (>5cm) rip ups imbrications indicate flow to N
8	
9	continuation of unit 8?
10	mostly small carbonate grains
11	bottom white then fines to silt
12	paleosol. carbonate nodules
13	very silty white streaks only in better sorted areas
14	thin beds <3in
15	paleosol
16	white base, muddy at top
17	white base
18	very high concentration of carbonate but still ss
19	paleosol
20	white base and in laminations
21	bi modal horizontal laminations
22	white in x-beds up until it becomes silty
23	white at top
24	white base and in laminations
25	thick mudstone
26	white in lower half
27	limestone with thin sand lenses
28	silty sand with high concentration of carbonate
29	white at top and in laminations

30	paleosol
31	white base and in laminations
32	thick mudstone
33	all white
34	bottom white
35	very few white streaks in bottom 3 feet
36	thin beds <3in
37	paleosol, lots of carbonate nodules
38	very silty
39	very silty
40	very silty
41	clastic dykes

Measured Units Owl Canyon

Unit	Lithology	Classification	Total (ft)	Complete White (ft)	Laminations White (ft)	Hand Sample	Thin Section
1	vf s	VFS/MUD	8.9	0	0	E1	E1
2	cong ss	TS	3	0	3	E2	E2
3	vf ss	VFS	7.6	0.5	0	E3,E4	E3,E4
4	mudstone	MUD	2	0	0		
5	vf ss	VFS	3.3	0.25	0	E5,E6	E5,E6
6	silty ss	MUD	4	0	0	E7	
7	m ss	TS/MS	4.1	0	0	E8	E7
8	c ss	TS/CSM	8.6	0	7.6	E9	E8
9	f/vf ss	VFS	36	1	0	E10	
10	mudstone	MUD	2.4	0	0	E11	E9
11	c ss	TS	7.5	1.3	6.1	E12, E13	E10,E11
12	vf ss	VFS	8	0	0		
13	siltstone	MUD	1.9	0	0		
14	vf ss	VFS	7.6	0.5	0	E14,E15	E12,E13
15	siltstone	MUD	1.4	0	0		
16	vf ss	VFS	21	1	1	E16,E17	E14,E15
17	siltstone	MUD	1.5	0	0		
18	c ss	SC	3.2	0.33	0		
19	vf ss	VFS	6	0	0		
20	vf ss	VFS	5	0	0		
					17.7 x 0.44		
	Total		143	4.88	8.3		

Measured Units Owl Canyon

Unit	Remarks
1	sandstone beds separated by thin paleosols
2	white in laminations
3	bi modal horizontal laminations, white top
4	thick paleosol, carbonate nodules
5	white bottom
6	thick paleosol, carbonate nodules
7	white bottom
8	white in laminations except at very top
9	white top. Strike and dip N15W,22E
10	paleosol
11	bottom white, white in laminations
12	
13	mudstone
14	white at top
15	thick paleosol
16	white bottom, few white streaks at bottom. Strike and dip N22W,24E
17	paleosol
18	white bottom
19	thin beds <3in
20	contact with Ingleside at thick limestone bed

Pattern of vertical arrangement of facies

1. Sequences begin with facies SC
2. Facies TS always follows facies SC
3. Facies CSM only follows facies SC but facies SC is not always overlain by facies CSM
4. Facies VFS usually follows either facies TS or facies CSM
5. Facies MUD usually follows facies VFS
6. Facies MS is rare and follows no apparent pattern
7. Facies LS is extremely rare and only appears near the top of sequences
8. Facies SC and TS may overlies any facies and reset the sequence

Composition of all minerals counted including grains, cement, and matrix n=13,098

Mineral	% of counted points
Quartz	42.8
Dolomite	15.4
Potassium Feldspar	11.8
Calcite	8.9
Hematite	5.8
Kaolinite	4.5
Other clays	3.4
Lithics	3.1
Biotite	1.3
Muscovite	1.0
Plagioclase Feldspar	0.8
Chlorite	0.5
Opaque minerals	0.4
Anhydrite	0.3
Gypsum	0.1
Zircon	0.1

Composition of all grains counted n=8,087

Mineral	% of counted grains
Quartz	69.0
Potassium Feldspar	19.3
Lithics	5.1
Biotite	2.2
Muscovite	1.7
Plagioclase Feldspar	1.4
Chlorite	0.7
Opaque minerals	0.6
Zircon	0.1

Whitening in relation to paleosol mudstones

Location	% of strata whitened <1ft above paleosol mudstone	% of strata whitened <1ft below paleosol mudstone	% of all other strata whitened
Hall Ranch	69%	48%	9%
Devil's Backbone	100%	60%	11%
Bobcat Ridge	50%	24%	8%
Blue Sky Trail	63%	47%	5%
Hwy 38	54%	36%	3%
Dixon Cove	55%	23%	8%
Owl Canyon	48%	42%	4%

Key to Symbols for Point Count Results

Quartz	Q
K-feldspar (not altered)	K
K-feldspar (altered)	Ka
Plagioclase feldspar (not altered)	P
Plagioclase feldspar (altered)	Pa
Lithics (plutonic)	Lp
Lithics (metamorphic)	Lm
Lithics (sedimentary clastics)	Lc
Lithics (sedimentary carbonate)	Lca
Biotite	B
Muscovite	M
Chlorite	C
Clay matrix	CM
Quartz cement	QC
Clay cement (kaolinite)	CCK
Clay cement (other)	CCo
Calcite cement	CaC
Dolomite cement	DoC
Opaque minerals	O
Hematite cement	HC
Anhydrite	A
Gypsum	G
Porosity	Por

Point count result remarks:

Sample A10 was a concretion

Samples C15 and E7 were taken at boundaries between whitened and non-whited rock so the samples were about half white and half red. Mineralogical differences can be seen between white and red rock even when they were close together

	Q	K	Ka	P	Pa	Lp	Lm	Lc	Lca	B	M	C	CM	QC	CCK	CCo	CalC	DoIC	O	HC	AG	Por
A1	51.2	8.8	5.2	0.8	0	2	0.4	0.4	0	1.2	1.2	0	1.6	0	0	1.6	0.4	16.4	0	6.4	0	2.4
A2	42	3.6	8.8	0	0.4	2.8	0	0.4	0	1.6	1.6	0.4	2.8	0	4.8	5.2	0	24.4	0	0	0.8	0.4
A3	53.2	3.6	12.4	0	1.2	1.2	0	0.4	0	0.4	0	0.4	1.2	0	6.8	8.4	0	7.2	0	0	0	3.6
A4	40.4	10.4	5.2	0	0	2.4	0	0.8	0	2	0.4	0	0.8	0	3.2	1.6	0	21.2	0.8	7.6	0.4	2.8
A5	50.4	10	5.6	0.4	0	2	0.4	0.8	0	1.6	0	0	0.4	2	1.6	2.4	0	16	0	3.6	0.8	2
A7	30	6.8	3.6	0.4	0	5.6	0.4	1.2	0.8	1.6	1.6	0	0.8	0	2.8	2	0	30.4	0.8	8.4	2.0	0.8
A8	43.6	2.4	13.6	0.4	0.4	5.6	0	0	0	0.4	2.4	0	2.4	0	1.6	3.6	0.4	17.6	0	0	0.4	5.2
A9	41.2	6.8	10.4	0.4	0	3.6	0.4	3.2	0	2.8	2	0	6.4	0	4.4	2.8	1.2	6	1.6	4	0	2.8
A10	4.8	0.8	0.4	0	0	0	0	0	0	0.4	0	0	3.6	0	0	0	0	87.2	0	0	2.8	0
A11	21.6	6.4	1.6	0	0	2	0	0.4	0	18	7.6	0.4	2.8	0	1.6	1.6	0	0	2.8	31.2	0	2
A12	46.8	3.2	12.8	0	0	6.4	0.4	4	0	1.6	1.2	0.8	2	0.8	2.8	7.6	0	4.4	0	0	0.8	4.4
A13	47.6	3.6	8.4	0	0.8	5.6	0	1.2	0	3.6	2	0	5.2	0.8	2.4	4.8	0	0	0	7.6	0	6.4
A14	52.8	2.8	13.2	0	0	2.8	0	2	0	1.2	1.6	0	2.8	0.4	6	7.2	0.4	0.8	0.4	0.4	0	5.2
A15	51.6	7.2	10.4	0	0.4	2	0	0.8	0	0.4	0	0	0.8	0.8	4	5.2	0	10.4	0	0	0	6

	Q	K	Ka	P	Pa	Lp	Lm	Lc	Lca	B	M	C	CM	QC	CCK	CCo	CaIC	DoIC	O	HC	AG	Por
B1	43.2	4	16.8	0	1.2	3.6	0	2.4	0	1.2	1.6	0	1.6	2.8	0.8	2.4	0.4	2.4	0.4	3.2	0	12
B2	32.4	3.2	16	0	0	4	0	0.4	0	0	0.4	0	1.2	0.4	0.4	1.6	3.6	25.2	0	4	0	7.2
B3	43.6	9.6	1.6	0	0	0.8	0	0.4	0	0	0	0	0	0.8	0	1.2	1.6	27.6	0	4.4	0	8.4
B7	47.2	7.6	11.2	0	0	3.6	0	2	0	1.6	1.6	0	2	0.8	3.2	6	0.4	4.4	0	0.8	0	7.6
B8	35.6	10.8	4.8	0.4	0	1.2	0	3.2	0	1.6	0.8	0	2.8	0	0.4	1.2	0.4	15.2	0.4	18.4	0	2.8
B9	36.8	9.6	7.2	0	0.4	5.6	0.8	2	0	0.4	0	0	1.2	0	1.2	0	0.8	26.8	0	2.8	0	4.4
B10	40.8	9.2	1.6	0	0	2	0.8	3.2	0	0.8	0.4	0	1.6	1.6	0.8	1.6	1.2	20	0.4	8	0	6
B11	44	5.2	5.2	0	0.4	1.6	0	2.8	0	0	0.8	0	0.8	0.4	11.2	5.6	0.4	14.8	0	0	0	6.8
B12	29.2	6.8	0.4	0.4	0	1.2	0.4	0.4	0	0	0	0	0	0	0.4	0.4	0.8	40.4	0.4	18	0	0.8
B14	44	6	11.2	0	0	2.8	0	2.8	0	0.4	1.6	0	0.8	0	5.6	2.4	1.2	14.8	0	0	0	6.4
B15	48.4	8	6.8	0	0	0.8	0.4	1.6	0	0.4	0.4	0	0	1.2	4.8	2	3.2	8.8	0	2.8	0	10.4

	Q	K	Ka	P	Pa	Lp	Lm	Lc	Lca	B	M	C	CM	QC	CCK	CCo	CaIC	DoIC	O	HC	AG	Por
B1	43.2	4	16.8	0	1.2	3.6	0	2.4	0	1.2	1.6	0	1.6	2.8	0.8	2.4	0.4	2.4	0.4	3.2	0	12
B2	32.4	3.2	16	0	0	4	0	0.4	0	0	0.4	0	1.2	0.4	0.4	1.6	3.6	25.2	0	4	0	7.2
B3	43.6	9.6	1.6	0	0	0.8	0	0.4	0	0	0	0	0	0.8	0	1.2	1.6	27.6	0	4.4	0	8.4
B7	47.2	7.6	11.2	0	0	3.6	0	2	0	1.6	1.6	0	2	0.8	3.2	6	0.4	4.4	0	0.8	0	7.6
B8	35.6	10.8	4.8	0.4	0	1.2	0	3.2	0	1.6	0.8	0	2.8	0	0.4	1.2	0.4	15.2	0.4	18.4	0	2.8
B9	36.8	9.6	7.2	0	0.4	5.6	0.8	2	0	0.4	0	0	1.2	0	1.2	0	0.8	26.8	0	2.8	0	4.4
B10	40.8	9.2	1.6	0	0	2	0.8	3.2	0	0.8	0.4	0	1.6	1.6	0.8	1.6	1.2	20	0.4	8	0	6
B11	44	5.2	5.2	0	0.4	1.6	0	2.8	0	0	0.8	0	0.8	0.4	11.2	5.6	0.4	14.8	0	0	0	6.8
B12	29.2	6.8	0.4	0.4	0	1.2	0.4	0.4	0	0	0	0	0	0	0.4	0.4	0.8	40.4	0.4	18	0	0.8
B14	44	6	11.2	0	0	2.8	0	2.8	0	0.4	1.6	0	0.8	0	5.6	2.4	1.2	14.8	0	0	0	6.4
B15	48.4	8	6.8	0	0	0.8	0.4	1.6	0	0.4	0.4	0	0	1.2	4.8	2	3.2	8.8	0	2.8	0	10.4

	Q	K	Ka	P	Pa	Lp	Lm	Lc	Lca	B	M	C	CM	QC	CCk	CCo	CalC	DolC	O	HC	AG	Por
C3	39.2	4.4	11.2	0	0	3.6	0.8	1.6	0	0.8	0.4	0	0	0	2.8	2	26.4	0	0	0	0	6.8
C4	36.4	9.2	11.2	0	0.4	5.6	0.4	1.6	0.8	0.4	0	0	0	0	0.8	1.6	28	0	0.4	1.6	0	1.6
C7	42.8	10	6	0	0.4	2	0	1.2	1.2	0.4	0	0	0	1.2	1.6	2	21.6	0.8	0.4	4.4	0	4
C8	52.8	1.6	4.4	0	0	0.8	0	0.4	0	0.4	0	0	0	1.2	2	1.6	32	0.8	0	0	0	2
C9	44	4.8	1.2	0.4	0	0.8	0	0.8	0	0	0.4	0	0	4	0	0.4	32.4	1.6	0.8	5.6	0	2.8
C11	1.6	0	0	0	0	0	0	0	0	0	0	0	0	0	0	0	98.4	0	0	0	0	0
C12	38	4.4	19.2	0	0	3.2	1.2	0.4	0	1.2	0.4	0	1.2	0	7.6	3.2	5.6	1.2	0	0	0	13.2
C13	48.8	2.4	17.2	0	0	3.6	0	0	0	0	0.8	0	0	0	9.2	6.4	3.6	1.2	0.4	0.8	0	5.6
C14	14.8	1.6	0	0	0	0	0	0.4	0	9.2	2.8	0	0	0	0	0.8	1.2	36.4	0	32.4	0	0.4
C15	48.4	3.6	4.4	0	0	0.4	0	0.8	0	0	0.4	0	0	0	6.4	1.2	1.6	24	0	5.6	0	3.2

	Q	K	Ka	P	Pa	Lo	Lm	Lc	Lca	B	M	C	CM	QC	CCK	CCo	CaIC	DoIC	O	HC	AG	Por
D1	37.2	2.8	16.8	0	1.2	8	2.4	0	0	2	3.2	1.2	0.8	0	8.8	3.6	2.8	0	2.4	1.6	0	5.2
D3	36.8	7.2	4.8	0.4	1.2	3.2	0	0	0	2.4	1.6	0	0	0	7.2	6	7.2	8.4	0.8	8.4	0	4.4
D4	8.4	2	0.4	0	0	0	0	0	0	0	0	0	0	0	0	0	86	0.4	0	2	0	0.8
D5	36.4	4	4.4	0	0.8	2	0.4	0.4	0	0.8	1.2	0	0.4	0	1.2	5.6	0	25.2	1.2	7.2	0	8.8
D6	43.2	4.4	1.6	1.2	0.4	0.8	0	0.8	0	1.6	1.2	0	0	0	0	1.6	17.6	5.6	1.6	18	0	0.4
D7	52.8	1.2	6.4	0	0.8	0	0	0	0	3.2	0.8	2.8	0	0.4	12.4	6.8	4	1.6	0	0	0	6.8
D8	38.8	2	11.6	0.4	0	2.8	0	0.8	0.4	0.8	0.4	0.4	0	0	5.2	2.4	28	0	0	0	0	6
D9	57.6	2	1.2	0.4	0	0	0	0	0	0	0	0	0	2.4	0	0.8	0	20.4	0	9.6	0	5.6
D13	56.8	3.2	7.6	0	0.8	0.4	0	0	0	1.6	2	3.2	0	0	6.8	3.6	13.2	0.4	0	0	0	0.4
D14	50	0.8	8.8	0	0.4	0.8	0	0	0	0	1.6	0	0	0	2	0.4	11.2	16.4	0.4	0	0	7.2
D15	52.4	4.4	6.8	0.4	1.6	1.2	0	0	0	0.4	2	0	0	0	2.8	1.2	3.2	12.4	0	3.6	0	7.6

	Q	K	Ka	P	Pa	Lp	Lm	Lc	Lca	B	M	C	CM	QC	CCk	CCo	CaIC	DoIC	O	HC	AG	Por	
E7	52	1.6	3.6	0	0.4	0	0	0	0	0.4	0.4	0.8	0	0	6	2	6	12.4	0.4	7.2	0	6.8	
E8	43.6	0	14.4	0	0.8	0.8	0	0	0	0.4	0.4	0	0.4	0	18	4.8	5.6	0	0.8	2.4	0	7.6	
E9	16.8	1.6	0	0.4	0	0	0	0	0	0	0.4	0	0	0	0	0	0	53.6	0	27.2	0	0	
E10	48.8	0	16.4	0	0.8	2	0	0	0	0.4	2.8	0.8	0.8	0	13.6	4.4	0	0	0	0	0	0	9.2
E12	29.2	1.6	2	0	0	0.4	0	0	0	1.2	0	0.4	0	0	0.4	0	1.6	50.4	1.2	9.2	0	2.4	
E13	38	0.8	7.2	0	1.2	0	0	0	0	0	0.8	3.2	0	0	9.2	2	2	28	0.8	0.8	0	6	
E14	46.8	0	5.6	0	0.8	0	0	0	0	1.6	1.6	5.6	0	0	16.8	4	1.2	12.4	0	0.8	0	2.8	
E15	39.2	2.8	4.8	0.4	0	0	0	0	0	0.4	0	0	0	0	2	1.2	2.4	22.8	0.8	14.4	0	8.8	

	Q	K	Ka	P	Pa	Lp	Lm	Lc	Lca	B	M	C	CM	QC	CCK	CCo	CalC	DoIC	O	HC	AG	Por
C15R	46.4	5.6	3.2	0	0	0.8	0	0.8	0	0	0	0	0	0	2.4	0.8	0.8	27.2	0	9.6	0	2.4
C15W	43.2	1.6	6.4	0	0	0	0	0.8	0	0	0.8	0	0	0	10.4	1.6	2.4	20.8	0	0	0	4
E7R	47.2	2.4	2.4	0	0.8	0	0	0	0	0	0	0	0	0	1.6	1.6	5.6	21.6	0	14.4	0	2.4
E7W	55.2	0.8	4.8	0	0.8	0	0	0	0	0.8	0.8	1.6	0	0	10.4	2.4	6.4	3.2	0.8	0	0	11.2

